ISSN 1023-9855

胸腔醫學

Thoracic Medicine

The Official Journal of Taiwan Society of Pulmonary and Critical Care Medicine

Vol.29 No.3 June 2014

第二十九卷 第三期

中華民國一〇三年六月

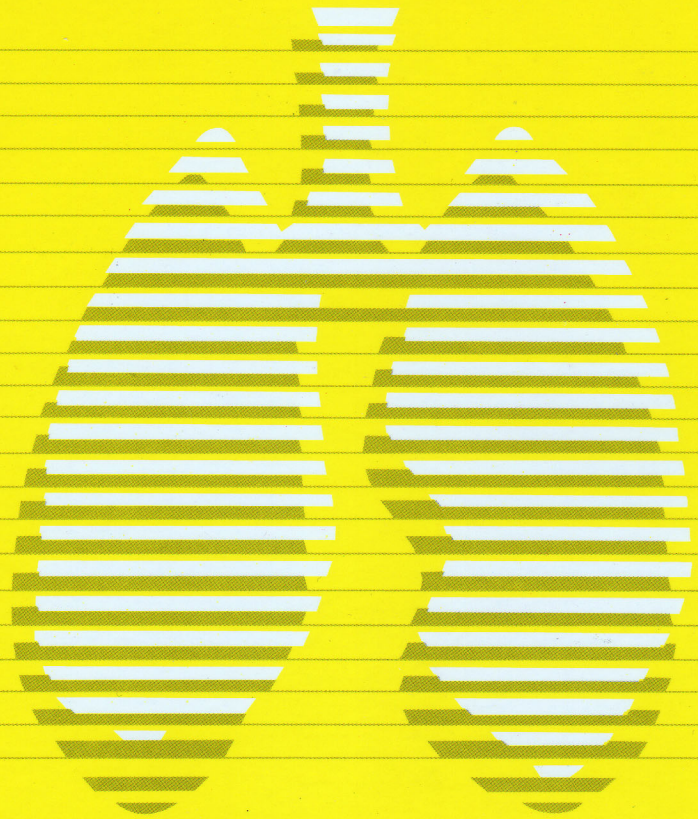

台灣胸腔暨重症加護醫學會

11217 台北市北投區石牌路二段201號

5.No.201, Sec. 2, Shipai Rd., Beitou District, Taipei City, Taiwan 11217, R.O.C.

ISSN 1023-9855

中華民國一〇三年六月　第二十九卷　第三期

ISSN 1023－9855

胸腔醫學

Thoracic Medicine

The Official Journal of Taiwan Society of Pulmonary and Critical Care Medicine

Vol.29 No.3 June 2014

原著

全身正子攝影對於肺小細胞癌診斷分期與存活的影響.....127~143
李適鴻，高國晉，何恭之，徐稟智，陳濘宏，楊政達，劉劍英

台灣痰抹片陰性肺結核患者的預測因子 .....144~151
連偉立，陳淑玲，許慧敏，余春慧，陳美芳

病例報告

肺腺纖維瘤：罕見良性肺部結節－病例報導 .....152~159
黃彥儒，朱國安，歐亭芸，吳冠陞，傅婷瑛，賴瑞生

以穿越肺裂之腫塊為表徵的肺部放射線菌病－病例報告 .....160~165
曾明雄，蕭世欣，鍾啟禮

氣管內原發性異生性大細胞淋巴瘤－病例報告與文獻回顧.....166~173
沈昱廷，劉大智，蔡志仁，楊志仁，王東衡，黃明賢

以支氣管內病灶為表現的後天免疫缺乏症候群相關之肺內卡波西氏肉瘤－病例報告及文獻回顧.....174~181
林士森，陳昱青，陳威宇，高尚志

免疫健全病人之瀰漫性禽結核分枝桿菌感染以肺部轉移癌表現－病例報告及文獻回顧 .....182~188
鄭人碩，巫政霖，張漢煜

克隆氏症病人的喉頭肉芽性炎症：結核病或是克隆氏症之腸外侵犯 .....189~193
鄭少仲，王振源

轉移性造釉細胞瘤（Metastasizing Ameloblastoma）－多處肺結節之罕見原因 .....194~199
鐘哲良，蔡子修，廖唯昱，余忠仁

中華民國一〇三年六月　第二十九卷　第三期

ISSN 1023－9855

Vol.29 No.3 June 2014

胸腔醫學

Thoracic Medicine

The Official Journal of Taiwan Society of Pulmonary and Critical Care Medicine

Orginial Articles

The Impact of Whole-body ^{18}F-Fluorodeoxy-D-Glucose Positron Emission Tomography - Computed Tomography (PET-CT) on the Staging and Outcome of Small Cell Lung Cancer Patients ..... 127~143
Shih-Hong Li, Kuo-Chin Kao, Kung-Chu Ho, Ping-Chih Hsu, Ning-Hung Chen, Cheng-Ta Yang, Chien-Ying Liu

Predicators of Pulmonary Tuberculosis in Patients with Sputum Smear-Negative Results in Taiwan ..... 144~151
Wei-Li Lien, Shu-Ling Chen, Hui-Min Hsu, Chun-Hui Yu, Mei-Fang Chen

Case Reports

Pulmonary Adenofibroma: A Rare Presentation of a Benign Lung Nodule – A Case Report ..... 152~159
Yen-Zu Huang, Kuo-An Chu, Ting-Yung Ou, Kuan-Sheng Wu, Ting-Ying Fu, Ruay-Sheng Lai

Pulmonary Actinomycosis Presenting as a Lung Mass Crossing the Fissure – A Case Report..... 160~165
Ming-Syong Zeng, Shih-Hsin Hsiao, Chi-Li Chung

Endotracheal Anaplastic Large Cell Lymphoma – A Case Report and Literature Review..... 166~173
Yu-Ting Shen, Ta-Chih Liu, Chee-Yin Chai, Chih-Jen Yang, Tung-Heng Wang, Ming-Shyan Huang

AIDS-related Intrapulmonary Kaposi's Sarcoma Presenting as Endobronchial Lesions: A Rare Presentation in Taiwan – A Case Report and Literature Review ..... 174~181
Shih-Sen Lin, Yu-Ching Chen, Wei-Yu Chen, Shang-Jyh Kao

Disseminated *Mycobacterium avium complex* Infection Mimicking Metastatic Lung Cancer in an Immunocompetent Patient – A Case Report and Literature Review ..... 182~188
Jen-Suo Cheng, Cheng-Lin Wu, Han-Yu Chang

Laryngeal Granulomatous Inflammation in a Patient with Crohn's Disease: Tuberculosis or Extra-intestinal Crohn's Disease ..... 189~193
Shao-Chung Cheng, Jann-Yuan Wang

Metastasizing Ameloblastoma (Malignant Ameloblastoma) – An Unusual Cause of Multiple Lung Nodules ..... 194~199
Che-Liang Chung, Tzu-Hsiu Tsai, Wei-Yu Liao, Chong-Jen Yu

The Impact of Whole-body ^{18}F-Fluorodeoxy-D-Glucose Positron Emission Tomography - Computed Tomography (PET-CT) on the Staging and Outcome of Small Cell Lung Cancer Patients

Shih-Hong Li, Kuo-Chin Kao, Kung-Chu Ho*, Ping-Chih Hsu, Ning-Hung Chen, Cheng-Ta Yang, Chien-Ying Liu

Background: Determining the appropriate therapy for small cell lung cancer (SCLC) is highly dependent on accurate staging, which may have an impact on disease outcome. We evaluated whether the introduction of whole-body positron emission tomography with the glucose analog ^{18}F-fluoro-2-deoxy-D-glucose (FDG-PET) improved the accuracy of staging, adequacy of therapy and clinical outcome of SCLC patients.

Methods: The study design included prospective recording and retrospective analysis. From September 2007 to July 2012, a total 117 of newly diagnosed SCLC patients (mean age: 62 years, male/female: 107/10, Eastern Cooperative Oncology Group performance status (ECOG): 0-2, were enrolled for analysis. Sixty-nine patients received conventional computed tomography (CT) for staging, and 48 patients underwent both FDG-PET and conventional image studies for staging. All patients received protocol-oriented therapy on an intention-to-treat basis Chang Gung Memorial Hospital.

Results: The clinical stage was changed in 14 of the 48 (29%) patients after FDG-PET (10 from limited-stage disease (LD) to extensive-stage disease (ED), 4 from ED to LD), and 34 remained at the same stage. The patients with LD as determined by FDG-PET had a longer median survival than those with LD by conventional staging (15.9±14.2 months versus 9.5±6.0 months; HR: 2.672; log-rank test p=0.0247). The median survival of patients with ED identified by FDG-PET staging was 9.3±4.6 months, compared to 10.1±8.2 months by CT scan (HR: 0.968; log-rank test p=0.9080).

Conclusions: For limited-stage SCLC patients, the application of FDG-PET had a positive impact on staging, management and outcome; however, there was less impact on extensive-stage SCLC. ***(Thorac Med 2014; 29: 127-143)***

Key words: small cell lung cancer, positron emission tomography (PET), computed tomography (CT), bone scan, overall survival

Department of Thoracic Medicine, *Department of Nuclear Medicine, Chang Gung Memorial Hospital and School of Medicine, Chang Gung University, Taipei, Taiwan
Address reprint requests to: Dr. Chien-Ying Liu, Department of Thoracic Medicine, Chang Gung Memorial Hospital and Chang Gung University, 5 Fushing Street, Gueishan Shiang, Taoyuan 333, Taiwan

Introduction

In Taiwan, lung cancer is the leading cause of cancer-related deaths among both women and men. Small cell lung cancer (SCLC) represented approximately 8.1% and 15% of all lung cancers in Taiwan and the United States, respectively [1-2]. Due to the rapid doubling of cancer cells, SCLC has a clinically aggressive nature and a tendency to become widespread metastatic disease. In 1957, the Veterans Affairs Administration Lung Cancer Study Group (VALG) classified SCLC into limited disease (LD) and extensive disease (ED) [3]. LD was defined as disease limited to 1 hemithorax with ipsilateral and contralateral hilar and mediastinal nodes that could be encompassed within a radiation portal; all other disease spread was classified as ED.

At the time of diagnosis, 28% to 37.2% of patients presented with LD and 53.3% to 72% with ED. For LD, concurrent chemoradiation therapy (CCRT) is the major treatment modality, and for ED, chemotherapy alone is used. The median survival of patients with LD was 10 to 14 months [4-7], which was better than the 5.6 to 7 months for ED patients [4-5,8]. Since the median survival of LD and ED is quite different, accurate staging of SCLC has significant implications for the choice of therapy and subsequent prognosis. In non-small cell lung cancer (NSCLC) patients, the sensitivity and specificity of integrated whole-body ^{18}F-fluorodeoxy-D-glucose positron emission tomography-computed tomography (^{18}F-FDG-PET/CT) for staging and diagnosis were higher than that of computed tomography (CT) [9]. For initial staging of SCLC, a conventional imaging study, such as CT of the thorax and abdomen, bone scan, cranial CT or magnetic resonance imaging (MRI), is performed. Accurate staging of LD is important for the introduction of the CCRT modality and improvement of disease outcome. As for ED, accurate staging could render thoracic radiation therapy unnecessary, so the use of ^{18}F-FDG-PET for staging may thereby reduce healthcare costs and allow ED SCLC patients to avoid the toxicity of radiation [10].

Several studies have revealed the value of ^{18}F-FDG-PET for initial staging and treatment planning of SCLC [11-17]. Whole-body ^{18}F-FDG-PET/CT was introduced into clinical cancer practice in our hospital in 2006. Therefore, to determine the prognostic value of ^{18}F-FDG-PET/CT for use in the staging of SCLC patients, we further analyzed the outcome of newly diagnosed SCLC patients using conventional staging tools and additional ^{18}F-FDG-PET/CT.

Patients and Methods

Study subjects

A prospective cancer recording system and retrospective analysis were used in the present study. From September 2007 to July 2012, the medical data of 3642 pathologically proven primary lung cancer patients were recorded in the cancer registration database at Lin-Kou Chang Gung Memorial Hospital. The screening criteria for this study were set as: 1) age ≥18 years old, 2) newly diagnosed SCLC, 3) Eastern Cooperative Oncology Group (ECOG) performance status: 0~2, and 4) having received CCRT or at least 2 cycles of standard chemotherapy after staging by ^{18}F-FDG-PET/CT or conventional imaging studies. The data of 340 newly diagnosed, untreated SCLC patients were recorded during this period. A total of 117 patients met the screening criteria and were enrolled for analysis. The

patients were grouped as LD or ED according to the VALG SCLC classification. Patients in these 2 groups were further divided into those staged with conventional imaging methods and those staged with additional ^{18}F-FDG-PET/CT. The conventional imaging methods included CT of the thoracic and upper abdomen, cerebral CT or MRI and bone scan. Standard therapy included systemic chemotherapy with a cisplatin and etoposide (EP) regimen for ED patients and systemic CCRT for LD patients. Forty ED SCLC patients received local radiation therapy for tumor control or palliation of symptoms. If pleural effusion was noted in any image study, diagnostic thoracentesis for cytological study was performed to confirm the etiology of the pleural effusion.

Image acquisition

Integrated whole-body ^{18}F-fluorodeoxy-D-glucose positron emission tomography- computed tomography

According to the protocol of the nuclear medicine department of Lin-Kou Chang Gung Memorial Hospital, all patients were requested to fast at least 4 hours before examination and had a glucose level less than 200 mg/dL. Intravenous contrast was not used. Fifty minutes after intravenous injection of FDG (333-407 MBq), integrated whole-body ^{18}F-FDG-PET/CT (Discovery ST16, GE Healthcare) images were obtained. The standard uptake value (SUV) for each voxel was calculated as follows: SUV= (measured activity concentration [Bq/mL])/(injected activity [Bq]/body weight [kg]×1,000).

Statistical analysis

Descriptive statistics were used to examine the demographic characteristics of the study population. Data were presented as mean± standard deviation (SD) or subject number. Fisher's exact test or chi-square (X_2) was used for categorical data and t tests for continuous measures to compare the differences between subgroups. Survival was determined as the duration from the date of diagnosis to the date of death, or the date of last follow-up, if the patients were still alive. Survival probabilities were presented by Kaplan-Meier curves, and the log-rank test was used to compare survival curves. Univariate Cox's proportional hazard modeling was used to analyze the hazard ratio (HR) with a 95% confidence interval (95% CI) for age at diagnosis, gender, cigarette exposure duration, cigarette exposure amount (pack-years), body mass index, comorbidity (coronary artery disease, cerebral vascular accident, chronic obstructive pulmonary disease, asthma, pulmonary tuberculosis infection, cancer history, hypertension and diabetes mellitus), number of conventional imaging studies for staging, chemotherapy, cycles of chemotherapy, ECOG performance status, radiation therapy, hyponatremia, superior vena cava syndrome and malignant pleural effusion. A p value less than 0.05 (2-sided) was considered statistically significant. Further multivariate Cox's proportional hazard modeling was performed if univariate Cox's regression showed statistical significance. Statistical analyses were performed using SPSS 19.0 for Windows (SPSS, Inc, Chicago, Ill) and GraphPad Prism 5.0 (GraphPad Software, San Diego, Ca).

Results

Patient population

From September 2007 to July 2012, 117 newly diagnosed SCLC patients were enrolled for analysis; 107 (91.5%) were male and 10

(8.5) were female. The mean age was 62.9±11.2 years, ranging from 28.7 to 83.3 years. Seventy-four patients (73.2%) were ED and 43 (36.8%) were LD. Sixty-nine patients underwent a conventional staging process and 48 patients had additional ^{18}F-FDG-PET/CT. In terms of performance status, 12 patients (10.2%) were ECOG 0, 95 (81.2%) were ECG 1, and 10 (8.5%) were ECOG 2 (Table 1).

Characteristics of patients

Group receiving ^{18}F-FDG-PET/CT imaging studies

In the subgroup of 48 patients receiving ^{18}F-FDG-PET/CT, 44 (91.7%) were male and 4 (8.3%) were female. The mean age was 60.2± 11.3 years. The proportion of smoking and non-smoking patients was 95.8% and 4.2%, respectively. The mean pack-years of smoking were 46.7±34.8. The mean BMI was 23.9±3.4. Seven patients (14.6%) were ECOG 0, 35 (72.9%) were ECOG 1, and 6 (12.5%) were ECOG 2. Twenty-four patients (50%) were LD and the others (n=24, 50%) were ED. The mean survival of the LD and ED patients was 15.9±14.2 and 9.3±4.6 months, respectively. One patient had ipsilateral malignant pleural effusion. The average cycles of chemotherapy with EP and with topoticam were 5.71±2.59 and 0.33±0.8, respectively. Only 22 (45.8%) patients received a bone scan. Cerebral CT was performed for 32 (66%) patients (Table 1).

Group receiving conventional imaging studies without ^{18}F-FDG-PET/CT

In the subgroup of 69 patients not receiving ^{18}F-FDG-PET/CT, 63 (91.3%) were male and 6 (8.7%) were female. The mean age was 64.8±10.7 years. The proportion of smoking and non-smoking patients was 94.2% and 5.8% respectively. The mean pack-years of smoking were 47.6±55.4. The mean BMI was 24.1±3.4. Five patients (7.2%) were ECOG 0, 60 (87.0%) were ECOG 1, and 4 (5.8%) were ECOG 2. Nineteen patients (27.5%) were LD and 50 (72.5%) were ED. The mean survival of the LD and ED patients was 9.5±6.0 and 10.1±8.2 months, respectively. Nine patients had ipsilateral malignant pleural effusion. The average number of chemotherapy cycles with the EP and the topoticam regimens was 4.96±2.03 and 0.58±1.48, respectively. Almost all patients (n=67, 97.1%) received a bone scan. Cerebral CT was performed for 40 patients (58%) (Table 1).

LD-SCLC patients receiving ^{18}F-FDG-PET/CT versus those undergoing conventional imaging studies

Of the 24 LD-SCLC patients receiving ^{18}F-FDG-PET/CT, 23 (95.8%) were male and 1 (4.2%) was female; 17 (89.5%) of the 19 patients receiving conventional imaging studies were male, and 2 (10.5%) were female. The mean age of the ^{18}F-FDG-PET/CT and conventional imaging study groups was 59.0±11.8 and 62.7±11.3 years, respectively. The mean pack-years of smoking of the ^{18}F-FDG-PET/CT and conventional imaging groups were 41.7±32.5 and 71.6±94.9, respectively, without statistical significance (p=0.086). The duration of smoking of the ^{18}F-FDG-PET/CT and conventional imaging groups was 30.6±13.5 and 40.2±12.8 years, respectively, which was statistically significant (p=0.023). Seven patients had ipsilateral pleural effusion, but only 1 had malignancy confirmed by cytology. The average cycles of chemotherapy with EP of the ^{18}F-FDG-PET/CT and conventional imaging groups were 6.3±2.9 and 4.9±1.3, respectively. The average cycles of

Table1. Characteristics of the Patients with Small Cell Lung Cancer

Characteristic	Total	Non-PET	PET	*p* value
Patient numbers	117	69	48	
Age, yr, mean±SD	62.9±11.2	64.8±10.7	60.2±11.3	0.021
Gender				1.000
Female	10	6 (8.7%)	4 (8.3%)	
Male	107	63 (91.3%)	44 (91.7%)	
Non-smoking	6	4 (5.8%)	2 (4.2%)	1.000
Smoking	111	65 (94.2%)	46 (95.8%)	
Smoking (pack*years)	47.3±47.9	47.6±55.4	46.7±34.8	0.967
ED		38.5±25.5	51.8±37.1	0.251
LD		71.6±94.9	41.7±32.5	0.086
BMI	24.1±3.4	24.1±3.4	23.9±3.4	0.692
Performance, ECOG				0.149
0	12	5 (7.2%)	7 (14.6%)	
1	95	60 (7.0%)	35 (72.9%)	
2	10	4 (5.8%)	6 (12.5%)	
Stage				0.013
ED	74	50 (72.5%)	24 (50%)	
LD	43	19 (27.5%)	24 (50%)	
Comorbidity				
Coronary artery disease	9	7	2	0.305
Cerebral vascular accident	9	5	4	1.000
Tuberculosis, lung	7	2	5	0.121
Diabetes mellitus	21	13	8	0.811
Hypertension	41	25	16	0.845
COPD	16	12	4	0.184
Asthma	2	1	1	1.000
Other cancer	9	6	3	0.735
Chemotherapy line	1.2±0.4	1.19±0.39	1.21±0.41	0.791
Cycles of chemotherapy				
EP	5.3±2.3	4.96±2.03	5.71±2.59	0.120
Topoticam	0.48±1.2	0.58±1.48	0.33±0.78	0.826
Dose of radiation, cGy	2662.74±2569.9	1872.5±2244.3	3798.8±2603.5	<0.001
Overall survival (months)				
LD	13.1±11.6	9.5±6.0	15.9±14.2	0.087
ED	9.8±7.2	10.1±8.2	9.3±4.6	0.243
Serum sodium	137.3±5.3	136.75±6.13	135.05±19.8	0.734
Hyponatremia	17	13	4	0.226
Malignant pleural effusion	10	9	1	0.046
ED	9	8	1	
LD	1	1	0	
Bone scan, done	89	67 (97.1)	22 (45.8)	<0.001
Bone scan, no	28	2 (2.9)	26 (54.2)	
Brain CT, done	72	40 (58)	32 (66.7)	0.342
Brain CT, no	45	29 (42)	16 (33.3)	

chemotherapy with topoticam of the ^{18}F-FDG-PET/CT and conventional imaging groups were 0.1±0.3 and 0.6±1.5, respectively. Six patients did not receive radiation therapy. There was no difference in the incidence of comorbidities between the patients with or without an ^{18}F-FDG-PET/CT study (Table 2).

ED-SCLC patients receiving ^{18}F-FDG-PET/CT versus those undergoing conventional imaging studies

Of the 24 ED-SCLC patients receiving ^{18}F-FDG-PET/CT, 21(87.5%) were male and 3 (12.5%) were female; 46 (92%) of the 50 patients undergoing conventional imaging studies were male, and 4 (8%) were female. The

Table 2. Characteristics of the patients with LD-SCLC and ED-SCLC

Patient number (percent)		LD			ED		
		PET	Non-PET	*p* value	PET	Non-PET	*p* value
Age at diagnosis		59.0±11.8	62.7±11.3	0.301	61.5±11.0	65.6±10.5	0.117
Gender	Male	23 (95.8)	17 (89.5)	0.411	21 (87.5)	46 (92.0)	0.675
	Female	1 (4.2)	2 (10.5)		3 (12.5)	4 (8.0)	
Cigarette smoking	Never	1 (4.2)	0 (0.0)	1.000	1 (4.2)	4 (8.0)	1.000
	Yes	23 (95.8)	19 (100.0)		23 (95.8)	46 (92.0)	
Cigarettes, pack/days		1.3±0.9	2.0±3.2	0.361	1.3±0.6	1.1±0.5	0.054
Cigarettes, years		30.6±13.5	40.2±12.8	0.023	35.6±17.5	33.0±15.9	0.523
Cigarettes, pack-years		41.7±32.5	71.6±94.9	0.086	51.8±37.1	38.5±25.5	0.076
Cigarette cessation	No	23 (95.8)	14 (73.7)	0.072	16 (66.7)	42 (84.0)	0.090
	Yes	1 (4.2)	5 (26.3)		8 (33.3)	8 (16.0)	
Body weight		67.2±13.2	65.7±13.6	0.720	62.2±9.6	62.4±10.4	0.923
Body height		164.8±5.8	163.8±7.4	0.602	163.3±6.7	160.9±6.3	0.152
Body mass index, BMI		24.6±3.8	24.4±3.9	0.865	23.3±2.8	24.0±3.3	0.327
Performance, ECOG	0	6 (25.0)	3 (15.8)	0.372	1 (4.2)	2 (4.0)	0.014
	1	17 (70.8)	13 (68.4)		18 (75.0)	47 (94.0)	
	2	1 (4.2)	3 (15.8)		5 (20.8)	1 (2.0)	
Therapy							
Cycles of chemotherapy, EP		6.3±2.9	4.9±1.3	0.068	5.1±2.1	5.0±2.3	0.685
Cycles of chemotherapy, topoticam		0.1±0.3	0.6±1.5	0.391	0.5±1.0	0.6±1.5	0.604
Lines of chemotherapy		1.2±0.4	1.2±0.4	0.717	1.3±0.4	1.2±0.4	0.486
Radiation therapy	No	1 (4.2)	5 (26.3)	0.432	11 (45.8)	23 (46.0)	0.989
	Yes	23 (95.8)	14 (73.7)		13 (54.2)	27 (54.0)	
Dose of radiation, cGy		5305.8±1845.2	3773.7±2468.9	0.031	2291.7±2388.9	1150.0±1678.2	0.045
Comorbidity							
Comorbidity	No	11 (45.8)	8 (42.1)	0.807	12 (50.0)	23 (46.0)	0.747
	Yes	13 (54.2)	11 (57.9)		12 (50.0)	27 (54.0)	

Coronary artery disease	No	23 (95.8)	17 (89.5)	0.575	23 (95.8)	45 (90.0)	0.657
	Yes	1 (4.2)	2 (10.5)		1 (4.2)	5 (10.0)	
Cerebral vascular disease	No	22 (91.7)	17 (89.5)	1.000	22 (91.7)	47 (94.0)	0.657
	Yes	2 (8.3)	2 (10.5)		2 (8.3)	3 (6.0)	
Diabetes mellitus	No	19 (79.2)	13 (68.4)	0.495	21 (87.5)	43 (86.0)	1.000
	Yes	5 (20.8)	6 (31.6)		3 (12.5)	7 (14.0)	
Hypertension	No	14 (58.3)	12 (63.2)	0.748	18 (75.0)	32 (64.0)	0.344
	Yes	10 (41.7)	7 (36.8)		6 (25.0)	18 (36.0)	
C.O.P.D.	No	23 (95.8)	16 (84.2)	0.306	21 (87.5)	41 (82.0)	0.740
	Yes	1 (4.2)	3 (15.8)		3 (12.5)	9 (18.0)	
Asthma	No	24 (100.0)	19 (100.0)		23 (95.8)	49 (98.0)	0.546
	Yes	0 (0.0)	0 (0.0)		1 (4.2)	1 (2.0)	
Tuberculosis	No	22 (91.7)	18 (94.7)	1.000	21 (87.5)	49 (98.0)	0.097
	Yes	2 (8.3)	1 (5.3)		3 (12.5)	1 (2.0)	
Other cancer	No	21 (87.5)	19 (100.0)	0.243	24 (100.0)	44 (88.0)	0.168
	Yes	3 (12.5)	0 (0.0)		0 (0.0)	6 (12.0)	
Clinical manifestations							
Dyspnea	No	16 (66.7)	13 (68.4)	0.903	9 (37.5)	34 (68.0)	0.013
	Yes	8 (33.3)	6 (31.6)		15 (62.5)	16 (32.0)	
Hemoptysis	No	18 (75.0)	15 (78.9)	1.000	17 (70.8)	45 (90.0)	0.048
	Yes	6 (25.0)	4 (21.1)		7 (29.2)	5 (10.0)	
Body weight loss	No	20 (83.3)	17 (89.5)	0.678	17 (70.8)	40 (80.0)	0.380
	Yes	4 (16.7)	2 (10.5)		7 (29.2)	10 (20.0)	
Chest pain	No	16 (66.7)	13 (68.4)	0.903	14 (58.3)	45 (90.0)	0.004
	Yes	8 (33.3)	6 (31.6)		10 (41.7)	5 (10.0)	
Cough	No	12 (50.0)	3 (15.8)	0.019	8 (33.3)	10 (20.0)	0.211
	Yes	12 (50.0)	16 (84.2)		16 (66.7)	40 (80.0)	
Serum sodium		137.9±4.8	135.5±7.8	0.343	138.0±2.7	137.2±5.5	0.485
Hyponatremia, Serum sodium <135	No	19 (79.2)	10 (52.6)	0.154	20 (83.3)	37 (74.0)	0.213
	Yes	3 (12.5)	4 (21.1)		1 (4.2)	9 (18.0)	
	U/A	2 (8.3)	5 (26.3)		3 (12.5)	4 (8.0)	
SIADH	No	0 (0.0)	0 (0.0)		0 (0.0)	0 (0.0)	
	Yes	0 (0.0)	0 (0.0)		0 (0.0)	0 (0.0)	
SVC syndrome	No	24 (100.0)	17 (89.5)	0.189	21 (87.5)	48 (96.0)	0.321
	Yes	0 (0.0)	2 (10.5)		3 (12.5)	2 (4.0)	
Pleural effusion	Negative	22 (91.7)	14 (73.7)	0.113	17 (70.8)	30 (60.0)	0.365
	Positive	2 (8.3)	5 (26.3)		7 (29.2)	20 (40.0)	
Malignant pleural effusion	Negative	2 (100.0)	4 (80.0)	0.495	6 (85.7)	12 (60.0)	0.214
	Positive	0 (0.0)	1 (20.0)		1 (14.3)	8 (40.0)	

mean age of the ^{18}F-FDG-PET/CT and conventional imaging patients was 61.5±11.0 and 65.6±10.5 years, respectively. The mean pack-years of smoking of the ^{18}F-FDG-PET/CT and conventional imaging groups were 51.8±37.1 and 38.5±25.5, respectively, without statistical significance (p=0.076). The patient number per ECOG performance status were statistically significant (p=0.014). Nine of 27 patients had ipsilateral malignant pleural effusion. The average cycles of chemotherapy with EP of the ^{18}F-FDG-PET/CT and conventional imaging groups were 5.1±2.1 and 5.0±2.3, respectively. The average cycles of chemotherapy with topoticam of the ^{18}F-FDG-PET/CT and conventional imaging groups were 0.5±1.0 and 0.6±1.5. There was no difference in the incidence of comorbidities between the patients with or without an ^{18}F-FDG-PET/CT study (Table 2).

Management and outcome of patients who altered their clinical stages after ^{18}F-FDG-PET/CT study

Fourteen (29%) of the 48 patients receiving an ^{18}F-FDG-PET/CT study altered their clinical stages (Table 3). Ten patients changed from LD to ED. The incongruent sites on ^{18}F-FDG-PET/CT and conventional imaging studies were the liver (n=5), bone or bone marrow (n=4), adrenal gland (n=5) and distal lymph nodes (n=4). Four patients changed from ED to LD, and the major incongruent sites were the adrenal gland and liver. The management of patients who altered clinical stages was based on the new stage status, i.e., CCRT for LD and chemotherapy only for ED. (Table 3). After the ^{18}F-FDG-PET/CT study, the overall survival of patients remaining as LD and ED was 16.2±14.9 months and 9.8±4.5 months, respectively. For patients changing stage from ED to LD and from LD to ED, overall survival was 14.2±11.6 months and 8.5±4.9 months, respectively. There was no overall survival difference between the LD/LD and ED/LD groups or between the LD/ED and ED/ED groups. However, a significant difference in overall survival was noted between the LD/LD and LD/ED groups (p=0.001). There was no statistically significant difference between ED/ED and ED/LD (p=0.306) (Table 4).

Survival of LD patients with or without an ^{18}F-FDG-PET/CT study

Median survival for the ^{18}F-FDG-PET/CT and conventional imaging groups was 15.9±14.2 months and 9.5±6.0 months, respectively (Table 1). Kaplan-Meier curves of the cumulative survival probabilities (Figure 1A) revealed that those in the ^{18}F-FDG-PET/CT group had a higher survival probability than those in the conventional imaging group, with an HR of 2.672 (p=0.0247, log-rank test). Cox's univariate analysis showed ECOG performance status 2 (p=0.039), BMI (p=0.027), cycles of chemotherapy with an EP regimen (p=0.027), no ^{18}F-FDG-PET/CT study (p=0.029) and positive pleural effusion (p=0.003) resulted in worse survival (Table 5). In Cox's multivariate analysis, cycles of chemotherapy with an EP regimen (p=0.016, HR=0.705) influenced survival (Table 5).

Survival of ED patients with or without an ^{18}F-FDG-PET/CT study

Median survival for the ^{18}F-FDG-PET/CT and conventional image groups was 9.3±4.6 and 10.1±8.2 months, respectively (Table 1). Kaplan-Meier curves of the cumulative survival probabilities (Figure 1B) revealed no difference between those in the ^{18}F-FDG-PET/CT and conventional imaging groups, with an HR of

Table 3. Patients who altered their clinical stages after ^{18}F-FDG-PET/CT study

Subject no.	Pre-PET stage	PET stage	Incongruence	Pre-PET planned management	Post-PET management	Overall survival (days)	Evaluation of discordance
1	LD	ED	1.Peritoneum at anterior middle upper abdomen 2.Hepatic hilar region	CCRT	chemotherapy	358	Progression of liver hilar lesion noted on CT 3 and 7 months later
2	LD	ED	Liver	CCRT	chemotherapy	215	Progression of liver lesion noted on CT 5 months later
3	LD	ED	Contralateral neck Lymph nodes	CCRT	chemotherapy	283	Confirmed by core needle aspiration
4	LD	ED	1.Pleural nodule closed to aorta arch 2.Neck lymph node bilateral	CCRT	chemotherapy	141	Progression of neck lymph node and pleural thickening noted on CT 1 month later
5	LD	ED	1.Liver 2.Multiple bones	CCRT	chemotherapy	169	Progression of liver and lumbar spine lesion noted on CT 4 months later
6	LD	ED	1.Liver 2.Bone marrow over upper thoracic spine and sternum	CCRT	chemotherapy	279	Progression of liver lesion noted on CT 3 months later
7	LD	ED	1.Bilateral supraclavicular lymph nodes 2.Right axillary lymph nodes 3.Cervical spine and thoracic spines	CCRT	chemotherapy	153	Progression of spine lesion noted on CT 3 months later
8	LD	ED	Left adrenal gland	CCRT	chemotherapy	174	Progression of left adrenal gland noted on CT 4 months later
9	LD	ED	1.Right axillary lymph node 2.right femoral bone	CCRT	chemotherapy	166	Progression of right femoral bone lesion on CT later
10	LD	ED	Left adrenal gland	CCRT	chemotherapy	620	Progression of left adrenal gland noted on CT 3 months later
45	ED	LD	Left adrenal gland	chemotherapy	CCRT	47	No evaluation, due to sudden massive hemoptysis and sudden death
46	ED	LD	Left adrenal gland	chemotherapy	CCRT	643	No progression on PET/CT at 6 months and on CT 1 year later
47	ED	LD	Liver	chemotherapy	CCRT	787	Stationary size noted on CT 6 months later
48	ED	LD	Bilateral adrenal glands	chemotherapy	CCRT	228	Stationary size noted on CT 6 months later

Table 4. Alteration of Stages and Overall Survival after Introduction of ^{18}F-FDG PET/CT Study

Group	Pre-PET stage	Post-PET stage	No. of patients	Overall survival (months) median±SD (range in days)	HR, *p* value
LD/LD	LD	LD	20	16.2±14.9 (35-1831)*	5.467
LD/ED	LD	ED	10	8.5±4.9 (141-620)+	0.001
ED/ED	ED	ED	14	9.8±4.5 (120-552)+	2.280
ED/LD	ED	LD	4	14.2±11.6 (47-787)*	0.306

* No difference between LD/LD and ED/LD groups

+ No difference between LD/ED and ED/ED groups

Table 5. Cox's Proportional Hazard Analysis for Overall Survival of LD-SCLC Patients

Variable		HR	95.0% CI		*p* value
			Lower	Upper	
Univariate					
Performance	ECOG 0-1	1			
	ECOG 2	3.294	1.062	10.221	0.039
BMI*		0.862	0.755	0.983	0.027
Cycles of chemotherapy, EP+		0.742	0.570	0.966	0.027
Pleural effusion	Without	1			
	With	3.904	1.610	9.467	0.003
PET	With	1			
	Without	2.422	1.095	5.358	0.029
Multivariate					
PET	With	1			
	Without	5.098	1.680	15.465	0.074
Cycles of chemotherapy, EP#		0.705	0.531	0.936	0.016

* Increase in HR for an increase in BMI, 1 kg/m^2

+ Increase in HR for an increase in the cycles of chemotherapy

0.968 (p=0.9080, log-rank test). Cox's univariate analysis showed comorbidity ≥3 (p=0.048), duration of smoking (p=0.041), ECOG performance status 2 (p=0.019), and cycles of chemotherapy with an EP regimen (p<0.001) resulted in worse survival (Table 6). In Cox's multivariate analysis, only cycles of chemotherapy with an EP regimen (HR=0.767, p=0.001) influenced survival (Table 6).

Detection of bone metastasis by bone scan imaging and ^{18}F-FDG-PET/CT studies

In the ^{18}F-FDG-PET/CT group, 5 incongruent bone metastatic sites were found in 22 patients who also received a bone scan imaging study. Four of the 5 revealed negative findings on bone scan but were found to have significant bone metastasis on PET/CT. Bone marrow metastasis was detected in 1 patient. The disease stage of 3 of the patients was changed from

(A) Overall survival of limited stage SCLC patients.

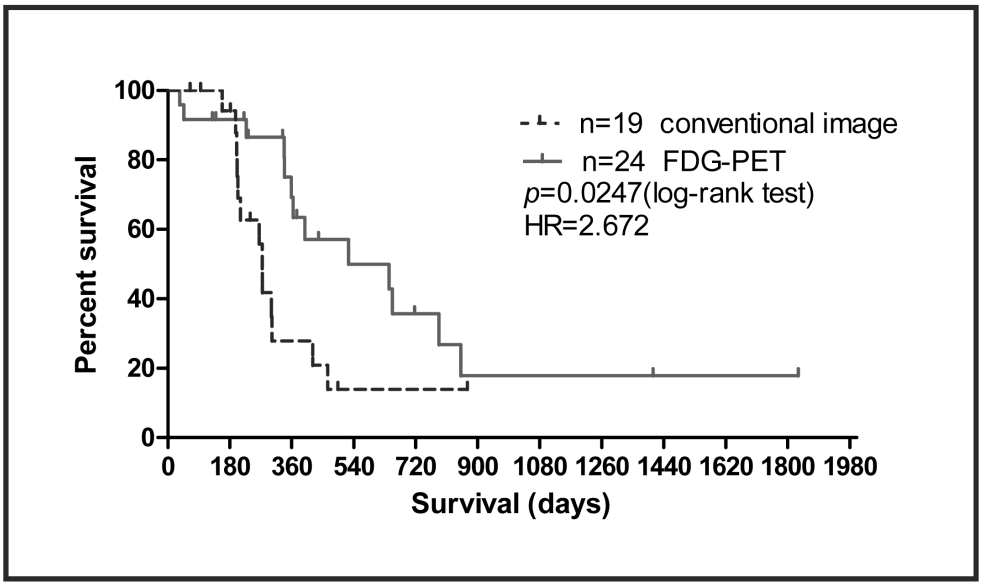

(B) Overall survival of extensive stage SCLC patients.

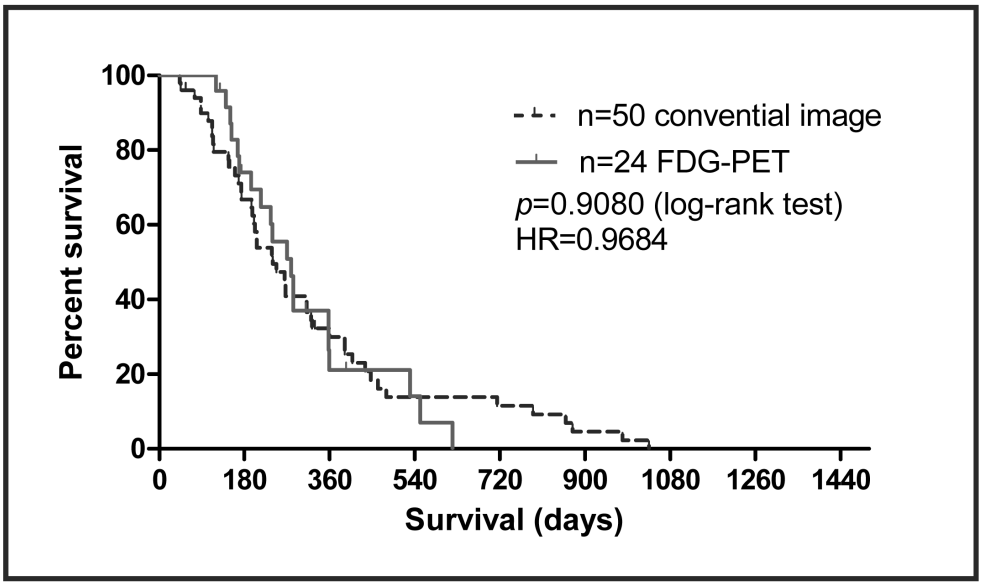

Fig. 1. (A) Overall survival of limited stage SCLC patients. (B) Overall survival of extensive stage SCLC patients.

LD to ED. One patient had consistent lumbar metastasis and the other had inconsistent bone metastasis between studies (Table 7).

Discussion

In the present study, after whole body ^{18}F-FDG-PET/CT examination of 48 SCLC patients, 10 of 24 LD patients were up-staged to

Table 6. Cox's Proportional Hazard Analysis for Overall Survival of ED-SCLC Patients

Variable		HR	95.0% CI		*p* value
			Lower	Upper	
Univariate					
Performance	ECOG 0-1	1			
	ECOG 2	3.294	1.210	8.436	0.019
Comorbidity	<3	1			
	≥3	2.283	1.007	5.177	0.048
Duration of smoking		1.016	1.001	1.032	0.041
Cycles of chemotherapy, EP*		0.750	0.644	0.874	<0.001
Multivariate					
Performance	ECOG 0-1	1			
	ECOG 2	1.472	0.484	4.474	0.495
Comorbidity	<3	1			
	≥3	1.770	0.764	4.098	0.183
Duration of smoking		1.015	1.000	1.031	0.054
Cycles of chemotherapy, EP		0.767	0.653	0.902	0.001

*Increase of HR for an increase in the cycles of chemotherapy with EP

Table 7. Detection of bone metastasis by bone scans versus 18F-FDG-PET/CT imaging study

Subject no.	Bone scan findings	PET findings	Influence of PET
6	Negative	Bone marrow metastasis at upper T spine and sternum	Changed stage and therapy (LD/ED)
7	Negative	C3 and thoracic spine	Changed stage and therapy (LD/ED)
9	Negative	Right femoral bone	Changed stage and therapy (LD/ED)
11	Left scapular, right 10^{th} rib	Right 9^{th} rib, sternum	No change in stage (ED/ED)
12	L5 spine lesion	L5 spine lesion	No change in stage (ED/ED)
24	Negative	Multiple bones	No change in stage (ED/ED)

ED, and 4 of 24 ED patients were down-staged to LD. The survival of patients with LD-SCLC evaluated by PET/CT was better than that evaluated by conventional imaging studies. Cox's multivariate analysis showed that cycles of chemotherapy for both LD and ED was an associated factor that influenced survival. The factor with the least HR of influencing the survival of LD-SCLC patients was accurate staging by PET/CT followed by adequate treatment. Our data supported the efficacy of whole body ^{18}F-FDG-PET/CT to detect distant metastasis and screen out under-staged LD patients and over-staged ED patients, compared with conventional imaging methods. Under-staged LD patients may receive unnecessary management such as

thoracic radiation therapy; in contrast, over-diagnosed ED patients may have inadequate radiation therapy for tumor control. All these may influence the disease outcome and survival of the patients.

No discrepant results in the evaluation of the primary tumor were found between ^{18}F-FDG-PET/CT and conventional imaging in the present study. However, compared with conventional images, ^{18}F-FDG-PET could detect more metastasis, except to the brain, suggesting it is a useful and practical diagnostic tool for accurate cancer staging. The most common metastatic sites of SCLC included bone, adrenal, liver and brain (detected by contrast CT or MRI). Three patients in our study had discordant findings between bone scan and whole body ^{18}F-FDG-PET/CT studies, resulting in alterations of clinical stages and planned management. The whole body ^{18}F-FDG-PET/CT also detected bone marrow metastasis in 1 patient with negative bone scan findings. Studies have shown that bone scan was insensitive to detecting bone marrow metastasis [18-19]. A higher sensitivity and accuracy of ^{18}F-FDG-PET/CT for bone metastasis in patients with SCLC [20-21] and NSCLC, compared with bone scan, have also been reported [19,22]. If the bone metastasis is confined to the bone marrow, ^{18}F-FDG-PET/CT can detect early-stage changes before bone remodeling, which can be detected on bone scan [19]. Five patients had discordant adrenal glands findings between studies and their clinical management was changed based on the PET/CT results. Integrated ^{18}F-FDG-PET/CT had a reported sensitivity of 97%, a specificity of 94%, and an accuracy of 95% for differentiating benign adrenal lesions from metastasis of lung cancer [23].

Small cell lung carcinoma often presents with mediastinal masses or lymph node conglomerates that mimic the presentation of some granulation diseases such as tuberculosis (TB), and they cannot be clearly distinguished. In our study, 5 patients received ^{18}F-FDG-PET/CT and had a history of *Mycobacterium tuberculosis* infection before the diagnosis of SCLC. Taiwan is a TB-endemic area, and ^{18}F-FDG-PET findings of mediastinal lymphadenopathy may be confused with TB or other granulation diseases. The real prevalence of pulmonary TB in our study may be higher than that reflected in the recorded data. Pathological diagnosis of mediastinal lymphadenopathy is important to distinguish TB from malignancy. Compared with endobronchial ultrasound-guided transbronchial aspiration (EBUS-TBNA) for lung cancer patients, the use of ^{18}F-FDG-PET for malignant diagnoses revealed low specificity (18.9%), a low positive predictive value (44%) and lower accuracy (47.4%) [24]. However, only 2 (4.8%) of the 43 lung cancer patients in the study had SCLC [24], and the accuracy of ^{18}F-FDG-PET for lymph node (N) staging of SCLC in a TB-endemic area may be questionable. Therefore, if the N stage was pivotal for the planning of therapy, pathologic survey of lymph nodes would be critically important.

The brain is a common metastatic site of SCLC, but ^{18}F-FDG-PET could identify only 61% of brain metastases [25]. Small size brain lesions were difficult to detect by ^{18}F-FDG-PET study [25], and different histological types of cerebral metastases may present with different FDG accumulations [26]. Only 26.7% of metastatic brain lesions in SCLC were revealed as hypermetabolic, which is significantly lower than the 80% in NSCLC [26]. Hence, brain metastases in our SCLC patients were detected mainly by brain CT or MRI, not by ^{18}F-FDG-

PET/CT study.

Smoking results in direct DNA damage, followed by p53 mutation in lung cancers [27]. Squamous cell carcinoma and SCLC have been reported to be strongly associated with cigarette smoking [28]. A smoking history has been identified as a significant poor prognostic factor in ED-SCLC [28], and female smokers with SCLC were also reported to have a higher mortality risk than males [28]. In our study, a higher proportion of males (94.9%) than females (4.3%) had a smoking history, which differed from previously reported data from Taiwan [4]. Cox's analysis showed that female patients did not have a statistically higher risk than males. This may have resulted from the lower proportion of female patients and smoking population in general in our SCLC study. Although the pack-years of smoking between the ^{18}F-FDG-PET/CT and conventional staging groups were not statistically different, the duration of smoking in the LD-SCLC subgroup was significantly longer in the PET/CT group. However, Cox's multivariate analysis of smoking-related factors including duration, pack-years and smoking cessation revealed no influence on overall survival. Accurate staging by PET/CT remained the most important contributing factor affecting LD-SCLC patient survival.

In our study, 111 of the 117 patients had received standard therapy, i.e., chemotherapy for ED patients and CCRT for LD patients. Six LD patients received chemotherapy only. The median survival of LD and ED patients in the ^{18}F-FDG-PET/CT group in our study was 15.9 and 9.3 months, respectively, which was better than previously reported data from Taiwan [4]. A cohort study in Taiwan between January 2004 and December 2006 revealed that LD (28%) and ED (72%) SCLC patients had overall survival of 10.3 and 5.6 months, respectively [4]. The LD patients receiving CCRT had better survival, and the ED patients undergoing chemotherapy had improved overall survival [4]. ^{18}F-FDG-PET/CT can provide more accurate staging followed by appropriate and adequate management, and our data supported the role of CCRT in improving the survival of LD-SCLC patients staged by ^{18}F-FDG-PET/CT study. As for ED-SCLC patients, it was found that most could be accurately staged by conventional imaging methods (contrast CT and bone scan), but there were still 4 subjects (22%) among the 18 SCLC patients who were staged initially as ED by conventional methods, but changed to LD after ^{18}F-FDG-PET/CT study. All these data support the major impact of PET/CT on the accurate staging of SCLC.

Thoracentesis was successfully performed 28 times among 34 patients due to pleural effusion discovered by imaging studies. Only 10 patients (8.54% of total) had malignant pleural effusion. All of the confirmed pleural effusions were located on the same side of the main tumor, and the malignant pleural effusion results did not change the stage and management. One study including 116 SCLC patients confirmed by cytology showed a low proportion (n=12, 10.3%) of malignant pleural effusion [29]. It was reported that for LD-SCLC patients with ipsilateral pleural effusion, completed chemotherapy may provide better long-term survival [30].

Although our study is a retrospective analysis of prospectively recorded data, some of the clinical information and biochemical data was not collected. Therefore, some known risk factors and predictive factors that may influence survival could not be evaluated comprehensively. The number of patients enrolled for

analysis was also small, and may represent only a part of the SCLC patient population. In addition, we selected only those patients with an ECOG performance status 0-2 for study. The application of PET/CT for patients with a poor performance status (ECOG >2) and the impact on management decision-making as well as on survival and outcome were not evaluated. The distant metastases detected by ^{18}F-FDG-PET and the discordant sites between studies were not confirmed by pathologic study, usually due to the difficulty in obtaining specimens.

In conclusion, for limited-stage SCLC patients, the application of ^{18}F-FDG-PET has a positive impact on accurate staging, appropriate management and disease outcome. Further study is needed to evaluate the efficacy of ^{18}F-FDG-PET/CT in extensive-stage SCLC. In a TB-endemic area, the development of tracers other than ^{18}F-FDG and specific to the biological characteristics of SCLC is also warranted.

Acknowledgements

The authors would like to thank Ms. Ya-Wen Chiu of the Department of Nursing and the Cancer Registry Center of Chang-Gung Memorial Hospital for their assistance with the recording and retrieval of data of the lung cancer patients. This work was supported in part by the National Science Council of Taiwan (NSC 100-2314-B-182A-052 and NSC 101-2314-B-182A-091-MY2) and Chang-Gung Memorial Hospital (CMRPG-3A0371, 3B0101, and 3B0102).

References

1. Govindan R, Page N, Morgensztern D, *et al*. Changing epidemiology of small-cell lung cancer in the United States over the last 30 years: analysis of the surveillance, epidemiologic, and end results database. J Clin Oncol 2006; 24: 4539-44.
2. Chen KY, Chang CH, Yu CJ, *et al*. Distribution according to histologic type and outcome by gender and age group in Taiwanese patients with lung carcinoma. Cancer 2005; 103: 2566-74.
3. Zelen M. Keynote address on biostatistics and data retrieval. Cancer Chemother Rep 3 1973; 4: 31-42.
4. Kuo YH, Lin ZZ, Yang YY, *et al*. Survival of patients with small cell lung carcinoma in Taiwan. Oncology 2012; 82: 19-24.
5. Gaspar LE, McNamara EJ, Gay EG, *et al*. Small-cell lung cancer: prognostic factors and changing treatment over 15 years. Clin Lung Cancer 2012; 13: 115-22.
6. Li AF, Hsu HS, Hsu CY, *et al*. A 20-year retrospective study of small-cell carcinomas in Taiwan. J Surg Oncol 2010; 102: 497-502.
7. Sundstrom S. Cisplatin and etoposide regimen is superior to cyclophosphamide, epirubicin, and vincristine regimen in small-cell lung cancer: results rrom a randomized phase III trial with 5 years' follow-up. J Clin Oncol 2002; 20: 4665-72.
8. Chute JP, Chen T, Feigal E, *et al*. Twenty years of phase III trials for patients with extensive-stage small-cell lung cancer: perceptible progress. J Clin Oncol 1999; 17: 1794-801.
9. Ung YC, Maziak DE, Vanderveen JA, *et al*. ^{18}Fluorodeoxyglucose positron emission tomography in the diagnosis and staging of lung cancer: a systematic review. J Natl Cancer Inst 2007; 99: 1753-67.
10. Ruben JD, Ball DL. The efficacy of PET staging for small-cell lung cancer: a systematic review and cost analysis in the Australian setting. J Thorac Oncol 2012; 7: 1015-20.
11. Bradley JD, Dehdashti F, Mintun MA, *et al*. Positron emission tomography in limited-stage small-cell lung cancer: a prospective study. J Clin Oncol 2004; 22: 3248-54.
12. Vinjamuri M, Craig M, Campbell-Fontaine A, *et al*. Can positron emission tomography be used as a staging tool for small-cell lung cancer? Clin Lung Cancer 2008; 9: 30-4.
13. Azad A, Chionh F, Scott AM, *et al*. High impact of ^{18}F-FDG-PET on management and prognostic stratification

of newly diagnosed small cell lung cancer. Mol Imaging Biol 2010; 12: 443-51.

14. Fischer BM, Mortensen J, Langer SW, *et al*. A prospective study of PET/CT in initial staging of small-cell lung cancer: comparison with CT, bone scintigraphy and bone marrow analysis. Ann Oncol 2007; 18: 338-45.
15. Kamel EM, Zwahlen D, Wyss MT, *et al*. Whole-body (18) F-FDG PET improves the management of patients with small cell lung cancer. J Nucl Med 2003; 44: 1911-7.
16. Schumacher T, Brink I, Mix M, *et al*. FDG-PET imaging for the staging and follow-up of small cell lung cancer. Eur J Nucl Med and Mol Imaging 2001; 28: 483-8.
17. Pandit N, Gonen M, Krug L, *et al*. Prognostic value of [18F]FDG-PET imaging in small cell lung cancer. Eur J Nucl Med Mol Imaging 2003; 30: 78-84.
18. Levitan N, Byren RE, Bromer RH, *et al*. The value of the bone scan and bone marrow biopsy in staging small cell lung cancer. Cancer 1985; 56: 652-4.
19. Ak I, Sivrikoz MC, Entok E, *et al*. Discordant findings in patients with non-small-cell lung cancer: absolutely normal bone scans versus disseminated bone metastases on positron-emission tomography/computed tomography. Eur J Cardiothorac Surg 2010; 37: 792-6.
20. Lee JW, Lee SM, Lee HS, *et al*. Comparison of diagnostic ability between (99m)Tc-MDP bone scan and (18)F-FDG PET/CT for bone metastasis in patients with small cell lung cancer. Ann Nucl Med 2012; 26: 627-33.
21. Kut V, Spies W, Spies S, *et al*. Staging and monitoring of small cell lung cancer using [18F]fluoro-2-deoxy-D-glucose-positron emission tomography (FDG-PET). Am J Clin Oncol 2007; 30: 45-50.
22. Hsia TC, Shen YY, Yen RF, *et al*. Comparing whole body ^{18}F-2-deoxyglucose positron emission tomography and technetium-99m methylene diophosphate bone scan to detect bone metastases in patients with non-small cell lung cancer. Neoplasma 2002; 49: 267-71.
23. Lu Y, Xie D, Huang W, *et al*. ^{18}F-FDG PET/CT in the evaluation of adrenal masses in lung cancer patients. Neoplasma 2010; 57: 129-34.
24. Kuo CH, Chen HC, Chung FT, *et al*. Diagnostic value of EBUS-TBNA for lung cancer with non-enlarged lymph nodes: a study in a tuberculosis-endemic country. PLoS One 2011; 6: e16877.
25. Rohren EM, Provenzale JM, Barboriak DP, *et al*. Screening for cerebral metastases with FDG PET in patients undergoing whole-body staging of non-central nervous system malignancy. Radiology 2003; 226: 181-7.
26. Lee HY, Chung JK, Jeong JM, *et al*. Comparison of FDG-PET findings of brain metastasis from non-small-cell lung cancer and small-cell lung cancer. Ann Nucl Med 2008; 22: 281-6.
27. Hainaut P, Pfeifer GP. Patterns of p53 G-->T transversions in lung cancers reflect the primary mutagenic signature of DNA-damage by tobacco smoke. Carcinogenesis 2001; 22: 367-74.
28. Khuder SA. Effect of cigarette smoking on major histological types of lung cancer: a meta-analysis. Lung Cancer 2001; 31: 139-48.
29. Domagala-Kulawik J, Gornicka B, Krenke R, *et al*. The value of cytological diagnosis of small cell lung carcinoma. Pneumonol Alergol Pol 2010; 78: 203-10.
30. Niho S, Kubota K, Yoh K, *et al*. Clinical outcome of chemoradiation therapy in patients with limited-disease small cell lung cancer with ipsilateral pleural effusion. J Thorac Oncol 2008; 3: 723-7.

全身正子攝影對於肺小細胞癌診斷分期與存活的影響

李適鴻　高國晉　何恭之*　徐稟智　陳濘宏　楊政達　劉劍英

背景：肺小細胞癌具有快速生長及極易遠端轉移之特性，臨床將其分為 limited disease (LD) 及 extensive disease (ED)。治療差別在於 LD 需要同時放射線治療加化學治療，而 ED 單純化學治療。平均存活時間 LD 是 10~14 月，ED 是 5.6~7 月。因此診斷分期的正確與否影響存活。在肺非小細胞癌診斷分期，正子攝影準確性高於傳統影像，對於遠端轉移更有其優異之處。近年來在肺小細胞癌診斷，正子攝影已有越來越多的研究證實對遠端轉移更能有效診斷。希望透過本研究以了解正子攝影對於肺小細胞癌分期與存活有何影響。

方法：找出自 2007 年 1 月至 2012 年 7 月的新診斷肺小細胞癌病患並符合以下條件者共 117 名：年紀大於等於 18 歲，病理診斷未治療肺小細胞癌，Eastern Cooperative Oncology Group performance status (ECOG) 小於等於 2 分，並且完成至少 2 次標準化學治療。依接受正子攝影與否分為二組，再依最後診斷分期為 LD 及 ED。並記錄病患流行病學資料、身體狀況、生化血液檢查、伴隨疾病（糖尿病、高血壓、慢性阻塞性肺病、氣喘、癌症、心血管疾病、腦血管疾病、肺結核）、影像學檢查（胸部 X 光、胸腹電腦斷層、腦部電腦斷層或核磁造影、骨頭攝影、正子掃描、胸部超音波）、病理學（切片病理學及細胞學檢查、肋膜積液細胞學檢查）、放射線治療、化學治療。Kaplan-Meier curve 及 log-rank test 來分析不同組別間存活差異，Cox's proportional hazards ratios 做單變項及多變項分析。

結果：經正子攝影檢查後，10 名病患由 LD 改變為 ED，而 4 名由 ED 改變為 LD。經正子攝影分期為 LD 病患比起傳統診斷工具診斷為 LD 病患有較長的存活（15.9±14.2 月 VS 9.5±6.0 月；HR: 2.672；log-rank test p=0.0247）但是對於 ED 病患，二者之間並無顯著差異（9.3±4.6 月 VS 10.1±8.2 月；HR: 0.968; log-rank test p=0.9080）。

結論：正子攝影對於 LD 肺小細胞癌病患分期與預後較具有影響，但對於 ED 肺小細胞癌影響不顯著。*(胸腔醫學 **2014; 29: 127-143**)*

關鍵詞：肺小細胞癌，正子攝影，電腦斷層，骨頭掃瞄，整體存活

長庚大學暨林口長庚紀念醫院　胸腔內科，* 核子醫學科
索取抽印本請聯絡：劉劍英醫師，林口長庚紀念醫院　胸腔內科，333 桃園縣龜山鄉復興街 5 號

Predicators of Pulmonary Tuberculosis in Patients with Sputum Smear-Negative Results in Taiwan

Wei-Li Lien, Shu-Ling Chen*, Hui-Min Hsu*, Chun-Hui Yu*, Mei-Fang Chen**

Introduction: Early identification of persons who have pulmonary tuberculosis (PTB) is necessary to provide early therapy and overall control. However, 25-60% of patients with culture-positive PTB may have negative smears, which delay the diagnosis. The aim of this study was to identify the predictors of PTB in patients that were sputum smear-negative.

Methods: This study was conducted at Kaohsiung Municipal United Hospital in southern Taiwan using a case-control design. In a retrospective review of hospital records, this study identified 516 suspected PTB patients who had 3 initial negative sputum smear samples from January 1, 2006 to December 30, 2009. We analyzed the factors, including demographic data, clinical symptoms, history of chronic diseases or taking medications, and radiographic findings to predict whether the patient had PTB or not.

Results: Multiple logistic analysis showed that significant predictors of PTB were cough (AOR=1.88, p=.022), hemoptysis (AOR=3.67, p=.001), diabetes (AOR=4.30, p<.001) and typical CXR findings (AOR=17.97, p<.001; AOR=0.38, p=.003).

Conclusion: This study revealed likely reliable predictors of smear-negative PTB. These results could provide a reference for physicians to provide an earlier and more precise diagnosis and treatment of PTB. ***(Thorac Med 2014; 29: 144-151)***

Key words: pulmonary tuberculosis, sputum smear, diabetes, cough, hemoptysis, CXR

Introduction

Pulmonary tuberculosis (PTB) is 1 of the most important health problems and infectious diseases in the world. Early identification of persons who have PTB is necessary to provide early therapy and overall control. However, 25-60% of patients with culture-positive PTB may have negative smears [1]. Patients with smear-negative PTB are responsible for about 13% of TB transmission [2]. Providing a prompt diagnosis of smear-negative PTB is a difficult task.

The majority of initial diagnoses of smear-negative PTB is usually based on clinical and chest radiographic (CXR) findings and individual judgment. However, the misdiagnosis rates have been estimated to be as high as 35% to 52% [3]. Diagnostic sensitivity in patients with smear-negative PTB may improve with nucleic acid amplification (NAA) tests, computed to-

Department of Internal Medicine, Kaohsiung Municipal United Hospital; *Department of Nursing, Kaohsiung Municipal United Hospital; **Department of Nursing, National Tainan Institute of Nursing
Address reprint requests to: Dr. Mei-Fang Chen, Department of Nursing, National Tainan Institute of Nursing, No. 78, Sec. 2, Minzu Rd., Tainan City 700, Taiwan, R.O.C.

mography (CT) of the chest and fiberoptic bronchoscopy with bronchoalveolar lavage (BAL) and lung biopsy. But, which patients are candidates for these examinations? We tried to identify the predictors based on demographic, clinical, and radiographic findings and risk factors, or a combination of these factors from smear-negative PTB to aid physicians in evaluating the likelihood of PTB. The principal aim of this study was to develop a prediction model for patients who need further aggressive interventions and avoid the adverse consequences of delayed treatment or missed treatment in patients with smear-negative PTB.

Methods

Design and sample

This study was conducted at Kaohsiung Municipal United Hospital in southern Taiwan using a case-control design. In a retrospective review of hospital records, this study identified 516 suspected PTB patients who had 3 initial negative sputum smear samples from January 1, 2006 to December 30, 2009. All patients had a medical chart with an outpatient department (OPD) note, microbiology results, and CXR interpretation by a board-certified radiologist and physician. The researchers carried out a review to obtain complete data on each patient.

In accordance with published experience [4-5], the researchers recorded risk factors for TB infection, including age, sex, and tobacco use. Clinical information recorded included the presence of fever, cough, sputum, body weight loss, hemoptysis, and other comorbidities associated with TB, cancer, diabetes, cerebral vascular accident (CVA) or steroid use, and Radiographic findings (Figure 1). The chart reviewer was blinded to the sputum-culture status of the patient. We categorized the CXR findings into 3 groups - typical, atypical and normal CXR presentations. Culture results and the initial smear interpretation of each sputum sample were verified. The study was performed with the approval of the hospital ethics committee.

Data analysis

Data were analyzed using SPSS/PC software Version 13.0. Descriptive statistics were used to describe the patients overall. For univariate analysis, a chi-square test was performed to investigate relationships between characteristics, variables and PTB. All p-values were 2-tailed and the a priori significance level was set as $p<.05$. All significant characteristic variables were entered into a multiple logistic regression model. The reference category was “no PTB”. All characteristics from the multiple logistic regression analysis with a p-value <.05 were used to construct the logistic regression model.

Results

Demographic, clinical symptoms, history of chronic diseases or taking medications and radiographic findings

Of the 516 patients, 143 (27.61%) had PTB, and 373 (72.29%) did not. The clinical symptoms of the patients in the PTB and no-PTB groups differed significantly in terms of fever ($p<.001$), cough ($p<.001$), hemoptysis ($p=.034$), cancer ($p=.003$), diabetes ($p<.001$), CVA ($p<.001$) and CXR findings ($p<.001$) (Table 1). Compared with patients in the no-PTB group, patients in the PTB group were more likely to have fever, cough, and hemoptysis, an underlying disease like cancer, diabetes, and CVA, and typical CXR findings.

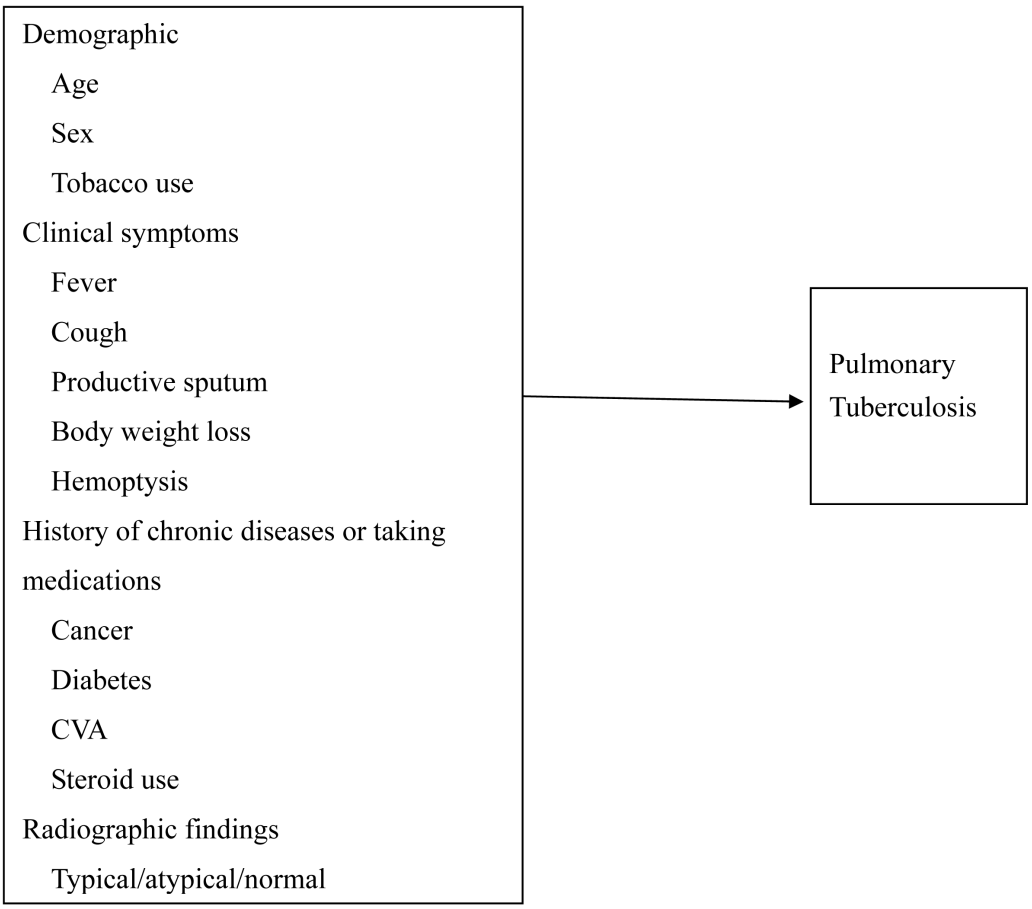

Fig. 1. Identifying Pulmonary Tuberculosis in Patients in Taiwan with Sputum Smear-Negative Results

Odds ratios for culture-positive PTB by patient demographics, clinical symptoms, and CXR

Multiple logistic analysis indicated that significant predictors of PTB were cough (AOR= 1.88, p=.022), hemoptysis (AOR=3.67, p=.001), diabetes (AOR=4.30, p<.001) and typical CXR findings (AOR=17.97, p<.001; AOR=0.38, p= .003) (Table 2). The best predicator of smear-negative PTB was typical CXR findings (AOR= 17.97, p<.001).

Discussion

In Taiwan, the incidence of TB was about 57/100,000 persons in 2010. Taiwan is a high incidence area for TB, and microscopic examination of sputum smear samples is often the most common diagnostic test for TB. However, patients with smear-negative TB do not receive a diagnosis in a timely manner; in these cases, the disease may develop further, initiation of treatment may be delayed, and further TB transmission may occur [6]. Patients with smear-negative TB include approximately one-quarter as many cases of TB as do patients with smear-positive TB, and are responsible for 10-20% of transmission [7]. Light microscopy can detect mycobacteria at a minimum density of 5000-10000 bacilli per ml of sputum, but only a few organisms in smear-negative PTB are infectious

Table 1. Bivariate analysis of associations of PTB with patient demographics, clinical symptoms, history of chronic diseases or taking medications and radiographic findings (n=516)

		PTB(-) (n=373) Number (%)	PTB(+) (n=143) Number (%)	*p* value
Age	≥65	87 (23.3)	34 (23.8)	.908
	<65	286 (76.7)	109 (76.2)	
Sex	Female	127 (34.0)	49 (34.3)	.521
	Male	246 (66.0)	94 (65.7)	
Tobacco	Yes	72 (19.3)	33 (23.1)	.392
	No	301 (80.7)	110 (76.9)	
Fever	Yes	34 (9.1)	0 (0.0)	<.001*
	No	339 (90.9)	143 (100)	
Cough	Yes	107 (28.7)	65 (45.5)	<.001*
	No	266 (71.3)	78 (54.5)	
Productive cough	Yes	41 (11.1)	13 (9.1)	.318
	No	330 (88.9)	130 (90.9)	
BWL	Yes	25 (6.7)	15 (10.5)	.108
	No	347 (93.3)	128 (89.5)	
Hemoptysis	Yes	28 (7.5)	19 (13.3)	.034*
	No	345 (92.5)	124 (86.7)	
Cancer	Yes	13 (3.5)	15 (10.5)	.003*
	No	360 (96.5)	128 (89.5)	
DM	Yes	201 (54.2)	120 (84.5)	<.001*
	No	170 (45.8)	22 (15.5)	
CVA	Yes	60 (16.1)	44 (30.8)	<.001*
	No	313 (83.9)	99 (69.2)	
Steroid use	Yes	34 (9.1)	18 (12.6)	.156
	No	339 (90.9)	125 (87.4)	
CXR	Typical	14 (3.8)	73 (51.0)	<.001*
findings	Atypical	165 (44.2)	17 (11.9)	
	Normal	194 (52)	53 (37.1)	

Abbreviations: BWL, body weight loss; DM, diabetes; CVA, cerebral vascular accident; CXR, chest x-ray

[8-9]. In spite of this, their overall contribution to disease transmission is considerable.

In this study, we attempted to determine useful predictors in smear-negative PTB patients. We found that cough (adjusted OR 1.88) and hemoptysis (adjusted OR 3.67) were positive predictors of clinical symptoms, and diabetes (adjusted OR 4.3) was the most important underlying disease for the prediction of smear-negative culture-positive PTB. In addition, the typical CXR presentation was the most reliable for predicting smear-negative culture-positive

Table 2. Odds ratios for culture-positive PTB by patient demographics, clinical symptoms, history of chronic diseases or taking medications and radiographic findings (n=516)

Determinants		Adjusted OR	95% CI	*p* value
Age	≥65	1.60	0.34-1.08	.091
	<65	1		
Sex	Female	1.11	0.63-1.93	.726
	Male	1		
Tobacco	Yes	1.19	0.62-2.29	.594
	No	1		
Cough	Yes	1.88	1.09-3.22	.022*
	No	1		
Productive cough	Yes	1.39	0.55-3.46	.486
	No	1		
BWL	Yes	1.06	0.43-2.64	.903
	No	1		
Hemoptysis	Yes	3.67	1.66-8.10	.001*
	No	1		
Fever	Yes	0	0	.998
	No			
Malignancy	Yes	2.30	0.85-6.20	.099
	No	1		
DM	Yes	4.30	2.28-8.10	<.001*
	No	1		
CVA	Yes	1.34	0.72-2.49	.360
	No	1		
Steroid use	Yes	1.23	0.52-2.93	.636
	No	1		
CXR findings	Typical	17.97	8.87-36-41	<.001*
	Atypical	0.38	0.20-0.72	.003*
	Normal	1		

Abbreviations: BWL, body weight loss; DM, diabetes; CVA, cerebral vascular accident; CXR, chest x-ray

PTB (adjusted OR 17.97).

The typical radiographic pattern of PTB is apical or upper lobe infiltrates or cavities. As we found, the best predictor of smear-negative TB is a typical CXR presentation. Atypical CXR findings, such as a lobar consolidation or a diffuse pattern (adjusted OR 0.38, *p*=.003) would most likely be another pulmonary disease process such as pneumonia, pulmonary fibrosis or pulmonary edema, rather than PTB.

Several studies have discussed the use of diagnostic tests to improve diagnostic sensitivity for patients with suspected smear-negative PTB. NAA tests have been arranged for patients

with suspected smear-negative PTB for a long time. However, the amplicor assay does not offer an advantage over the empirical approach [10]. Hence, we do not recommend the use of amplicor assay in the routine diagnosis of smear-negative PTB.

Some studies have advocated the use of fiberoptic bronchoscopy in the diagnosis of PTB [11-12]. However, bronchoscopy is expensive, uncomfortable for the patient, relatively risky and insensitive. Mohan *et al*. compared BAL with empirical treatment and concluded that presumptive treatment is more cost-effective [13].

Cigarette smoking was not associated with smear-negative PTB in this study. This result is compatible with those of most studies that reported a negative correlation [14]. Only 1 study showed that current cigarette smoking was strongly associated with PTB [15]. However, smoking has been reported to be associated with an increased risk of developing TB disease [16], a slow healing process, delayed sputum conversion [17], and a high death rate [18].

Knowing how to make an adequate prediction and correct decision for patients with suspected active, smear-negative PTB whose culture specimens ultimately prove to be positive is very important. A precise prediction and decision may avoid adverse consequences. Withholding treatment for patients with true PTB may lead to infection of others in the community, but overestimating the condition and treatment of patients without PTB may leave them exposed unnecessarily to possible drug toxicity. Thus, a decision to treat may or may not implicate a public health effect [19-21].

The findings in our study can be used by physicians as a simple guide for clinical practice regarding smear-negative PTB. However, a limitation of this study may be that these findings are localized to 1 hospital only. It is unclear whether these results are suitable for the whole country or not. Further studies are necessary to confirm our results in cohorts of patients in different hospitals.

In summary, empirical judgment with regard to smear-negative PTB may be a more practical method than the amplicor assay or bronchoscopy. Our study results may be helpful in providing physicians with more reliable information on making an earlier definitive diagnosis of smear-negative cases to improve clinical treatment and public health outcomes.

Conclusion

In conclusion, this study revealed the likely reliable predictors of smear-negative PTB, which include cough, hemoptysis, diabetes and typical CXR findings. These results could provide a reference for physicians in making an earlier and more precise diagnosis and decision on treatment.

References

1. Garay SM. Pulmonary tuberculosis. In: Rom WN, Garay SM (eds). Tuberculosis. Little Brown, NY, USA, 1996; 373-412.
2. Alma T, Sandra VK, Nico AK, *et al*. Tuberculosis transmission by findings patients with smear-negative pulmonary tuberculosis in a large cohort in The Netherlands. CID 2008; 47: 1135-42.
3. Gordin FM, Slutkin G, Schecter G, *et al*. Presumptive diagnosis in treatment of pulmonary tuberculosis based on radiographic findings. Am Rev Respir Dis 1989; 139: 1090-3.
4. Kanaya AM, Glidden DV, Chambers HF, *et al*. Identifying pulmonary tuberculosis in patients with negative sputum smear results. Chest 2001; 120(2): 349-55.
5. Mello FC, Bastos LG, Soares SL, *et al*. Predicting smear-

negative pulmonary tuberculosis with classification trees and logistic regression: a cross-sectional study. BMC Public Health 2006; 6(43), from http://www.biomedcentral.com/1471-2458/6/43.

6. Siddiqi K, Lambert ML, Walley J, *et al*. Clinical diagnosis of smear negative pulmonary tuberculosis in low-income countries: the current evidence. Lancet Infect Dis 2003; 3: 288-96.
7. Behr MA, Warren SA, Salamon H, *et al*. Transmission of Mycobacterium tuberculosis from patients smear-negative for acid-fast bacilli. Lancet 1999; 353: 444-9.
8. Yeager HJ, Lacy J, Smith LR, *et al*. Quantitative studies of mycobacterial populations in sputum and saliva. Am Rev Respire Dis 1967; 95: 998-1004.
9. Hobby GL, Holman AP, Iseman MD, *et al*. Enumeration of tubercle bacilli in sputum of patients with pulmonary tuberculosis. Antimicrob Agents Chemother 1973; 4: 94-104.
10. Rau NV, Libman MD. Laboratory implementation of the polymerase chain reaction for confirmation of pulmonary tuberculosis. Eur J Chin Microbiol Infect Dis 1999; 18: 35-41.
11. Danek SJ, Bower JS. Diagnosis of pulmonary tuberculosis by flexible fiberoptic bronchoscopy. Am Rev Respir Dis 1979; 119: 677-9.
12. Gracia JDe, Currull V, Vidal R, *et al*. Diagnostic value of bronchoalveolar lavage in suspected pulmonary tuberculosis. Chest 1988; 93: 329-32.
13. Mohan A, Pande JN, Sharma SK, *et al*. Bronchoalveolar lavage in pulmonary tuberculosis: A decision analysis approach. QJM 1995; 88: 269-76.
14. Kanaya AM, Glidden DV, Chambers HF, *et al*. Identifying pulmonary tuberculosis in patients with negative sputum smear results. Chest 2001; 120: 349-55.
15. Range N. Risk factors for smear negative and culture positive results among pulmonary tuberculosis patients in Mwanza, Tanzania: The Open Tropical Med J, 2008; 1: 68-73.
16. Gupta KP, Gupta R. Association between smoking and tuberculosis. Indian J Tuberc 2003; 50: 5-7.
17. Gajalakshmi V, Peto R, Kanaka TS, *et al*. Smoking and mortality from tuberculosis and other disease in India: retrospective study of 43000 adult male deaths and 35000 controls. Lancet 2003; 362: 507-15.
18. Hassmiller KM. The association between smoking and tuberculosis. Salud Public Mex 2006; 48(Suppl 1): S201-16.
19. Scott B, Schmid M, Nettleman MD, *et al*. Early identification and isolation of inpatients at high risk for tuberculosis. Arch Intern Med 1994; 154: 326-30.
20. El-Solh A, Mylotte J, Sherif S, *et al*. Validity of a decision tree for predicting active pulmonary tuberculosis. Am J Respir Crit Care Med 1997; 155: 1711-6.
21. Redd JT, Susser E. Controlling tuberculosis in an urban emergency department: a rapid decision instrument for patient isolation. Am I Public Health 1997; 87: 1543-7.

台灣痰抹片陰性肺結核患者的預測因子

連偉立　陳淑玲 *　許慧敏 *　余春慧 *　陳美芳 **

背景：早期診斷肺結核患者可以提供早期治療與整體控制。然而，有 25-60% 痰培養陽性患者剛開始的痰抹片為陰性而延遲診斷時間。本研究目的為確定在痰抹片陰性患者罹患肺結核之預測因子。

方法：採病例對照法，在南台灣高雄聯合醫院收案。採回朔性研究法，從 2006 年 1 月 1 日至 2009 年 12 月 30 日，收取 516 位初次三套痰抹片為陰性的疑似結核病個案。分析因子包括人口學變項、臨床症狀、慢性疾病或藥物使用與影像學檢查來預測是否為肺結核。

結果：多因素邏輯式回歸分析發現肺結核之預測因子包括咳嗽（AOR=1.88, *p*=.022）咳血（AOR=3.67, *p*=.001），糖尿病（AOR=4.30, *p*<.001）與典型胸部 X 光（AOR=17.97, *p*<.001; AOR=0.38, *p*=.003）。

結論：本文提供痰抹片陰性肺結核患者之預測因子。這結果可供醫師提早診斷與治療肺結核的參考。
*(胸腔醫學 **2014; 29: 144-151**)*

關鍵詞：肺結核，痰抹片，糖尿病，咳血，咳嗽，胸部 X 光

高雄市立聯合醫院　胸腔內科，* 高雄市立聯合醫院　護理科，** 國立台南護理專科學校　護理科
索取抽印本請聯絡：陳美芳醫師，國立台南護理專科學校　護理科，700 台南市中西區民族路二段 78 號

Pulmonary Adenofibroma: A Rare Presentation of a Benign Lung Nodule – A Case Report

Yen-Zu Huang*, Kuo-An Chu*, Ting-Yung Ou*, Kuan-Sheng Wu**,
Ting-Ying Fu***, Ruay-Sheng Lai*,****

Pulmonary adenofibroma is a rare primary benign mesenchymal lung tumor that has been seldom reported in the currently available literature. Unusual lung tumors constitute a broad range of histological types that unsurprisingly have a wide spectrum of imaging appearances and clinical presentations. Herein, we report a 60-year-old male who complained of low-grade fever and general malaise, and was tentatively diagnosed as having acute hepatitis and pleural effusion, accompanied with the incidental finding of pulmonary nodule on chest computed tomography (CT), which was ultimately diagnosed as pulmonary adenofibroma. The initially challenging frozen section reading raised the suspicion of malignancy, but ultimately the diagnosis was revised to benign pulmonary adenofibroma. This case can increase our awareness of this extremely rare benign lesion in the future. ***(Thorac Med 2014; 29: 152-159)***

Key words: adenofibroma, benign pulmonary tumor, frozen section, pulmonary nodule

Introduction

Primary mesenchymal tumors of the lung are rare, with an incidence of less than 1% of all primary lung tumors according to the current literature [1], and often resemble their soft tissue counterparts. Adenofibroma is a mixed biphasic tumor with glandular and fibrous proliferation. Most adenofibromas have been reported in the ovary and breast. Pulmonary adenofibroma is an even rarer type of benign soft-tissue tumor that comprises epithelial and stromal components, both of which are histologically benign, and resembles adenofibroma of the female genital tract. To the best of our knowledge, only a few cases of pulmonary adenofibroma have been formally reported to date [2-3]. Because of the rarity and incidental finding of this tumor with its unusual histologic appearance, we face a diagnostic challenge in distinguishing this pulmonary nodule from malignancy. Herein, we report the case of a middle-aged male who initially presented with dyspnea on exertion as well as cough-related pain in

*Division of Chest Medicine, Department of Internal Medicine, Kaohsiung Veterans General Hospital, Kaohsiung, Taiwan; **Division of Infectious Diseases, Department of Internal Medicine, Kaohsiung Veterans General Hospital, Kaohsiung, Taiwan; ***Department of Pathology and Laboratory Medicine, Kaohsiung Veterans General Hospital, Kaohsiung, Taiwan; ****National Yang-Ming University School of Medicine, Taipei, Taiwan
Address reprint requests to: Dr. Kuo-An Chu, Division of Chest Medicine, Department of Internal Medicine, Kaohsiung Veterans General Hospital, 386 Ta-Chung 1st Road, Kaohsiung 813, Taiwan

the right subcostal region. During a later imaging survey for differential diagnosis during the patient's hospitalization, we incidentally noted the abnormal chest CT finding of a pulmonary nodule that was ultimately pathologically diagnosed as pulmonary adenofibroma. Clinical suspicion in this case increased our awareness of this rare benign lesion.

Case Report

A 60-year-old male presented with the compliant of low-grade fever with general malaise and poor appetite for the past 1 week, associated with cough-related pain in the right subcostal region. The patient had been a social cigarette smoker for less than 5 years as a teenager and had quit smoking decades earlier. He had never experienced such discomfort before this episode, and he sought medical assistance at another hospital due to intractable cough-related chest pain with a persistent low-grade fever. He was referred to our hospital for further evaluation and management with the following initial vital signs: body temperature, 37.6°C; heart rate, 82 beats/min; respiratory rate, 18 breaths/min; and blood pressure, 120/72 mmHg. His illness history showed that he had initially suffered from poor appetite and easy satiety with normal defecation approximately 5 days earlier, followed by a low-grade fever and diarrhea along with dry cough for 2 days and eventual right subcostal region pain. His pain was dull in nature, but included intermittent sharp sensations without obvious radiation that worsened with deep breathing. There was no evidence of hereditary disease in his extended family or in the traceable recent cluster and travel history.

Physical examinations revealed the following: clear breathing sounds in the bilateral lung fields, but a rough, scratchy friction rub with basal crackles in the right lower chest, as well as local tenderness without rebounding pain at the right upper abdominal quadrant. In addition, normal active bowel sounds and a lack of skin discoloration, edematous changes in the lower extremities, and palpable lymph nodes were noted.

Laboratory examinations revealed a white blood cell (WBC) count of 5700/mm^3 with a predominant neutrophil count (87%), and abnormal liver function with glutamate oxaloacetate transaminase (GOT)/glutamic pyruvic transaminase (GPT) of 311/181 U/L, and an international normalized ratio of 1.19. Urine and stool analyses revealed no specific finding.

No prior imaging studies were available for comparison. Chest radiography at presentation showed right costophrenic angle blunting, apical pleural thickening, prominent bilateral hilar vascular shadows with pulmonary vascular redistribution, and bilateral lower lung field reticulonodular infiltration (Figure 1). We performed an echocardiogram as well as chest and abdominal ultrasounds, and then a diagnostic thoracocentesis followed by closed drainage of the patient's pleural effusion. No space-occupying lesion of the liver parenchyma or biliary tract dilatation were found. We observed preserved left ventricular systolic function with an estimated left ventricular ejection fraction of 68% in the absence of cardiac chamber dilatation. Besides, mild pulmonary regurgitation, moderate mitral valve regurgitation and mild tricuspid valve regurgitation with an estimated pulmonary artery systolic pressure of approximately 37 mmHg were mentioned in the echocardiogram report. The pleural fluid was found to be exudative in nature with a predominance of lymphocytes, (lactate dehydrogenase: 488 U/

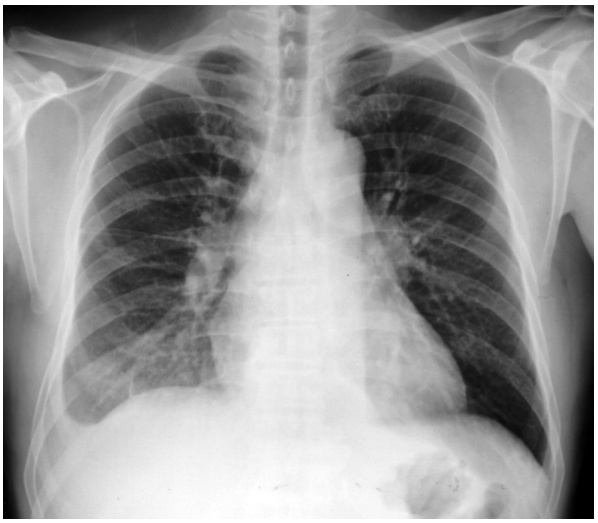

Fig. 1. Chest radiography: right costophrenic angle blunting.

L; protein: 3.2 g/dL; sugar: 98 mg/dL; WBC: 2140/mm^3; RBC: 10000/mm^3; differential neutrophil/lymphocyte/monocyte count ratio: 1/92/7). Hepatitis markers, including hepatitis A IgM antibody, hepatitis B surface antigen, antibody to hepatitis B surface antigen and IgM antibody to hepatitis C virus were screened with negative findings.

Under supportive care, the patient's constitutional symptoms greatly improved with the exception of a mild cough. We then performed sputum analysis and culture with no positive findings. We repeated the laboratory examination, and a series of liver function tests with GOT/GPT revealed a decreasing trend toward normal serum values. The follow-up CXR revealed a sharp costophrenic angle after removing the pigtail drainage. In this situation, our tentative diagnosis became acute hepatitis with reactive right-side pleural effusion, which was suspected to be related to viral infection; the differential diagnosis was acute hepatitis combined with a lymphocyte-predominant exudative pleural effusion of unknown etiology, which was suspected to be related to pulmonary tuberculosis with pleurisy or to malignancy. Chest CT scan revealed a 1-cm nodule with a well-defined and smooth margin at the right upper lobe (Figure 2A) without mediastinal lymph node enlargement, and focal ground glass opacity at the right lower lung field with minimal atelectasis (Figure 2B), likely due to the previous pleural effusion. We could not confidently define this incidental finding of a nodule as a solitary pulmonary nodule (SPN) due to the exis-

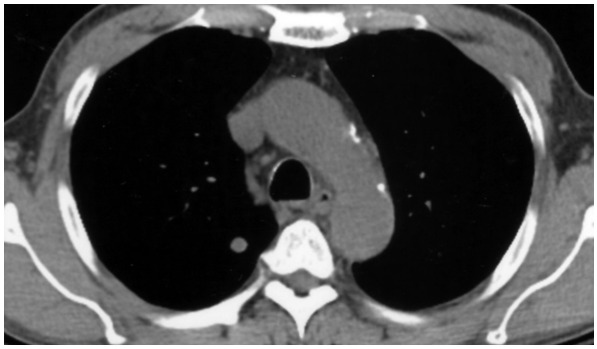

Fig. 2A. Axial view of chest CT scan (mediastinal window): a 1-cm nodule with a well-defined and smooth margin at the right upper lobe

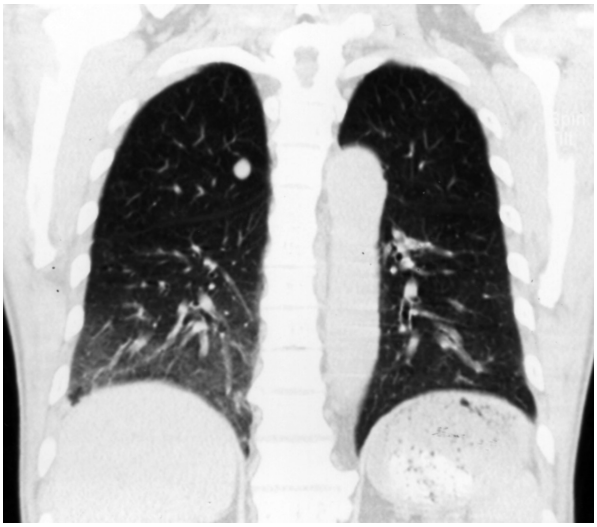

Fig. 2B. Coronal view of chest CT scan (lung window): focal ground glass opacity at the right lower lung field with minimal atelectasis

tence of the not fully explained pleural effusion. We assessed the probability of malignancy, the surgical risk and the patient's preference, and then consulted the chest surgeon for thoracoscopic right upper lobe nodule wedge resection and pleural biopsy.

After discussing the possible etiology of the right upper lobe nodule with the patient, he agreed to go ahead with the diagnostic surgical intervention. The frozen section of the excisional biopsy of the wedge resection was originally reported to comprise a gray-white tissue, measuring 1.1 × 1.0 × 0.3 cm, that was indicative of adenocarcinoma, as it contained clusters of moderately differentiated neoplastic cells in acinar and focal papillary patterns. Later, the final pathological report was revised to indicate a benign adenofibrous lesion, because a further large specimen had shown well-circumscribed features without local tissue invasion. The submitted wedge resection specimen consisted of 1 piece of tissue measuring 5.3 × 2.2 × 1.5 cm in size with a white tumor that measured 1.1 × 0.8 × 0.7 cm, and was 0.7 cm distant from the cut end. Hematoxylin and eosin (H&E) stain of the tumor revealed a well circumscribed but not encapsulated lesion composed of a proliferation of bland-looking epithelial cells and stroma in cleft-like and glandular patterns (Figure 3A). No mitoses, necrosis or cytologic atypia was observed (Figure 3B). The immunohistochemistry (IHC) stain of the lining epithelial cells was positive for thyroid transcription factor-1 (TTF-1) and high molecular weight cytokeratin (HMCK), and focally positive for p63. The IHC stain of the tumor cells was negative for cytokeratin 5/6 (CK 5/6), and the IHC stain of the stroma was positive for desmin and smooth muscle actin (SMA) (Figure 3C), consistent with the presence of smooth muscles (Figure 3D). The lesion met the diagnostic criteria of pulmonary adenofibroma with a smooth muscle component. In addition, the pleura excisional biopsy comprised 5 pieces of gray-white soft tissue, measuring up to 2.1 × 1.2 × 0.2 cm, indicating mesothelial cell hyperplasia, acute and chronic inflammatory cell infiltration and fibrosis. Granuloma was not present. Neither mycobacteria nor fungi could be identified with the acid-fast and PAS stains. The TTF-1 stain result was negative and there was no evidence of malignancy in the examined sections.

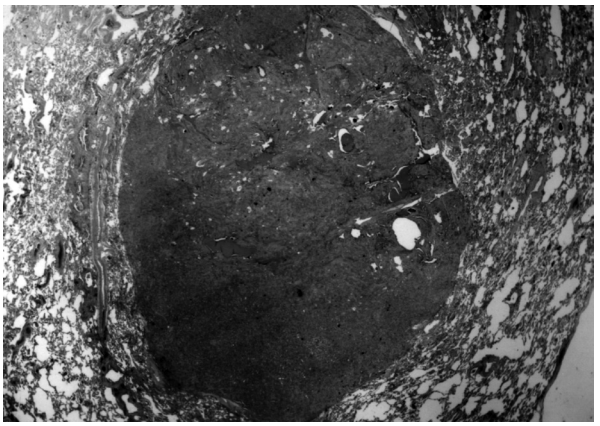

Fig. 3A. H&E stain X20: well-circumscribed papillary structures lined with a layer of simple cuboidal epithelium.

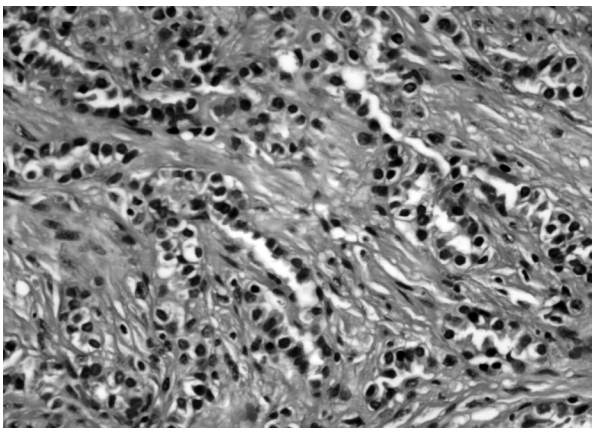

Fig. 3B. H&E stain X400: the epithelium lining the gland-like spaces is bland and devoid of cytologic atypia

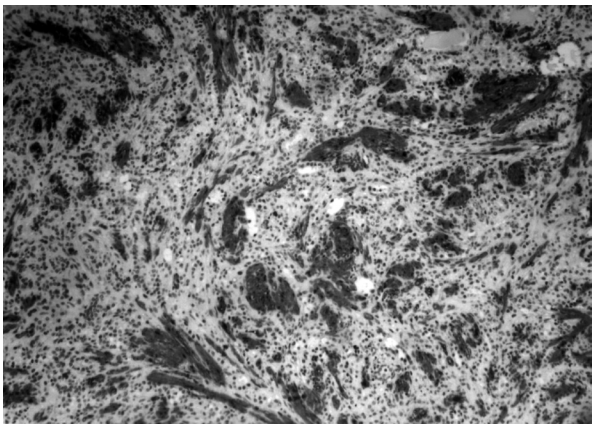

Fig. 3C. SMA IHC stain of X200: the stroma is positive for desmin and SMA, consistent with the presence of smooth muscles.

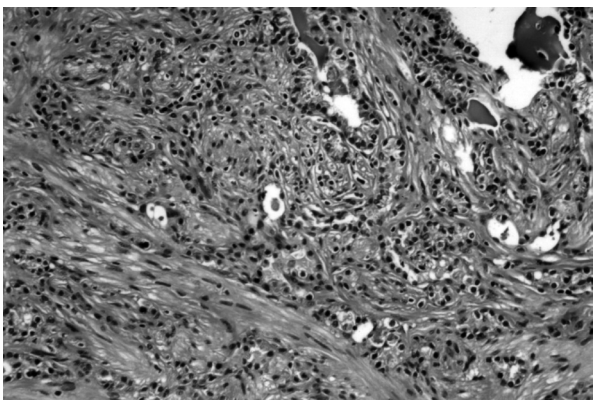

Fig. 3D. H&E stain X200: spindle stromal cells show a fascicular pattern of growth with focal presence of smooth muscle cells.

Discussion

Pulmonary nodules [4-7] are an important problem in our daily practice. Estimates of their frequency range from 0.2% in older studies using chest radiography to approximately 40-60% in lung cancer screening trials using low-dose CT [8-11]. Possible causes of pulmonary nodules include many benign diseases, but the primary concern is bronchogenic carcinoma. Unusual lung tumors constitute a broad range of histological types that unsurprisingly have a spectrum of imaging appearances [12-13].

Pulmonary adenofibroma is a very rare benign tumor that appears on chest radiograph as a SPN, a well-defined soft-tissue nodule that is detected incidentally in middle-aged adults. The most common causes of benign SPN were healed or nonspecific granulomas, which account for 25% of all benign nodules. Another 15% of benign nodules were caused by active granulomatous infections, including tuberculosis, coccidioidomycosis, histoplasmosis, cryptococcosis, and aspergillosis. Hamartomas comprised an additional 15% of benign lesions. Less common miscellaneous causes of benign nodules included nonspecific inflammation and fibrosis, lung abscesses, round pneumonia, round atelectasis, bronchogenic cysts, healed pulmonary infarcts, focal hemorrhages, hemangiomas, and arteriovenous malformations. The border characteristics of a nodule in CT imaging can also be used to help estimate the probability of malignancy. Nodules with irregular, lobulated, or spiculated borders are associated with a progressively higher probability of malignancy than those with a smooth border [14]. Furthermore, nodules with a purely ground-glass or semisolid appearance have a higher probability of malignancy than purely solid lesions [15]. Benign calcification patterns (diffuse, central, laminated, or popcorn patterns) and intranodular fat density are associated with an extremely low probability of malignancy. Stippled and eccentric calcification patterns do not exclude malignancy, and thus further work-ups are required.

Adenofibroma is a mixed biphasic benign tumor with glandular and fibrous proliferation. Most adenofibromas have been reported in the ovary and breast. Even rarer cases of uterine endometrium adenofibroma [16], uterine cervical

adenofibroma [17], paratesticular adenofibroma [18], biliary adenofibroma of the liver, and pulmonary adenofibroma have been formally reported, but to the best of our knowledge, these are extremely rare in the current literature. To make the diagnosis of pulmonary adenofibroma, there should be a histological finding of dominant pseudopapillae covered by bland cuboidal epithelium and bland spindle cell-rich sclerotic stroma, as well as findings of positive cytokeratin and TTF-1 epithelium stains and negative cytokeratin and S-100 stroma stains.

With regard to our patient, the initial report from the frozen section obtained during intraoperative sampling was adenocarcinoma, moderately differentiated; however, the final report was revised after the larger specimen was sampled and the examination was completed. We attempted to determine the possible cause of such an extreme difference, and concluded that careful specimen sampling with an adequate margin from the cut end and delicate high-power field reading with a better resolution are crucial when diagnosing this rare benign tumor.

Pulmonary nodules are frequently first diagnosed by frozen section, immediately followed by lobectomy or other procedures. The frozen section diagnoses of pulmonary nodules can be difficult, since inflammatory and fibrotic lesions can be confused with malignancies, thus creating intraoperative dilemmas for pathologists and thoracic surgeons [19]. The discrepancies between the frozen section and the permanent section were mainly due to the interpretation error, and sampling errors and technical artifacts, and partly due to a lack of interdepartmental communication. The causes of the false positive diagnosis were the interpretation error and the unavoidable freezing artifacts. The sampling error was the main reason for the false negative diagnosis. In a few cases, the diagnosis has been deferred to the permanent section, mainly due to a lack of adequate clinical information and inadequate material. In our case, delicate structures such as ciliated epithelial cells devoid of cytologic atypia, which were not definitively observed in the frozen section due to freezing artifacts, were identified in the permanent section, and thus the final pathological report was revised to a benign adenofibrous lesion.

In summary, advanced imaging modalities combined with clinical information and histopathological findings assisted by IHC staining are still needed for the definite diagnosis. Adequate preoperatively diagnostic imaging-guided or intraoperative sampling with careful readings may facilitate diagnoses and decisions regarding whether to perform major surgery. Finally, pulmonary adenofibroma should be taken into consideration when encountering a lung tumor that comprises bland stromal and epithelial cells in the microscopic examination, and should be carefully distinguished from pulmonary harmartoma, leiomyoma, pulmonary blastoma, intrapulmonary solitary fibrous tumor, and metastases from soft tissue and visceral sarcoma.

References

1. Weissferdt A, Moran CA. Mesenchymal Tumors of the Lungs. Diagnostic Pathology of Pleuropulmonary Neoplasia. Springer London, 2012; 243-96.
2. Cavazza A, Rossi G, De Marco L, *et al*. Solitary fibrous pseudopapillary tumor of the lung: Pulmonary fibroadenoma and adenofibroma revisited. Pathologica 2003; 95: 162-6.
3. Suster S, Moran CA. Pulmonary adenofibroma: report of two cases of an unusual type of hamartomatous lesion of the lung. Histopathology 1993; 23: 547-51.
4. Ost DE, Gould MK. Decision making in patients with pulmonary nodules. Am J Respir Crit Care Med 2012;

185(4): 363-72.

5. Gould MK, Fletcher J, Iannettoni MD, *et al*. Evaluation of patients with pulmonary nodules: when is it lung cancer?: ACCP evidence-based clinical practice guidelines (2nd edition). Chest 2007; 132 (3 Suppl): 108S-130S.
6. Macmahon H, Austin JH, Gamsu G, *et al*. Guidelines for management of small pulmonary nodules detected on CT scans: a statement from the Fleischner Society. Radiology 2005; 237 (2): 395-400.
7. Naidich DP, Bankier AA, MacMahon H, *et al*. Recommendations for the management of subsolid pulmonary nodules detected at CT: a statement from the Fleischner Society. Radiology 2013; 266 (1): 304-17.
8. van Klaveren RJ, Oudkerk M, Prokop M, *et al*. Management of lung nodules detected by volume CT scanning. N Engl J Med 2009; 361: 2221-9.
9. Swensen SJ, Jett JR, Hartman TE, *et al*. CT screening for lung cancer: five-year prospective experience. Radiology 2005; 235: 259-65.
10. McWilliams A, Mayo J, MacDonald S, *et al*. Lung cancer screening: a different paradigm. Am J Respir Crit Care Med 2003; 168: 1167-73.
11. Diederich S, Wormanns D, Semik M, *et al*. Screening for early lung cancer with low-dose spiral CT: prevalence in 817 asymptomatic smokers. Radiology 2002; 222 (3): 773-81.
12. Bhatia K, Ellis S. Unusual lung tumours: an illustrated review of CT features suggestive of this diagnosis. Cancer Imaging 2006; 6: 72-82.
13. Gimenez A, Franquet T, Prats R, *et al*. Unusual primary lung tumors: a radiologic-pathologic overview. Radiographics 2002; 22(3): 601-19.
14. David Ost, Alan M, Steven H, *et al*. The solitary pulmonary nodule. N Engl J Med 2003; 348: 2535-42.
15. Gould MK, Fletcher J, Iannettoni MD, *et al*. Evaluation of patients with pulmonary nodules: when is it lung cancer?: ACCP evidence-based clinical practice guidelines (2nd edition). Chest 2007; 132 (3 Suppl): 94S-107S.
16. Bettaieb I, Mekni A, Bellil K, *et al*. Endometrial adenofibroma: a rare entity. Arch Gynecol Obstet 2007; 275(3): 191-3.
17. Ishiko O, Sumi T, Ueda K, *et al*. Uterine cervical adenofibroma associated with Turner's syndrome in a young woman. Arch Gynecol Obstet 2002; 267(1): 49-50.
18. Janane A, Ghadouane M, Alami M, *et al*. Paratesticular adenofibroma. Scand J Urol Nephrol 2003; 37(2): 179-80.
19. Marchevsky AM, Changsri C, Gupta I, *et al*. Frozen section diagnoses of small pulmonary nodules: accuracy and clinical implications. Ann Thorac Surg 2004; 78: 1755-9.

肺腺纖維瘤：罕見良性肺部結節－病例報導

黃彥儒 * 朱國安 * 歐亭芸 * 吳冠陞 ** 傅婷瑛 *** 賴瑞生 *,****

肺腺纖維瘤是一種非常罕見的良性間葉細胞瘤，在目前的文獻資料庫裡只有極少數的臨床病例報告。不常見的肺部腫瘤由各種不同組織型態的細胞所構成，也會有不同的影像學表徵以及臨床表現。我們報導了一位六十歲男性以輕微發燒及全身倦怠就診，初步理學檢查及配合實驗室和影像學診斷為急性肝炎及右側肋膜積液，肋膜積液抽吸檢查顯示淋巴細胞為主的滲出液；進一步安排胸部電腦斷層檢查發現右上肺一個邊緣清楚的結節。經手術取得檢體冰凍切片初步報告為中度分化的肺腺癌，然而最終病理報告修正為良性腫瘤。藉由此病例報告讓臨床醫師增加對此良性肺腫瘤的了解。*(胸腔醫學 **2014; 29: 152-159**)*

關鍵詞：腺纖維瘤，良性肺腫瘤，冷凍病理切片，肺結節

* 高雄榮民總醫院　胸腔內科，** 感染科，*** 病理檢驗部，**** 國立陽明大學醫學院
索取抽印本請聯絡：朱國安醫師，高雄榮民總醫院　內科部　胸腔內科，高雄市左營區大中一路 386 號

Pulmonary Actinomycosis Presenting as a Lung Mass Crossing the Fissure – A Case Report

Ming-Syong Zeng, Shih-Hsin Hsiao, Chi-Li Chung

Pulmonary actinomycosis, a rare bacterial lung infection, usually presents with nonspecific clinical symptoms and radiological patterns and is prone to being a delayed diagnosis or misdiagnosed as malignancy, tuberculosis, or pneumonia. We report a 59-year-old man who suffered from chronic, repeated hemoptysis. The chest radiograph and CT image revealed a left upper lung mass that extended across the major fissure into the left lower lobe. A CT-guided biopsy of the lung mass was done and revealed acute and chronic inflammation. The hemoptysis symptom and the lung lesion persisted despite short courses of empirical antibiotic treatment. Therefore, surgical resection was performed and the pathology showed a lung abscess with "sulfur granules", a finding pathognomonic of actinomycosis. The patient received amoxicillin/clavulanate for 8 months with complete relief of symptoms and no recurrence of lung infiltrates. This case report reminds us that, in addition to malignancy, tuberculosis, nocardiosis and fungal infection, actinomycosis should be included in the differential diagnosis of a lung lesion crossing the fissure, in order to provide prompt diagnosis and treatment. ***(Thorac Med 2014; 29: 160-165)***

Key words: actinomycosis, crossing the fissure, sulfur granule

Introduction

Actinomycetes, a Gram-positive, filamentous, predominantly anaerobic, prokaryotic bacteria, is conspicuous among normal flora in the oral cavity and gastrointestinal tract and can infect virtually every organ or body site in humans [1]. Actinomycosis in humans has been well known since the 19th century, but is now a rare disease with low mortality [2]. However, patients with either a delayed or missed diagnosis of actinomycosis may have considerable morbidities, signifying the importance of early and accurate diagnosis of this disease [1].

Up to 15% of the infections caused by Actinomycetes generally involves the thorax, and probably results from aspiration of this microorganism from the oropharyngeal cavity or from the gastrointestinal tract [2]. Clinical presentations and radiological findings are both nonspecific and vary widely among individuals [1]. Therefore, pulmonary actinomycosis is

Division of Pulmonary Medicine, Department of Internal Medicine, Taipei Medical University Hospital, Taipei, Taiwan
Address reprint requests to: Dr. Shih-Hsin Hsiao, Division of Pulmonary Medicine, Department of Internal Medicine, Taipei Medical University Hospital, No. 252, Wu-Hsing Street, Taipei 11031, Taiwan

likely to be misdiagnosed as malignancy, tuberculosis, fungal infection or lung abscess, and the average duration of illness before definitive diagnosis is about 6 months [3].

Herein, we report the case of a patient with pulmonary actinomycosis who presented with intermittent hemoptysis for a long period and a mass lesion crossing the lung fissure.

Case Report

A 59-year-old man with a history of diabetes mellitus had intermittent cough with blood-tinged sputum for 1 year and a long-standing left lung infiltrate. In February 2011, he was admitted to our hospital with worsened hemoptysis. He did not have a history of smoking, drinking, animal contact, or foreign travel. Also, his family history was not contributory. On physical examination, he had clear consciousness and was not in apparent distress. His vital signs and oxygen saturation were as follows: body temperature, 36.6°C; pulse rate, 84 beats/minute; blood pressure, 126/77 mmHg; respiratory rate, 20 breaths/minute; and O_2 saturation, 99% in room air, respectively. No specific abnormality was detected by physical examination except extensive dental caries.

The results of blood tests, including complete blood count, coagulation, electrolytes, liver function, renal function and tumor markers, were all within the reference range. Only normal pharyngeal flora was cultured from his sputum, and sputum acid-fast staining and culture for Mycobacterium were negative. Serial imaging studies, including chest radiographs and a computed tomography (CT) scan of the chest (Figure 1), revealed a mass-like lesion with a diameter of 5.2 cm at the widest portion, located in the left upper lobe (LUL). This lesion not only invaded the visceral pleura but also crossed the major fissure into the left lower lobe (Figure 1B), a radiological finding suggestive of malignancies, tuberculosis or other uncommon infections.

To explore the etiology of the mass-like lesion, we performed bronchoscopy and found that there were some blood clots but no other obvious lesions within the bronchial trees. In addition, CT-guided biopsy of the lung mass was performed and the pathology revealed acute and chronic inflammation, without evidence of malignancy, granulomatous inflammation or any specific microorganisms. Thus, empirical antibiotics were administered during his hospitalization and follow-up at the outpatient department. However, the symptom of hemoptysis did not improve completely after multiple courses of 1-2 weeks of oral amoxicillin 500 mg every 6 hours, and serial follow-up chest radiographs showed no resolution of the lesion.

Therefore, to exclude the possibility of lung malignancy, the patient underwent LUL lobectomy and left lower lobe (LLL) wedge resection in June 2011. A $5 \times 4 \times 3$ cm tumor located mainly in the LUL, crossing the major fissure and extending to the superior segment of the LLL was found (Figure 2A). The histological examination revealed an abscess formation with some actinomyces-like "sulfur granules" within the mass lesion (Figure 2B), and the Gram staining demonstrated clusters of radiated, filamentous, Gram-positive microorganisms. As a result, pulmonary actinomycosis was diagnosed.

The patient received treatment for his dental caries and an 8-month course of oral amoxicillin/clavulanate 1 g every 12 hours for pulmonary actinomycosis. The chest radiograph obtained 5 months after treatment revealed

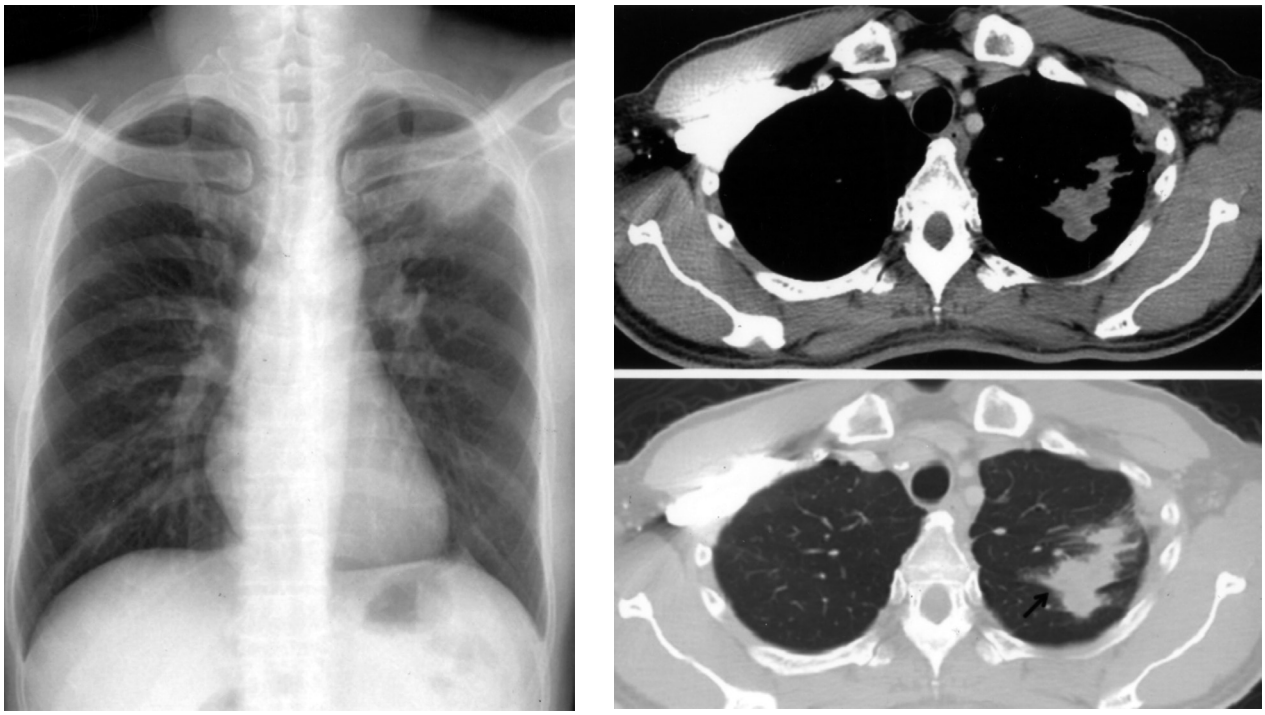

(A) (B)

Fig. 1. (A) Chest radiograph revealed a mass-like lesion located at the left upper lobe. (B) CT imaging of the chest demonstrated an infiltrating mass-like lesion located in the left upper lobe and crossing the major fissure (arrow) into the left lower lobe.

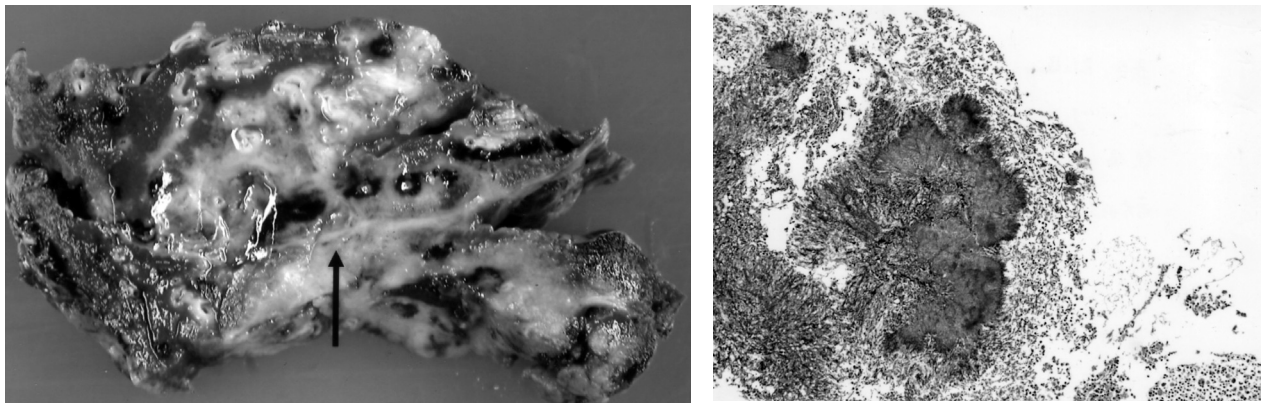

(A) (B)

Fig. 2. Pathology of the lung mass after resection. (A) Gross examination revealed a mass-like lesion crossing the major fissure of the left lung (arrow). (B) Histological examination revealed an abscess formation with some actinomyces-like "sulfur granules" within the mass lesion (40 X, H & E stain).

residual fibrosis at the left lung and no recurrence of lung infiltrates (Figure 3). The patient no longer had hemoptysis and was still asymptomatic 1 year after completion of the antibiotic

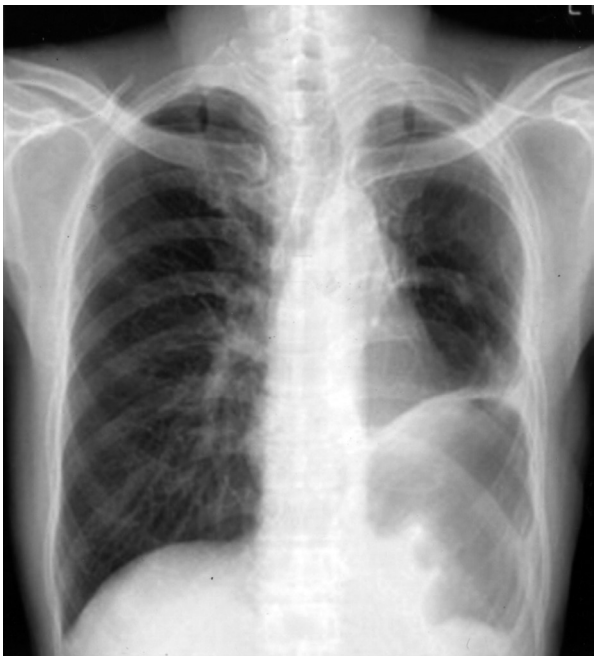

Fig. 3. Chest radiograph obtained 5 months after completion of antibiotic treatment revealed the post-lobectomy status and the residual fibrosis at the left lung.

treatment.

Discussion

We reported a patient with symptomatic pulmonary actinomycosis, which presented as a mass-like lesion crossing the major fissure of the left lung and was diagnosed by surgical intervention 4 months after his first visit.

There are diverse radiological patterns of pulmonary actinomycosis, including a peculiar transfissural extension into the neighboring pulmonary lobe (crossing the fissure) [4-6]. Few diseases have been reported to invade across the lung fissure; they include malignancy, tuberculosis, nocardiosis, fungal infections and actinomycosis [7-8]. The present case presented with the "crossing the fissure" sign in a long-standing mass-like lesion, which provided a valuable signal in identifying the underlying etiologies.

For a definite diagnosis of pulmonary actinomycosis, a positive culture from an adequate specimen and the histopathological demonstration of sulfur granules in infected tissue are required [1]. Therefore, an invasive diagnostic biopsy procedure or surgical excision is usually needed [4,7,9]. The etiology was not confirmed in our patient until he agreed to undergo excisional biopsy 4 months after his first visit.

The traditional recommendation for treatment of actinomycosis is administration of penicillin, delivered intravenously for 2-6 weeks, followed by an oral form for 6-12 months [1]. Medical treatment for less than 3 months in patients without debulking surgery might be associated with an increased risk of recurrence [9]. The patient in this case had received multiple brief courses of amoxicillin before the diagnosis, which might explain the relapsing hemoptysis and poor radiological response.

In conclusion, the radiological feature of transfissural extension into the neighboring pulmonary lobe is a useful sign for determining the etiology of an unresolved pulmonary infiltrate. This case report reminds us that, in addition to malignancy, tuberculosis, nocardiosis and fungal infection, actinomycosis should be included in the differential diagnosis of a lung lesion crossing the fissure, in order to provide prompt diagnosis and treatment.

References

1. Mabeza GF, Macfarlane J. Pulmonary actinomycosis. Eur Respir J 2003; 21: 545-51.
2. Russo TA. Agents of actinomycosis. In: Mandell GL, ed. Principles and Practice of Infectious Disease. 5th ed. New York, Churchill Livingstone, 1995; 2645-54.
3. Weese WC, Smith IM. A study of 57 cases of actinomycosis over a 36-year period. A diagnostic 'failure' with

good prognosis after treatment. Arch Intern Med 1975; 135: 1562-8.
4. Flynn MW, Felson B. The roentgen manifestations of thoracic actinomycosis. Am J Roentgenol Radium Ther Nucl Med 1970; 11: 707-16.
5. Webb WR, Sagel SS. Actinomycosis involving the chest wall: CT findings. AJR Am J Roentgenol 1982; 139: 1007-9.
6. Kim TS, Han J, Koh WJ, *et al*. Thoracic actinomycosis: CT features with histopathologic correlation. AJR Am J Roentgenol 2006; 186: 225-31.
7. Hsieh MJ, Liu HP. Thoracic actinomycosis. Chest 1993; 106: 336-70.
8. Hathur B, Mahesh PA, Babu SM, *et al*. A cavitary lesion in the lung crossing the fissure. Lung India 2011; 28: 222-5.
9. Choi J, Koh WJ, Kim TS, *et al*. Optimal duration of IV and oral antibiotics in the treatment of thoracic actinomycosis. Chest 2005; 128: 2211-7.

以穿越肺裂之腫塊爲表徵的肺部放射線菌病－病例報告

曾明雄　蕭世欣　鍾啟禮

放射線菌病是少見的肺部細菌感染，其臨床與影像學表現多不具特異性，常被延遲診斷或誤認為腫瘤、結核病或肺炎。本病例為 59 歲男性病人，臨床表現為長期且反覆性的咳血，胸部 X 光及電腦斷層掃描發現一左上肺葉腫塊，穿越大肺裂，並侵入到左下肺葉。腫塊之電腦斷層導引切片僅顯示有急慢性發炎現象，因此先給予短期經驗性抗生素治療，但咳血及病灶仍然持續，所以進行外科手術切除，病理切片發現肺膿瘍及硫顆粒放射線菌，因此診斷為肺部放射線菌病，經有效抗生素長期治療後痊癒，後續追蹤並未復發。回顧文獻，在影像學上發現肺部有橫跨肺裂之病灶時，除了考慮腫瘤、肺結核、諾卡菌病或真菌感染之外，需進一步檢查是否有放射線菌感染，以利儘早治療。*(胸腔醫學 **2014; 29: 160-165**)*

關鍵詞：放射線菌病，穿越肺裂，硫顆粒

台北醫學大學附設醫院　內科部　胸腔內科
索取抽印本請聯絡：蕭世欣醫師，台北醫學大學附設醫院　內科部　胸腔內科，台北市信義區吳興街 252 號

Endotracheal Anaplastic Large Cell Lymphoma – A Case Report and Literature Review

Yu-Ting Shen*, Ta-Chih Liu**,*****, Chee-Yin Chai***,******,
Chih-Jen Yang*,****,******, Tung-Heng Wang*,*******, Ming-Shyan Huang*,******

We describe a 52-year-old man who presented with hemoptysis. The chest radiograph showed a widened carinal angle, and the computed tomography (CT) of the chest revealed subcarinal lymphadenopathy with invasion into the trachea and left main bronchus. A mass at the main carina with nearly total obstruction of the left main bronchus was found with bronchoscopy. Biopsy of the lesion revealed anaplastic lymphoma kinase (ALK)-negative anaplastic large cell lymphoma (ALCL). No other organ or lymph node involvement was found on positron emission tomography. The patient had a complete remission after treatment with chemotherapy and radiotherapy. He has been followed up in the clinic without incident for more than a year. Endotracheal/endobronchial ALCL is very rare. All reported patients were younger than 30 years, and all of them had ALK-positive ALCL. To our knowledge, ours is the first case of endobronchial ALCL in a patient more than 50 years old and with ALK-negative ALCL. This case suggests that lymphoma should be included in the differential diagnoses of endobronchial tumor in older adults. ***(Thorac Med 2014; 29: 166-173)***

Key words: large cell lymphoma, endotracheal tumor, bronchoscopy

Introduction

Non-Hodgkin's lymphoma (NHL) initially identified as mediastinal lymphadenopathy on chest radiography is uncommon; endobronchial NHL is very rare and often occurs in teenagers. In this report, we present a rare case of endobronchial NHL presenting with hemoptysis and a widened carinal angle on chest radiography. We also reviewed related literature.

Case Presentation

This 52-year-old man with a history of type 2 diabetes mellitus under regular control and chronic hepatitis B experienced 3 hemoptysis

*Division of Pulmonary and Critical Care Medicine, Department of Internal Medicine; **Division of Hematology and Oncology, Department of Internal Medicine; *** Department of Pathology, Kaohsiung Medical University Hospital; ****Department of Internal Medicine, Kaohsiung Municipal Ta-Tung Hospital; *****Institute of Clinical Medicine, College of Medicine; ******Department of Internal Medicine, School of Medicine, College of Medicine; *******Department of Respiratory Therapy, College of Medicine, Kaohsiung Medical University, Kaohsiung, Taiwan
Address reprint requests to: Dr. Ming-Shyan Huang, Division of Pulmonary and Critical Care Medicine, Department of Internal Medicine, Kaohsiung Medical University Hospital, Kaohsiung Medical University, No. 100, Tzyou 1st Road, Kaohsiung 807, Taiwan

events within a month, and expectorated about 100 ml of blood each time. He felt little chest tightness before the episodes, and he denied having sore throat, fever, palpitation, dyspnea, orthopnea, nausea, vomiting, tarry stool, epigastric pain, hunger pain or midnight abdominal pain. He also denied having night sweating, poor appetite or weight loss in the previous month. No history of contact with tuberculosis was noted.

He therefore came to the emergency department, presenting with normal vital signs. Leukocytosis (16400/μL) and an elevated C-reactive protein level (19.06 mg/dL) were found. The chest radiograph showed sub-segmental atelectasis in the left lower lung field (Figure 1A); interval widening of the carinal angle compared with the previous chest radiograph was also noted (Figure 1B). The computed tomography (CT) of the chest revealed a carinal mass with invasion into the left main bronchus (Figure 2). He was then admitted for suspected endotracheal cancer.

After admission, bronchoscopy located a mass at the main carina with nearly total obstruction of the left main bronchus and partial obstruction of the right main bronchus (Figure 3). Cytological examination of the endobronchial brushing and washing found scattered dysplastic squamous cells. Pathological exam of the specimens from bronchoscopic biopsy, especially the immunohistochemical stain, which was positive for CD3 and CD30 but negative for cytokeratin and anaplastic lymphoma kinase (ALK), revealed anaplastic large cell lymphoma (ALCL) (Figure 4).

Positron emission tomography (PET) scan revealed lymphoma involving lymph nodes in the subcarinal and left lower paratracheal regions with endotracheal/endobronchial extension (Figure 5); no other lymph node involvement was noted. Standard chemotherapy with cyclophosphamide, hydroxydaunorubicin, vincristine and prednisone for 6 cycles was given, followed by radiotherapy for another month. The follow-up chest CT showed gradual shrinkage of the lymphoma. He has been followed up in the clinic without incident for more than a year, and the follow-up chest CT showed gradual shrinkage of the lymphoma, without evidence of relapse (Figure 6).

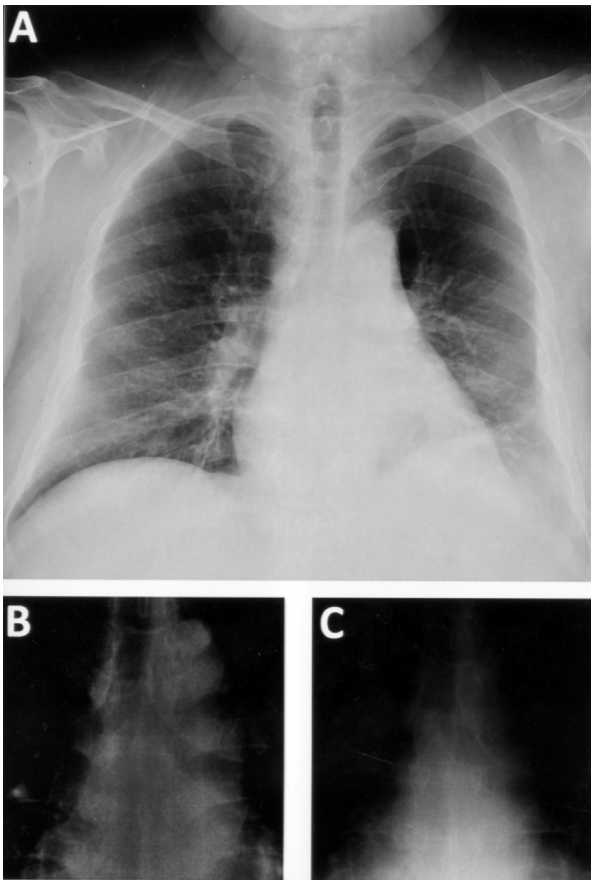

Fig. 1. The chest radiograph taken on presentation (A) showing sub-segmental atelectasis in the left lower lung field. The carinal angle in this film (B), a focused magnification of (A) is obviously widened compared with the chest radiograph taken about 1.5 years previous to this (C).

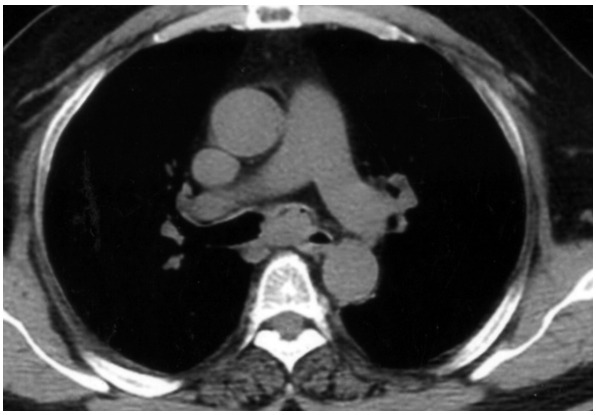

(A)

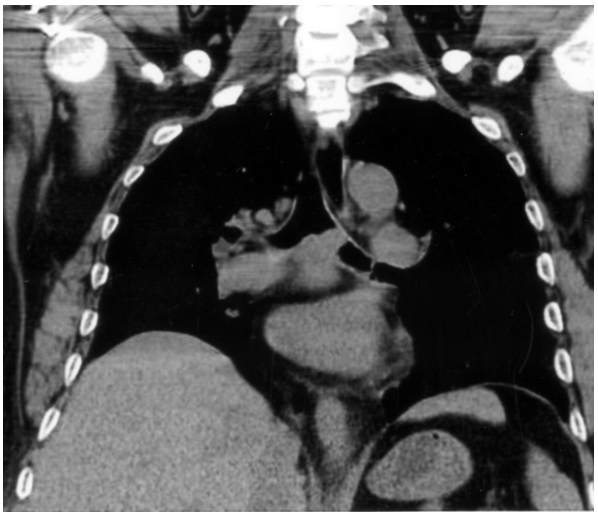

(B)

Fig. 2. Computed tomography of the chest reveals a subcarinal mass with invasion into the left main bronchus.

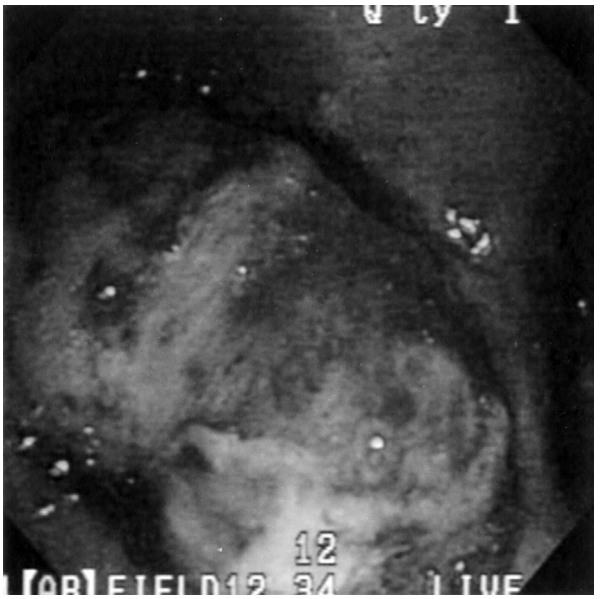

Fig. 3. Bronchoscopy shows a mass at the main carina with occlusion of the left main bronchus, an irregular surface and erythematous mucosa.

Discussion

NHLs often occur in middle-aged and older adults, and the incidence has increased compared with a few decades before. About 20% of patients with NHLs have mediastinal lymphadenopathy on presentation. Peripheral T-cell lymphoma is a heterogeneous group of generally aggressive neoplasms that constitute less than 15% of all NHLs that present in adults, and ALCL is 1 of them [1]. Some ALCLs are associated with the ALK gene. ALK-positive ALCLs and ALK-negative ALCLs have similar symptoms, histologic presentations, and patterns of surface receptor expression; however, patients with ALK-negative ALCLs are about 25 years older than patients with ALK-positive ALCLs [2].

Even if the major symptoms of ALCLs are "B symptoms", such as night sweating, body weight loss and fever, patients with only painless lymphadenopathy are common. The lymphadenopathy may be at retroperitoneal and peripheral nodal sites. Extranodal sites including bone marrow, peripheral blood, bone, lung, pleural fluid, liver, spleen and gastrointestinal tract may be involved [2-4]. Primary pulmonary NHLs are uncommon, and those presenting as endotracheal/endobronchial tumors are even rarer. Since the first case of endobronchial ALCL was described in 1998 [5], only about 10

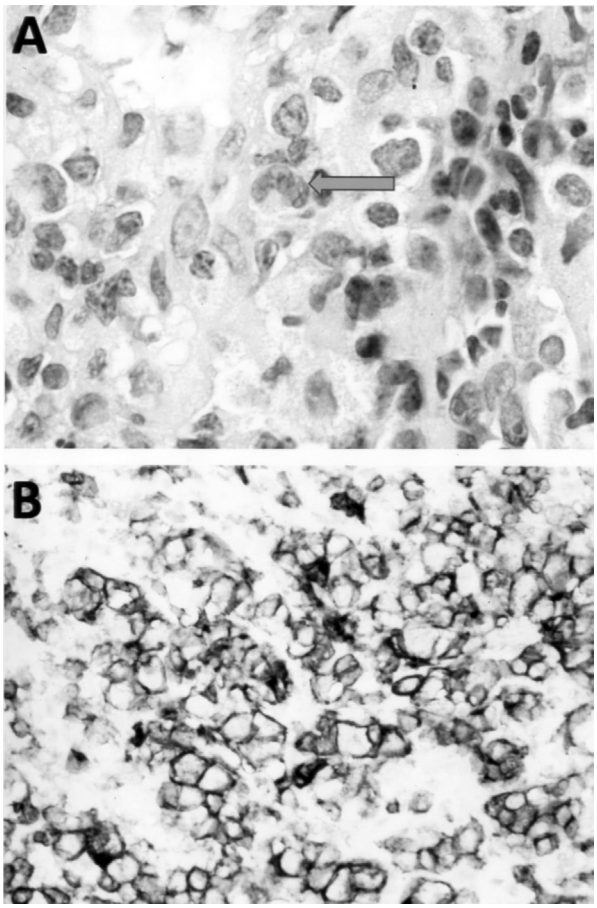

Fig. 4. Pathological examination of the specimens from bronchoscopic biopsy discloses diffuse infiltration of pleomorphic large lymphocytes with prominent nucleoli and abundant eosinophilic cytoplasm involving the bronchial epithelium and adjacent tissues. Mitotic activity with some atypical forms is prominent. Characteristic horseshoe- or doughnut-shaped nuclei (hallmark cells) (arrows) are also seen (A). The tumor cells are immunoreactive for CD30 (B). (A) H&E stain, original magnification, 1000×. (B), 400× immunohistochemistry for CD30.

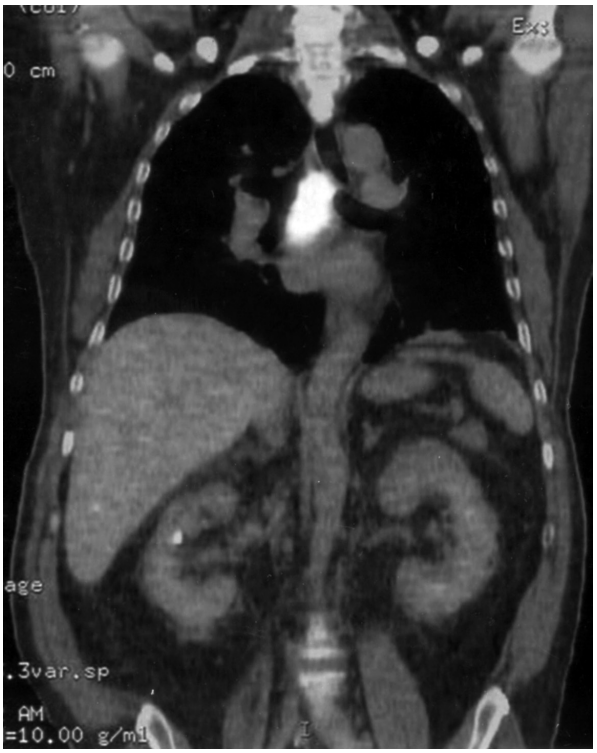

Fig. 5. Positron emission tomography shows high-grade FDG-avid lymphoma involving lymph nodes of the subcarinal and left lower paratracheal regions with extension to the left bronchus.

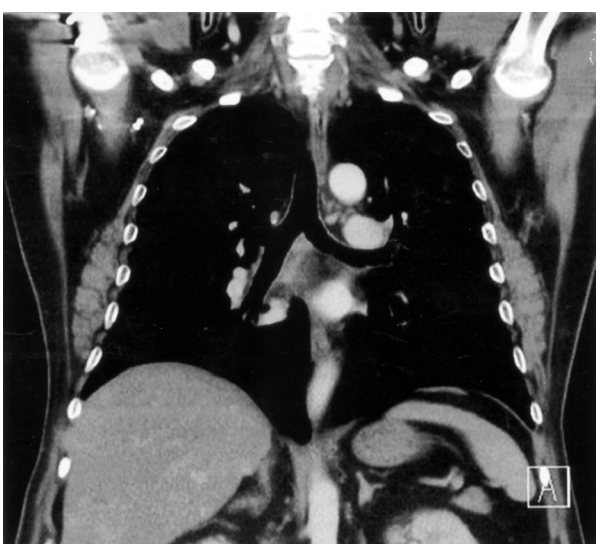

Fig. 6. The serial follow-up chest CT taken 12 months later shows marked shrinking of the subcarinal lymphoma.

cases have been reported [5-12].

Endobronchial lymphoma has been classified into 2 types [13]. Type 1 is characterized by the presence of diffuse submucosal nodules lining bronchoscopically visualized airways in individuals with clinically apparent systemic lymphoma, and frequently presents as pneumonitis on chest radiograph. Type 2 involves a localized endobronchial mass in the central airway that

may be an extension of adjacent lymph nodes external to the bronchi. The signs observed in type 2 patients are uniformly related to airway obstruction -- our patient presented with respiratory symptoms such as wheezing and cough, rather than "B symptoms" such as fever, sweating or weight loss, and chest CT revealed endobronchial invasion from the parabronchial lymphadenopathy. These presentations were compatible with those in the report cited above [13].

All of the cases of endotracheal/endobronchial ALCLs found in a literature review were type 2 endobronchial lymphomas, and two-thirds of the patients were male. Except for our case, all patients were younger than 30 years old, and most of them were less than 20 years old. Ours was the only case among all tested cases with an ALK-negative tumor, and our patient was obviously older than the others. Nearly all patients had atelectasis. The patient reported by Pavlov *et al*. [12] had hyperinflation of the lung on the same side as the endobronchial mass. The symptom of hemoptysis was found only in the case reported by Bollag *et al*. [10] and in ours, since hemoptysis is not a common symptom of endobronchial lymphoma. The case reported by Chen *et al*. [8] was the only case involving multiple nodules in the respiratory tract. Most patients presented with various B symptoms, and low-grade fever and weight loss were more commonly reported than sweating. These findings are incompatible with the description reported above [13], but more cases are needed to identify the prevalence of B symptoms in patients with type 2 endobronchial lymphoma (Table 1).

The standard induction therapy for lymphoma consists of cyclophosphamide, hydroxydaunorubicin, vincristine and prednisone. Although the regimens used for ALCLs are the same as for other subtypes of peripheral T-cell lymphomas, the outcome of ALCLs is generally better [2]. The International Prognostic Index (IPI) has been used for years to predict the outcome of patients with primary systemic ALCL, but in the most recent 15 years, the ALK gene of the tumor has become a main predictor, according to several retrospective studies [2,14-15]. The outcomes of ALK-positive patients are generally better than those of ALK-negative ALCL patients [2]. According to the International Peripheral T-cell Lymphoma (IPTL) Project, the 5-year survival rate of ALK-positive patients and ALK-negative patients is 70% and 49%, respectively [2].

To our knowledge, this is the first reported case of endobronchial ALK-negative ALCL in a patient over 50 years old in the medical literature. This case suggests that lymphoma should be included in the differential diagnoses of endobronchial tumor in older adults. Our case also highlights the importance of a systematic approach to reading chest radiographs and comparing them with previous films. Through a careful assessment of the carinal angle the diagnosis was made in time in our case.

In conclusion, we report an uncommon case of ALCL presenting with a carinal tumor. In patients with endobronchial tumor, the possibility of lymphoma should be considered. A careful review of serial chest radiographs in those patients presenting with hemoptysis and prompt bronchoscopic examination remain the keystone for a correct diagnosis of endobronchial tumor.

Table 1. Recent reports of endotracheal/endobronchial anaplastic large cell lymphoma

Authors, Year	Age/Sex	B symptoms	Atelectasis	Hemoptysis	Location of lymphoma	ALK
Kim *et al.*, 1998 [5]	28/M	Weight loss	+	-	Left main bronchus	unknown
Bhalla *et al.*, 2003 [6]	17/F	Nil	+	-	Left main bronchus	unknown
Guerra *et al.*, 2006 [7]	9/F	Low-grade fever	+	-	Left main bronchus	+
Chen *et al.*, 2008 [8]	17/M	Weight loss, low-grade fever	+	-	Trachea, left main bronchus, bronchus intermedius	unknown
Escobosa Sanchez *et al.*, 2009 [9]	10/M	Low-grade fever	+	-	Right main bronchus	+
Bollag *et al.*, 2010 [10]	26/M	Nil	-	+	Trachea	+
Zhang *et al.*, 2012 [11]	16/M	Weight loss, fever, night sweating	+	-	Right main bronchus	+
Pavlov *et al.*, 2013 [12]	13/F	Nil	-	-	Right main bronchus	+
Present case	52/M	Nil	+	+	Left main bronchus	-

References

1. Morton LM, Wang SS, Devesa SS, *et al*. Lymphoma incidence patterns by WHO subtype in the United States, 1992-2001. Blood 2006; 107: 265-76.
2. Savage KJ, Harris NL, Vose JM, *et al*. ALK- anaplastic large-cell lymphoma is clinically and immunophenotypically different from both ALK+ ALCL and peripheral T-cell lymphoma, not otherwise specified: report from the International Peripheral T-Cell Lymphoma Project. Blood 2008; 111: 5496-504.
3. Reiter A, Schrappe M, Tiemann M, *et al*. Successful treatment strategy for Ki-1 anaplastic large-cell lymphoma of childhood: a prospective analysis of 62 patients enrolled in three consecutive Berlin-Frankfurt-Munster group studies. J Clin Oncol 1994; 12: 899-908.
4. de Jong D, Vasmel WL, de Boer JP, *et al*. Anaplastic large-cell lymphoma in women with breast implants. JAMA 2008; 300: 2030-5.
5. Kim DH, Ko YH, Lee MH, *et al*. Anaplastic large cell lymphoma presenting as an endobronchial polypoid mass. Respiration 1998; 65: 156-8.
6. Bhalla R, McClure S. Pathologic quiz case: a 17-year-old adolescent girl with a short history of dyspnea. Endobronchial, anaplastic large cell lymphoma, T-cell phenotype. Arch Pathol Lab Med 2003; 127: e430-1.
7. Guerra J, Echevarria-Escudero M, Barrio N, *et al*. Primary endobronchial anaplastic large cell lymphoma in a pediatric patient. P R Health Sci J 2006; 25: 159-61.
8. Chen SC, Shih CM, Su JL, *et al*. Anaplastic large-cell lymphoma presenting as an endobronchial polypoid tumor. J Clin Oncol 2008; 26: 4845-7.

9. Escobosa Sanchez OM, Herrero Hernandez A, Acha Garcia T. Endobronchial anaplastic large cell lymphoma in childhood. An Pediatr (Barc) 2009; 70: 449-52.
10. Bollag R, Ramalingam P, Davis B, *et al*. Fine needle aspiration cytology of an endotracheal mass: report of a case with an unusual presentation of anaplastic large cell lymphoma. Acta Cytol 2010; 54: 328-32.
11. Zhang Y, Wang L, Huang J, *et al*. Anaplastic large cell lymphoma presenting as an endobronchial polypoid mass. Leuk Lymphoma 2012; 53: 2078-9.
12. Pavlov N, Pavlov V, Culic S, *et al*. Endobronchial ALK+ anaplastic large-cell lymphoma resembling asthma in a 13-year-old girl. J Pediatr Hematol Oncol 2013; 35: e4-6.
13. Rose RM, Grigas D, Strattemeir E, *et al*. Endobronchial involvement with non-Hodgkin's lymphoma. A clinical-radiologic analysis. Cancer 1986; 57: 1750-5.
14. Gascoyne RD, Aoun P, Wu D, *et al*. Prognostic significance of anaplastic lymphoma kinase (ALK) protein expression in adults with anaplastic large cell lymphoma. Blood 1999; 93: 3913-21.
15. Schmitz N, Trumper L, Ziepert M, *et al*. Treatment and prognosis of mature T-cell and NK-cell lymphoma: an analysis of patients with T-cell lymphoma treated in studies of the German High-Grade Non-Hodgkin Lymphoma Study Group. Blood 2010; 116: 3418-25.

氣管內原發性異生性大細胞淋巴瘤－病例報告與文獻回顧

沈昱廷 *　劉大智 **,*****　蔡志仁 ***,******　楊志仁 *,****,******
王東衡 *,*******　黃明賢 *,******

我們在此報告一個病例：五十二歲男性，主訴咳血，胸部 X 光片發現主支氣管分支角度增大，胸部電腦斷層發現主氣管分支下方有一腫瘤伴隨氣管與左側主支氣管內侵犯，支氣管鏡檢查發現有一腫瘤位於主氣管分支並伴隨左側支氣管近乎完全阻塞，切片檢查發現此腫瘤為一 anaplastic lymphoma kinase（ALK）基因陰性之異生性大細胞淋巴瘤，正子造影檢查無發現其他器官或淋巴侵犯。經化學治療及放射治療後腫瘤完全緩解，並已在門診追蹤超過一年。氣管或支氣管內發生之異生性大細胞淋巴瘤為非常罕見之病例，目前已發表的案例報告均發生在三十歲以下，且均為 ALK 陽性。據我們所知，此病例為首次發現之五十歲以上及 ALK 陰性之支氣管內異生性大細胞淋巴瘤。因此，在年紀較大患者發生之支氣管內腫瘤應將此病列為鑑別診斷。*(胸腔醫學 **2014; 29: 166-173**)*

關鍵詞：大細胞淋巴瘤，氣管內腫瘤，支氣管鏡

高雄醫學大學附設中和紀念醫院　內科部　胸腔內科 *，內科部　血液腫瘤內科 **，病理部 ***，大同醫院內科 ****
醫學院臨床醫學研究所 *****，醫學系 ******，醫學院呼吸治療學系 *******
索取抽印本請聯絡：黃明賢醫師，高雄醫學大學附設中和紀念醫院　內科部　胸腔內科，高雄市 807 自由一路 100 號

AIDS-related Intrapulmonary Kaposi's Sarcoma Presenting as Endobronchial Lesions: A Rare Presentation in Taiwan – A Case Report and Literature Review

Shih-Sen Lin, Yu-Ching Chen*, Wei-Yu Chen**, Shang-Jyh Kao

Kaposi's sarcoma (KS) is a complication suffered by patients infected with human immunodeficiency virus (HIV). KS forms most frequently in the mucocutaneous zone, but can also be found in other parts of the body. Intrapulmonary KS may lead to respiratory symptoms, such as coughing, hemoptysis, and exertional dyspnea. Pneumocystic jeroveci pneumonia, cytomegalovirus pneumonia, and pulmonary tuberculosis may be caused by diseases or factors other than intrapulmonary complications of HIV, so the differential diagnosis of intrapulmonary KS could potentially be overlooked. We reported the case of a patient with HIV who was brought to the hospital due to respiratory symptoms. Pulmonary tuberculosis medications were given initially, but the symptoms worsened, and the chest x-ray showed progression of the condition. As a result of computed tomography (CT) and bronchoscopy findings, we further suspected the possibility of intrapulmonary KS. Pathological diagnosis confirmed our impression. With the use of anti-viral medications and chemotherapy, the patient showed improvement in clinical symptoms and chest x-ray findings. We completed an extensive literature review, and believe this experience will help doctors in Taiwan identify KS more quickly when encountering patients with respiratory complications possibly related to HIV. ***(Thorac Med 2014; 29: 174-181)***

Key words: Kaposi's sarcoma, human immunodeficiency virus (HIV), acquired immunodeficiency syndrome (AIDS), intrapulmonary complications

Introduction

Kaposi's sarcoma (KS) is a well-known complication experienced by individuals infected with human immunodeficiency virus (HIV). KS is typically found on the skin but can also be found on other parts of the body where intrapulmonary lesions are relatively uncommon. Although KS has been reported in many international review papers and case reports,

Division of Chest Medicine, Department of Internal Medicine, Shin Kong Wu Ho-Su Memorial Hospital, Taipei, Taiwan; *General Education Center, Ching-Kuo Institute of Management and Health, Keelung, Taiwan; **Division of Infectious Diseases, Department of Internal Medicine, Shin Kong Wu Ho-Su Memorial Hospital, Taipei, Taiwan
Address reprint requests to: Dr. Shang-Jyh Kao, Division of Chest Medicine, Department of Internal Medicine, Shin Kong Wu Ho-Su Memorial Hospital, No. 95, Wen Chang Road, Shih Lin District, Taipei City, Taiwan

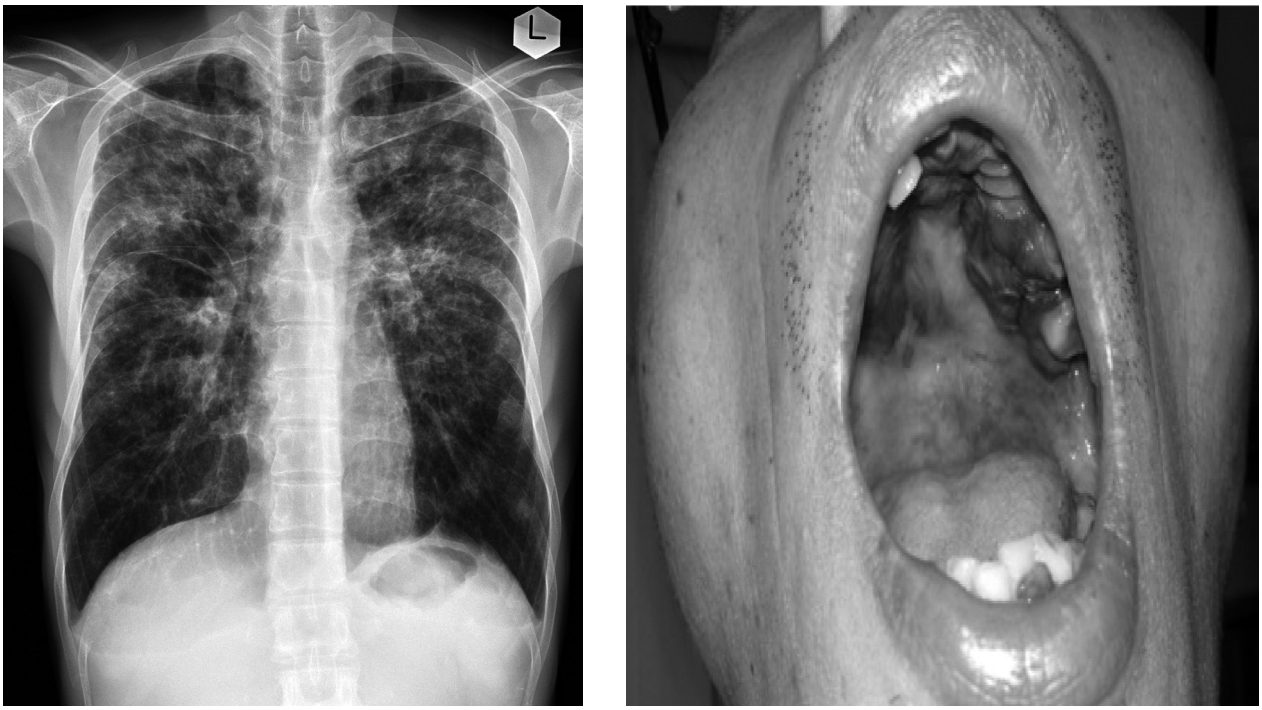

(A) (B)

Fig. 1. (A) Initial chest x-ray showed bilateral fibroinfiltration with multiple nodular opacities (B) Oral thrush developed during hospitalization

few classical imaging and bronchoscopy findings have been reported from Taiwan. Herein, we report a patient with acquired immunodeficiency syndrome (AIDS)-related KS. We initially suspected the case was related to AIDS and treated the complications accordingly, including the administration of anti-tuberculosis (TB) drugs. However, the patient's condition worsened after treatment. We performed chest computed tomography (CT), bronchoscopy, and endobronchial biopsy and eventually confirmed KS. The symptoms and imaging findings of the patient improved significantly after administering antiviral medications and chemotherapy.

Case Report

A 45-year-old male homosexual presented with a dry cough that had persisted for 2 months, accompanied with progressive shortness of breath. The symptoms were especially exaggerated during physical exertion, and were reduced after rest. The patient visited our pulmonology outpatient department, where a chest x-ray revealed fibronodular infiltration in the bilateral upper lung field (Figure 1A). The patient was admitted under the impression of pulmonary TB, and anti-TB medications were started after respiratory isolation. During the period of hospitalization, oral thrush developed (Figure 1B) and HIV screening showed positive results. The absolute CD4 count was only 167 cells per microliter (cells/uL), with an extremely high HIV viral load (598,189 copies per milliliter). AIDS was diagnosed, and antiretroviral therapy (ART) was started on the 5th day after admis-

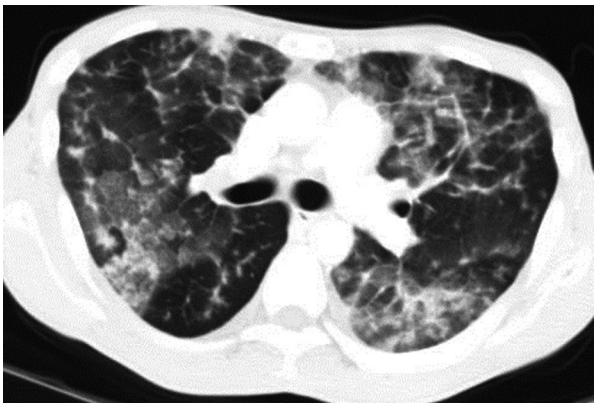

(A)

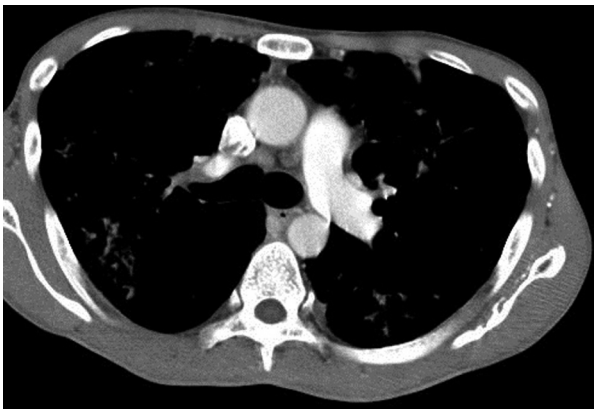

(B)

Fig. 2. Chest CT (A) showed peribronchial thickening, multiple ill-defined, irregular peribronchovascular lesions with subpleural airspace opacities, patchy ground-glass opacities and bilateral interlobular septal thickening, and (B) retrotracheal and bilateral hilar lymphadenopathy

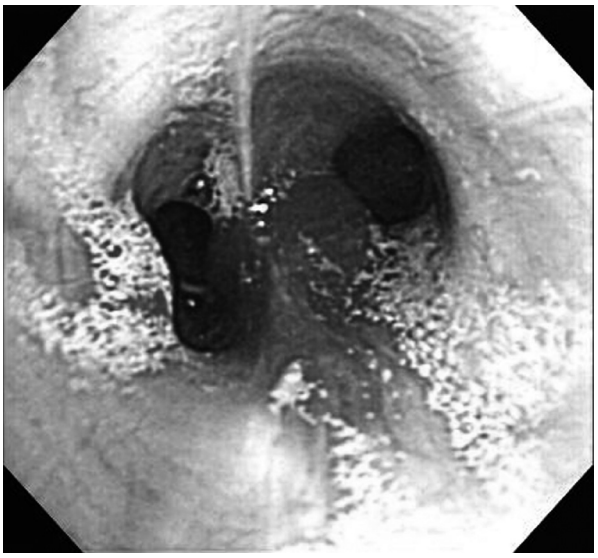

(A)

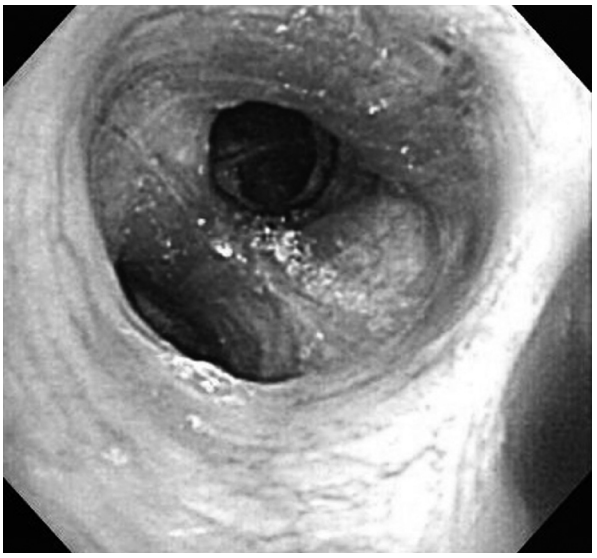

(B)

Fig. 3. Bronchoscopy showed (A) multiple violaceous lesions with spotty bleeding, and (B) swelling and red mucosa at the bifurcation of the segmental bronchi

sion. However, the patient suffered from more severe symptoms, including coughing with blood-tinged sputum and exertional dyspnea. Chest CT revealed peribronchial thickening, multiple ill-defined, irregular peribronchovascular lesions with subpleural airspace opacities, patchy ground-glass opacities, and bilateral interlobular septal thickening. The retrotracheal bilateral hilar and axillary lymph nodes were also enlarged (Figure 2A, 2B). Bronchoscopy showed endobronchial violaceous lesions diffused with spotty bleeding (Figure 3A, 3B). The biopsy revealed a spindle cell tumor, which was compatible with a diagnosis of KS (Figure 4A, 4B). We discontinued anti-TB treatment and started chemotherapy with doxorubicin on the 22nd day of hospitalization. After completing

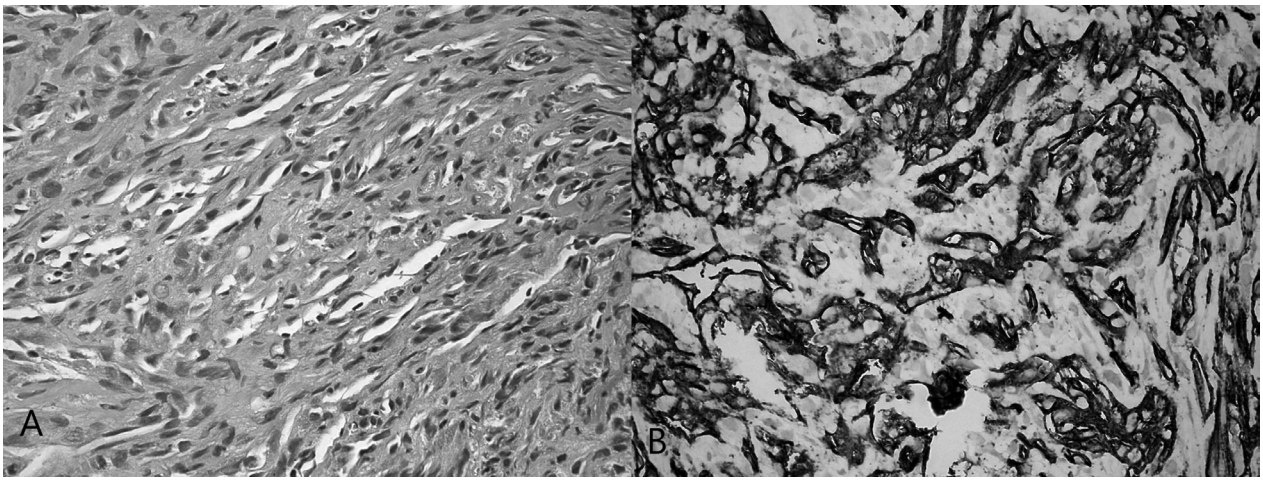

Fig. 4. Photomicrograph showed (A) proliferation of spindle cells arranged in a fascicular pattern with slit-like spaces filled with red blood cells. (HE 400X) (B) The spindle cells show positive reactivity for CD34 staining (CD34 400X).

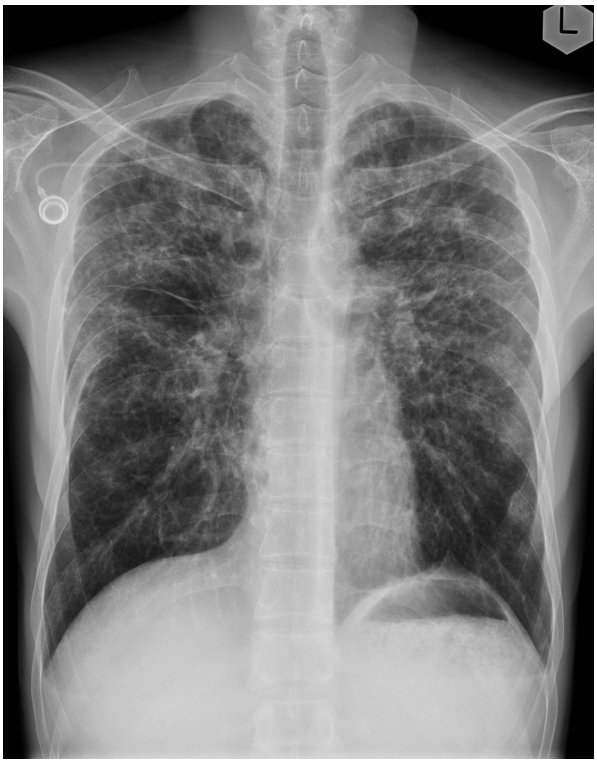

Fig. 5. The chest x-ray showed much improvement after antiretroviral therapy and systemic chemotherapy

the course of chemotherapy, the patient's condition and chest x-ray pattern were markedly improved (Figure 5) and his respiratory symptoms had subsided. The patient was discharged, and outpatient follow-up was arranged.

Discussion

KS is a type of angiosarcoma caused by the human herpes virus 8 (HHV-8) and is also known as KS-associated herpes virus (KSHV). KS is classified into 4 subtypes: AIDS-related or epidemic, endemic or African, organ transplant-associated, and classic. Among these types, AIDS-related KS is the most common tumor observed in HIV-infected patients and is also considered an AIDS-defining illness by the US Centers for Disease Control and Prevention.

Although the literature shows KS can occur in any population at risk of AIDS, homosexual and bisexual men are in the highest risk category. AIDS-related KS is relatively uncommon in heterosexual drug abusers, blood recipients, hemophilia patients, women, and children [1].

In AIDS-related KS patients, the CD4 count is the most important marker of disease progression. Porter *et al*. performed a study of 70 newly diagnosed KS patients; after receiving

ART, the rate ratio (RR) of KS for patients who had a CD4 count of fewer than 200 cells/uL, 200-349 cells/uL, and 350-499 cells/uL was 18.9, 3.6, and 4.1, respectively [2]. This study showed that if an AIDS patient has a lower CD4 count, the risk of KS must be considered.

KS may develop in any part of the body and can be categorized into cutaneous KS and visceral KS. Cutaneous is the most common form of KS; most early symptoms start as cutaneous KS. Visceral KS can appear at all visceral sites, including the lymph nodes, liver, pancreas, heart, bones, bone marrow, and skeletal muscle [3-4]. The most common sites of visceral KS are the oral cavity, GI tract, and respiratory system.

In KS patients whose lungs were affected, 80-90% of the cases were shown to be related to mucocutaneous diseases [5-6]. For these patients, the airway, lung parenchyma, pleura, and intrathoracic lymph nodes were affected. If the lung parenchyma and airway were affected, symptoms of dyspnea, hypoxemia, and hemoptysis, and a dry cough were reported to develop and progress within a few weeks [7]. Therefore, if an AIDS patient has cutaneous lesions accompanied with the aforementioned respiratory symptoms, KS invasion of the lungs should be strongly suspected. First, clinicians can check the CD4 count and viral load to determine the degree of immunosuppression caused by HIV. In KS patients whose lungs were affected, the CD4 counts were reported to be less than 50 cells per cubic millimeter, and the viral load was greater than 10,000 copies per millimeter [8]. However, because of the immunosuppression caused by AIDS, opportunistic infections such as pneumocystic jeroveci pneumonia, cytomegalovirus (CMV) infection, and pulmonary TB may produce the symptoms listed above.

KS must be differentiated from other opportunistic infections, and a radiographic study is essential for the differential diagnosis. In previous reports, 60% of the patients showed patchy reticular opacities with a peribronchovascular distribution, and 25% showed ill-defined nodular densities on chest x-rays [9-10]. On chest CT images, hilar densities extending into the parenchyma along the perivascular or peribronchial pathways and a characteristic septal or nodular pattern (the so-called “frame-shape appearance”) were highly suggestive of intrapulmonary KS [11].

Bronchoscopy plays an important role in diagnosing intrapulmonary or endobronchial KS. The goal of bronchoscopy is to confirm endobronchial lesions, to aid pathological sampling by providing related sites of the lesion, and to perform bronchoalveolar lavage (BAL) and bronchial brushing to facilitate microbiological and cytological examinations. KS endobronchial lesions often presented as violaceous or bright red and were macular or maculopapular lesions, especially at the bifurcations of the airway [12]. Biopsy of endobronchial lesions is not performed routinely for several reasons: bronchial biopsy samples have a poor diagnostic yield, and the procedure cannot be repeated frequently due to the risk of significant bleeding; the diagnosis is difficult to make histologically on bronchial biopsy specimens because crush artifacts and reactive fibrous tissue have similar appearances; most intrapulmonary KS are related to mucocutaneous presentations and are also effective in following chemotherapy targeted at KS [13-14]. However, the definite diagnosis still relies on pathological examination of the specimen obtained by bronchoscopy in cases of atypical clinical symptoms and diagnostic imaging. To confirm the diagnosis,

the characteristic architecture of spindle cells surrounding thin vascular channels should be observed on pathological slides.

ART is currently the main treatment for intrapulmonary KS. Before the development of ART, the prognosis of pulmonary AIDS-related KS was poor, with a median survival period of only 2-10 months [15]. However, ART alone in the treatment of pulmonary AIDS-related KS is not adequate. The latest literature indicates that ART combined with systemic chemotherapy drugs, such as bleomycin, doxorubicin, and vincristine, effectively reduces lung lesions [16]. This treatment was especially effective in patients (such as our patient) whose lung condition continued to deteriorate after ART.

In conclusion, pulmonary AIDS-related KS is a common HIV complication with symptoms that may be similar to symptoms of other AIDS-related lung complications. Therefore, detailed patient medical histories, laboratory examinations, and imagining techniques are needed for the differential diagnosis. If a clinical diagnosis cannot be made with the above measures, a bronchoscopic biopsy is needed. The current mainstream treatment of pulmonary AIDS-related KS is ART combined with systemic chemotherapy. In our case, the patient showed quick and obvious improvement in clinical symptoms and diagnostic imaging findings after the treatment. Since cases of pulmonary AIDS-related KS have seldom been identified in Taiwan, we encourage doctors to diagnose pulmonary AIDS-related KS quickly and accurately, and to start effective treatment immediately when encountering patients with symptoms of possible pulmonary AIDS-related KS.

References

1. Beral V, Peterman TA, Berkelman RL, *et al*. Kaposi's sarcoma among persons with AIDS: a sexually transmitted infection? Lancet. 1990; 335: 123-8.
2. Lodi S, Guiguet M, Costagliola D, *et al*. Kaposi sarcoma incidence and survival among HIV-infected homosexual men after HIV seroconversion. CASCADE Collaboration J Natl Cancer Inst. 2010; 102: 784-92.
3. Ioachim HL, Adsay V, Giancotti FR, *et al*. Kaposi's sarcoma of internal organs. A multiparameter study of 86 cases. Cancer. 1995; 75: 1376-85.
4. Caponetti G, Dezube BJ, Restrepo CS, *et al*. Kaposi sarcoma of the musculoskeletal system: a review of 66 patients. Cancer. 2007; 109: 1040-52.
5. Haramati LB, Wong J. Intrathoracic Kaposi's sarcoma in women with AIDS. Chest. 2000; 117: 410-4.
6. Huang L, Schnapp LM, Gruden JF, *et al*. Presentation of AIDS-related pulmonary Kaposi's sarcoma diagnosed by bronchoscopy. Am J Respir Crit Care Med. 1996; 153: 1385-90.
7. Joshi M, Markelova N, Palacio D, *et al*. A patient with HIV, dyspnea, and multiple pulmonary nodules: pulmonary Kaposi sarcoma. Chest. 2006; 130: 1924-8.
8. El Amari EB, Toutous-Trellu L, Gayet-Ageron A, *et al*. Predicting the evolution of Kaposi sarcoma in the highly active antiretroviral therapy era. AIDS. 2008; 22: 1019-28.
9. Davis SD, Henschke CI, Chamides BK, *et al*. Intrathoracic Kaposi sarcoma in AIDS patients: radiographic-pathologic correlation. Radiology. 1987; 163: 495-500.
10. Miller RF, Tomlinson MC, Cottrill CP, *et al*. Bronchopulmonary Kaposi's sarcoma in patients with AIDS. Thorax. 1992; 47: 721-5.
11. Wolff SD, Kuhlman JE, Fishman EK. Thoracic Kaposi sarcoma in AIDS: CT findings. J Comput Assist Tomogr. 1993; 17: 60-2.
12. Yoo DJ, Lee KH, Munderi P, *et al*. Clinical and bronchoscopic findings in Ugandans with pulmonary Kaposi's sarcoma. Korean J Intern Med. 2005; 20: 290-4.
13. Cadranel J., Mayaud C. Intrathoracic Kaposi's sarcoma in patients with AIDS. Thorax. 1995; 50: 407-14.
14. Miller R. HIV-associated respiratory diseases. Lancet 1996; 348: 307-12.
15. Cadranel JL, Kammoun S, Chevret S, *et al*. Results of

chemotherapy in 30 AIDS patients with symptomatic pulmonary Kaposi's sarcoma. Thorax. 1994; 49: 958-60.
16. Mosam A, Shaik F, Uldrick TS, *et al*. A randomized controlled trial of highly active antiretroviral therapy versus highly active antiretroviral therapy and chemotherapy in therapy-naive patients with HIV-associated Kaposi sarcoma in South Africa. J Acquir Immune Defic Syndr. 2012; 60: 150-7.

以支氣管內病灶爲表現的後天免疫缺乏症候群相關之肺內卡波西氏肉瘤－病例報告及文獻回顧

林士森　陳昱青 *　陳威宇 **　高尚志

卡波西氏肉瘤 (Kaposis sarcoma) 是相當常見的人類免疫缺乏病毒感染之病人併發症之一，最常發生在黏膜表皮處，但是其他部位也有可能會發生。其中若發生在肺內會產生許多呼吸道相關症狀如咳嗽，咳血，運動性氣促等等相關症狀。由於人類免疫缺乏病毒感染相關的肺內併發症如肺囊蟲肺炎，巨細胞病毒肺炎，或是肺結核在國內較為常見，若發生以上所述之症狀時常會疏忽肺內卡波西氏肉瘤的診斷。我們在這裡提出一個人類免疫缺乏病毒感染的病例，由於呼吸道症狀入院，起初以肺結核藥物處理，但是症狀及胸部影像仍然持續惡化。經由典型的電腦斷層及支氣管鏡圖片，懷疑是肺內的卡波西氏肉瘤而進行支氣管鏡檢查及病理切片，切片結果證實我們的憶測。在使用了抗病毒藥物及化學治療後，病人的症狀及胸部影像有顯著且快速的進步。我們也瀏覽了許多的文獻，希望這個經驗可以讓國內的醫師在遇見人類免疫缺乏病毒感染患者罹患呼吸道併發症的同時可以更快速的診斷出卡波西氏肉瘤。*(胸腔醫學 **2014; 29: 174-181**)*

關鍵詞：卡波西氏肉瘤，人類免疫缺乏病毒，後天免疫缺乏症候群，肺內併發症

新光吳火獅紀念醫院　內科部　胸腔內科，* 經國管理暨健康學院　通識教育中心
** 新光吳火獅紀念醫院　內科部　感染科
索取抽印本請聯絡：高尚志醫師，新光吳火獅紀念醫院　內科部　胸腔內科，台北市 111 士林區文昌路 95 號

Disseminated *Mycobacterium avium complex* Infection Mimicking Metastatic Lung Cancer in an Immunocompetent Patient – A Case Report and Literature Review

Jen-Suo Cheng, Cheng-Lin Wu*, Han-Yu Chang

Mycobacterium avium complex (MAC) infection often occurs in patients with pre-existing pulmonary disease or in those with an immunocompromised status. The classic radiographic features of pulmonary MAC are pleural thickening, bronchiectasis, centrilobular nodules and cavities. A lung mass-like lesion is rarely seen in pulmonary MAC. Herein, we report a rare case of a patient without chronic lung disease or immunosuppression, presenting with a lung mass and anemia, and with the final diagnosis of pulmonary MAC with bone marrow involvement. ***(Thorac Med 2014; 29: 182-188)***

Key words: disseminated *mycobacterium avium complex*, immunocompetent

Introduction

Mycobacterium avium complex (MAC) is the most frequently identified pathogen in non-tuberculous mycobacterial (NTM) lung disease in the United States [1]. It has been found to colonize natural water, soil, indoor water systems, and hot tubs, and it can be isolated from the sputum of apparently healthy individuals [2]. Pulmonary disease from MAC usually affects immunocompetent hosts with pre-existing lung disease [3] such as chronic obstructive pulmonary disease (COPD), bronchiectasis, cystic fibrosis, pneumoconiosis, prior pulmonary tuberculosis (TB), pulmonary alveolar proteinosis, and esophageal motility disorders. However, extrapulmonary or disseminated forms of MAC infections are mainly noted in immunocompromised hosts [4].

The signs and symptoms of pulmonary MAC infections are variable and non-specific. Chronic cough, anorexia, weight loss, night sweats and hemoptysis are the constitutional symptoms. Anemia is a rare presentation. The radiologic features of pulmonary MAC infections are pleural thickening, bronchiectasis, nodules and cavities [5]. A pulmonary mass is a rare presentation of pulmonary MAC infection.

In this report, we describe the case of a 58-year-old immunocompetent man with the

Division of Pulmonary Medicine, Department of Internal Medicine; *Department of Pathology, National Cheng Kung University Hospital, Tainan, Taiwan
Address reprint requests to: Dr. Han-Yu Chang, Division of Pulmonary Medicine, Department of Internal Medicine, National Cheng Kung University Hospital, No. 138, Sheng-Li Rd., Tainan 704, Taiwan

presentations of anemia and a pulmonary mass. His human immunodeficiency virus (HIV) screening test was negative. The cultures from sputum and biopsied lung tissue both grew MAC. For anemia of unknown etiology, bone marrow biopsy was also done, which revealed MAC infection, as well.

Case Report

A 58-year-old male, a working man who denied any previous systemic disease, experienced cough with purulent sputum beginning 2 months prior to visiting the chest outpatient department. He complained of poor appetite and gradual body weight loss of about 3 kilograms. Low-grade fever developed in the most recent 2 weeks. At the chest outpatient department, chest roentgenogram showed a mass in the right upper lung field (Figure 1). Chest computed tomography (CT) showed a spiculated mass lesion in the right upper lung (Figure 2a), enlarged lymph nodes in the right paratracheal and subcarinal areas (Figure 2b, 2c), and lung-to-lung metastasis (Figure 2d). CT-guided lung biopsy was performed and pathology revealed granulomatous inflammation (Figure 3a). The culture from biopsied lung tissue grew MAC. The patient's sputum also yielded MAC. The HIV screening test was negative. Anti-NTM medications were prescribed and his fever subsided 2 days later; he was then discharged. However, he presented himself with general malaise and a pale appearance 3 weeks later. Hemoglobin had dropped from 10 mg/dL to 6.7 mg/dL. He was then re-admitted to our ward. Bone marrow biopsy revealed granulomatous inflammation (Figure 3b) and bone marrow culture also revealed MAC infection. Anti-NTM medications were continued and his anemia improved gradually.

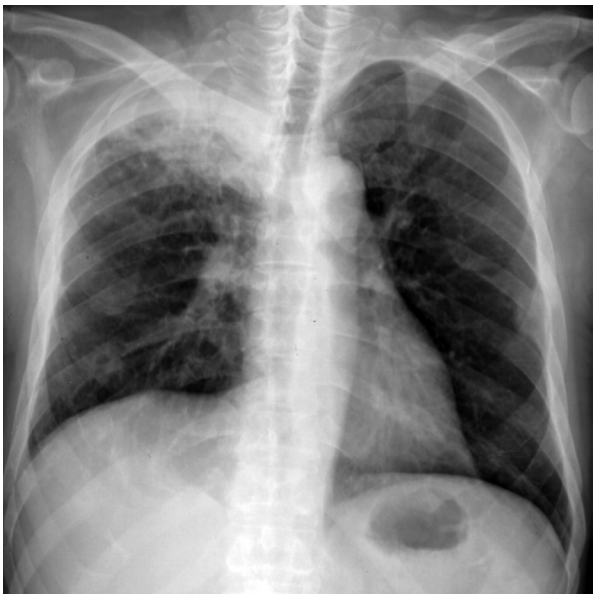

Fig. 1. Chest radiograph showed right upper lobe consolidation or lung mass lesion.

Discussion

NTM is increasingly recognized as a cause of chronic pulmonary infection worldwide. This phenomenon is due not only to better diagnostic techniques or the state of HIV infection, but more importantly to environmental exposure, host immune response and preexisting lung disease [6]. Genotypes, phenotypes, and female sex hormones are also contributors to NTM infection among immunocompetent patients [12]. MAC is the most commonly identified pathogen in NTM infections.

MAC organisms have been isolated from various environmental sources, such as soil, water, and animals (e.g., birds, pigs, and cattle) [7]. In terms of host immunity, IFN-γ, TNF-α, and IL-12 have been reported to contribute to protecting against MAC, whereas IL-10 suppresses host defenses against MAC [8].

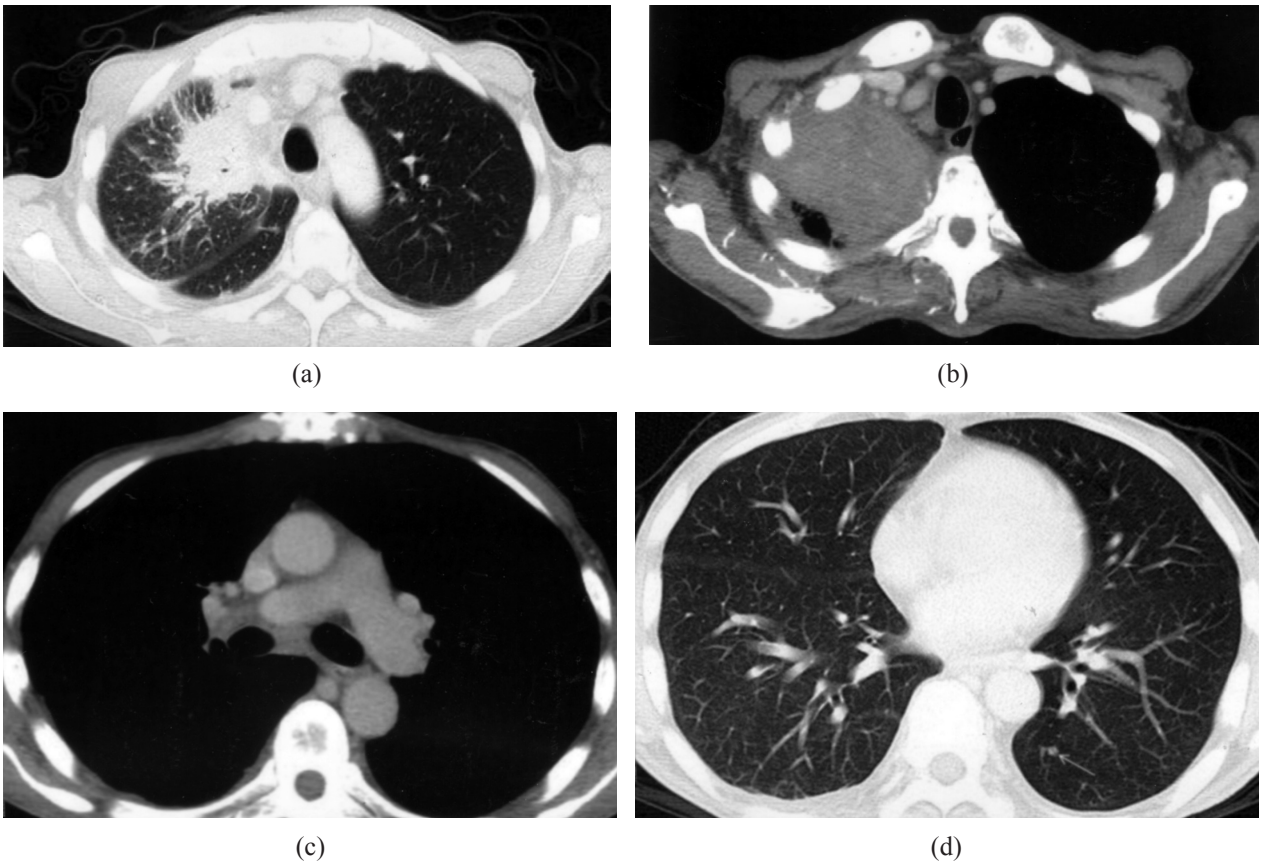

Fig. 2. CT scan of the chest showed a spiculated mass in the right upper lung (a), enlarged lymph nodes in the right paratracheal (b) and subcarinal areas (c), and a left lung nodule (white arrow) suspected of being lung metastasis (d)

A subgroup of patients with pulmonary MAC disease presents with nodular and interstitial nodular infiltrates involving the right middle or left lingual lobes. MAC disease usually appears in postmenopausal, nonsmoking, white women [9-10], and is labeled "Lady Windomere syndrome" [11]. This form of disease is also known as "nodular-bronchiectasis" or "nodular bronchiectatic disease". This may hint that there is a specific genotype or phenotypes in this subgroup of pulmonary MAC disease. In a recent study, a possible molecular mechanism responsible for the abnormal induction of leptin, adiponectin, IFN-γ, and IL-10 in patients with NTM lung disease was reported [12].

The symptoms and signs of pulmonary MAC disease are variable and non-specific. Chronic cough (productive or dry), fatigue, malaise, weakness, dyspnea, and chest discomfort are all included. Hemoptysis may occur secondary to bronchiectasis or endobronchial disease, or as a manifestation of preexisting lung disease. There is less fever and body weight loss in these patients than in those with typical TB. Since these infections frequently coexist with underlying lung diseases, such as COPD, pneumoconiosis or bronchiectasis, the physical findings in the chest are usually similar to those of

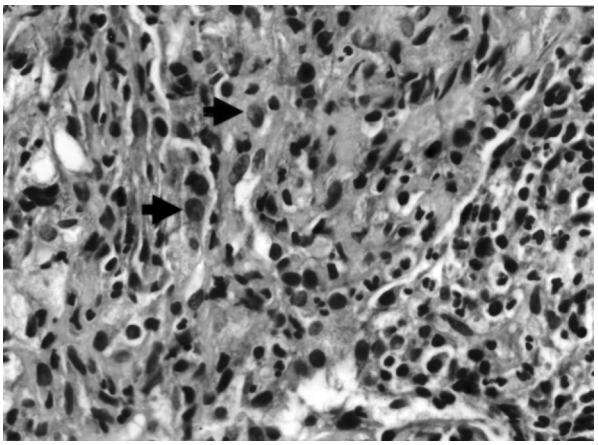

(a)

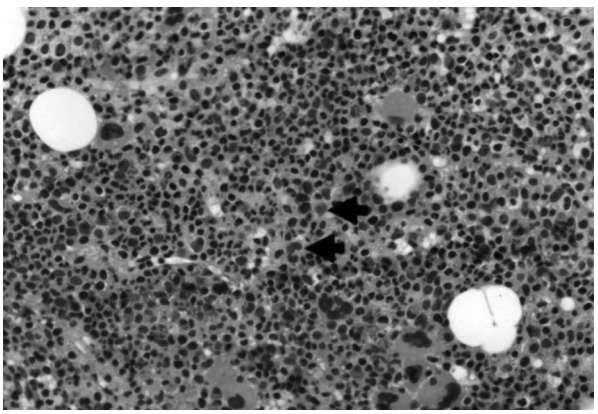

(b)

Fig. 3. Lung CT-guided biopsy with hematoxylin and eosin (H&E) stain 400X showed granulomatous inflammation without caseous necrosis (a) and bone marrow biopsy with H&E 200X showed myeloid hyperplasia with granulomatous inflammation and myelofibrosis (b); both images had epithelioid histiocytes infiltration (black arrow).

the underlying disease [1].

Two major clinical presentations are described in pulmonary MAC infections. One is the above-mentioned "Lady Windomere syndrome", the typical symptoms of which are persistent cough with purulent sputum, but no fever or body weight loss. The mean duration of cough before diagnosis was 25 weeks [3]. The other is disease in those with a known underlying disease. Patients are usually middle-aged to elderly men and often smokers with underlying pulmonary disease. The symptoms resemble typical pulmonary TB with cough and body weight loss. The upper lung is usually involved with cavities formation [13].

The classic radiographic pictures of pulmonary MAC infections are indistinguishable from those of pulmonary TB. Christensen and colleagues [5] reviewed 114 cases of pulmonary MAC documented between 1959 and 1979; 92% of pulmonary MAC infection was infiltrates at the apical or posterior segment of the upper lobes, and 88% of images was cavitary lesions. Endobronchial spread accounted for 80% of images. The follow-up images showed atelectasis or scarring lesions (70%). There was no presentation of focal mass-like lesions [5,15]. In Woodring *et al*.'s study [14], focal masses were present in only 3 of 40 NTM patients studied. The presentation of a focal mass is almost exclusively associated with pulmonary MAC [16]. In the previous study, the focal mass-like presentations of pulmonary MAC infection sometimes revealed calcification and were often accompanied with surrounding fibroproductive (satellite) lesions [16,24]. These may distinguish pulmonary MAC infection from lung cancers, which usually present as an irregular shape with lobulation and notching lesions, and are accompanied with a pleural tail [23]. However, in previous case series, the diagnosis was often made at resection for suspected malignancy [24].

The diagnosis of pulmonary NTM infection not only requires 3 clinical criteria: first, pulmonary signs and symptoms, second, chest radiograph or CT findings, and third, appropriate exclusion of other diseases, but also requires meeting microbiologic criteria, including posi-

tive culture from 2 separate sputum cultures or positive culture from at least 1 bronchial wash or lavage, or lung tissue biopsy revealing mycobacterial histopathologic features (granulomatous inflammation) with positive culture findings from tissue culture, or 1 or more bronchial washings, or 1 or more sputum cultures. Regarding the collection of sputum specimens, 3 early-morning specimens on different days is preferred. Sputum can also be induced for those patients unable to produce it; if sputum cannot be obtained, bronchoscopy with or without lung biopsy may be necessary [1].

The indications for treatment of pulmonary NTM infections are compatible respiratory or constitutional symptoms with radiographic abnormalities plus either consistent isolation of NTM in moderate to high numbers from more than 1 specimen of pulmonary secretions or histologic evidence of pulmonary parenchymal involvement. The treatment regimen for pulmonary MAC infections should be adjusted according to the severity and status of the disease. The initial therapy for nodular-bronchiectatic disease is clarithromycin 1000 mg or azithromycin 500-600 mg plus ethambutol 25 mg/kg and rifampin 600 mg 3 times weekly. For cavitary disease, the regimen is clarithromycin 500-1000 mg or azithromycin 250-300 mg plus ethambutol 15 mg/kg and rifampin 450-600 mg daily with or without streptomycin or amikacin. In advanced or previously treated disease, it is suggested streptomycin or amikacin can be added to the regimen for cavitary disease and rifabutin may be used instead of rifampin [1].

Disseminated NTM infection was defined as isolation of NTM from blood or bone marrow, from a liver biopsy specimen, or from specimens from 2 or more noncontiguous sites like the respiratory tract, lymph node, ascites, pleural effusion, pericardial effusion, joint fluid, or cerebral spinal fluid [17]. Disseminated NTM infection is mostly associated with immunosuppressed conditions like renal or cardiac transplantation, an immunosuppressive therapy history, HIV infection and leukemia, and has rarely been reported in immunocompetent subjects [19]. There have been increasing numbers of case reports of disseminated NTM infections in immunocompetent hosts recently [20-22]. MAC was the most common species involved in disseminated NTM diseases in Taiwan. The abnormalities of disseminated NTM infections seen in chest images included patchy consolidation (35.3%), an interstitial pattern (29.4%), and nodular or cavitary lesions (23.5%) [18].

In conclusion, we reported a rare case of disseminated MAC infection in a non-HIV infected and immunocompetent middle-aged man without a pre-existing lung condition. His chest images of a solitary spiculated mass in the right upper lung with several mediastinal lymphadenopathies resembling metastatic lung cancer has been rarely reported previously.

References

1. Griffith DE, Aksamit T, Brown-Elliott BA, *et al*. An official ATS/IDSA statement: diagnosis, treatment, and prevention of nontuberculous mycobacterial diseases. Am J Respir Crit Care Med 2007; 175: 367-416.
2. Tobin-D'Angelo MJ, Blass MA, *et al*. Hospital water as a source of Mycobacterium avium complex isolates in respiratory specimens. J Infect Dis 2004; 189(1): 98-104.
3. Prince DS, Peterson DD, Steinger RM, *et al*. Infection with Mycobacterium avium complex in patients without predisposing conditions. N Engl J Med 1989; 321: 863-8.
4. Azzam HC, Gahunia MK, Sae-Tia S, *et al*. Mycobacterium avium-associated typhlitis mimicking appendicitis in an immunocompetent host. Am J Med Sci 2009; 337: 218-20.
5. Christensen EE, Dietz GW, Ahn CH, *et al*. Pulmonary

manifestations of Mycobacterium intracellularis. AJR Am J Roentgenol 1979; 133: 59-66.

6. Glassroth J. Pulmonary disease due to nontuberculous mycobacteria Chest 2008; 133(1): 243-51.
7. Maekawa K, Ito Y, Hirai T, *et al*. Environmental risk factors for pulmonary Mycobacterium avium-intracellulare complex disease. Chest 2011; 140(3): 723-9.
8. Vankayalapati R, Wizel B, Samten B, *et al*. Cytokine profiles in immunocompetent persons infected with Mycobacterium avium complex. J Infect Dis 2001; 183: 478-84.
9. Hartman TE, Swensen SJ, Williams DE. Mycobacterium avium intracellulare complex: evaluation with CT. Radiology 1973; 17: 23-6.
10. Primack SL, Logan PM, Hartman TE, *et al*. Pulmonary tuberculosis and Mycobacterium avium-intracellulare: a comparison of CT findings. Radiology 1905; I94: 413-7.
11. Reich JM, Johnson RE. Mycobacterium avium complex pulmonary disease presenting as an isolated lingular or middle lobe pattern: the Lady Windermere Syndrome. Chest 1992; 101: 1605-9.
12. Kartalija M , Ovrutsky AR, Bryan CL, *et al*. Patients with nontuberculous mycobacterial lung disease exhibit unique body and immune phenotypes Am J Respir Crit Care Med 2013 Jan; 187(2): 197-205.
13. Teirstein AS, Damsker B, Kirschner PA, *et al*. Pulmonary infection with Mycobacterium avium-intracellulare: diagnosis, clinical patterns, treatment. Mt Sinai J Med 1990; 57: 209.
14. Woodring JH, Vandiviere HM, Melvin IG, *et al*. Roentgenographic features of pulmonary disease caused by atypical mycobacteria. South Med J 1987; 80(12): 1488-97.
15. Albelda SM, Kern JA, Marinelli DL, *et al*. Expanding spectrum of pulmonary disease caused by nontuberculous mycobacteria. Radiology 1985; 157: 289-96.
16. Levin DL. Radiology of pulmonary Mycobacterium avium intracellulare complex. Clin Chest Med 2003; 23: 603-12.
17. Lai CC, Lee LN, Ding LW, *et al*. Emergence of disseminated infections due to nontuberculous mycobacteria in non-HIV-infected patients, including immunocompetent and immunocompromised patients in a university hospital in Taiwan. J Infect 2006; 53: 77-84.
18. Chou CH , Chen HY, Chen CY, *et al*. Clinical features and outcomes of disseminated infections caused by nontuberculous mycobacteria in a university hospital in Taiwan, 2004-2008. Scand J Infect Dis 2011; 43: 8-14.
19. Kim WY, Jang SJ, Ok T, *et al*. Disseminated Mycobacterium intracellulare infection in an immunocompetent host. Tuberc Respir Dis 2012; 72: 452-6.
20. Song JY, Park CW, Kee SY, *et al*. Disseminated Mycobacterium avium complex infection in an immunocompetent pregnant woman, BMC Infect Dis 2006; 6: 154.
21. Okada H, Yoshioka K. Acute disseminated encephalomyelitis associated with meningitis due to Mycobacterium intracellulare. Intern Med 2010; 49: 2113-6.
22. Azzam HC, Gahunia MK, Sae-Tia S, *et al*. Mycobacterium avium-associated typhlitis mimicking appendicitis in an immunocompetent host. Am J Med Sci 2009; 337: 218-20.
23. Hansell DM, Armstrong P, Lynch DA, *et al*. Imaging of diseases of the chest. 4th edition. Elsevier Mosby 2005: 107-18.
24. Miller Jr WT. Spectrum of pulmonary nontuberculous mycobacterial infection. Radiology 1994; 191: 343-50.

免疫健全病人之瀰漫性禽結核分枝桿菌感染以肺部轉移癌表現－病例報告及文獻回顧

鄭人碩　巫政霖*　張漢煜

禽結核分枝桿菌感染通常發生在肺部之前就有疾病或者是免疫不全的病人，典型的放射影像學上多以肺結節，肺空洞，支氣管擴張或肋膜增厚表現。以肺部腫瘤表現的肺部禽結核分枝桿菌是相當罕見的。在這裡我們分享一個之前肺部正常且沒有免疫不全的中年男性，以肺部腫瘤及貧血表現。最後診斷是瀰漫性禽結核分枝桿菌感染的個案。*(胸腔醫學 **2014; 29: 182-188**)*

關鍵詞：瀰漫性禽結核桿菌，免疫健全病人

成功大學附設醫院　內科部　胸腔內科，* 成功大學附設醫院　病理部
索取抽印本請聯絡：張漢煜醫師，成功大學附設醫院　內科部　胸腔內科，704 台南市北區勝利路 138 號

Laryngeal Granulomatous Inflammation in a Patient with Crohn's Disease: Tuberculosis or Extra-intestinal Crohn's Disease

Shao-Chung Cheng, Jann-Yuan Wang*

Crohn's disease and tuberculosis are both granulomatous inflammation in histology and are hardly distinguishable if there is neither caseous necrosis nor acid-fast bacilli. We presented a 31-year-old woman with stable Crohn's disease complicated with culture-confirmed pulmonary tuberculosis. Histological examination of the laryngeal biopsy indicated granulomatous inflammation without caseous necrosis or acid-fast bacilli. After standard anti-tuberculosis treatment, her laryngeal lesion recovered. ***(Thorac Med 2014; 29: 189-193)***

Key words: acid-fast bacilli, caseous necrosis, Crohn's disease, granulomatous inflammation, laryngeal tuberculosis

Introduction

Crohn's disease is a chronic inflammatory bowel disease characterized by remittent chronic inflammation mainly affecting the gastrointestinal tract. Incidence of extra-intestinal manifestations of Crohn's disease is around 25% [1]. However, the precise incidence of laryngeal involvement in Crohn's disease remains uncertain. The prevalence of otolaryngologic involvement in Crohn's disease ranges from 0.5% to 13%, and most cases affect the oral mucosa [2]. Bronchopulmonary involvement in even rarer; it has been reported to be, as low as 0.4% [3]. Histological examination of the gastrointestinal tract may reveal focal chronic inflammation, focal crypt irregularity and granulomas [4], but extra-intestinal involvement may show only non-caseous granulomas [5]. Granulomas can also be found in tuberculosis (TB). Laryngeal TB (less than 1% [6]) is a rare manifestation of TB that, for the most part, was considered to be secondary spread from pulmonary TB. Crohn's disease and TB are difficult to differentiate histologically if there is a lack of caseous necrosis and acid-fast bacilli (AFB). Herein, we report a case of Crohn's disease complicated with laryngeal TB.

Case Report

A 31-year-old woman was diagnosed as

Department of Internal Medicine, Tauyuan General Hospital, Tauyuan, Taiwan; *Department of Internal Medicine, National Taiwan University Hospital, Taipei, Taiwan
Address reprint requests to: Dr. Jann-Yuan Wang, Department of Internal Medicine, National Taiwan University Hospital, No. 7, Zhongshan South Road, Taipei 100, Taiwan

having Crohn's disease by intestinal biopsy in February 2007. Under the control of a non-steroid anti-inflammatory drug (mesalamine 1000 mg 3 times per day), she was in a remittent status as assessed by the Crohn's disease activity index (CDAI) [7]. The latest colofibroscopy performed in May 2011 showed no lesion. She began experiencing sore throat, odynophagia and low-grade fever in July 2011. Laryngoscopy (Figure 1) showed granular change with multiple ulcers at the bilateral aryepiglottic folds, epiglottis and vocal cords. She was treated as having epiglottitis with oral empiric amoxycillin with clavulanate, naproxen and acetaminophen for 2 weeks. No steroid had been used before this episode. Biopsy of the laryngeal lesion showed granulomatous inflammation with ulceration, but there was neither caseous necrosis nor AFB. Chest radiography (Figure 2) was arranged and showed infiltrations in the right upper lung field. Computed tomography (CT) of the chest (Figure 3) revealed scattered nodular opacities and tree-in-bud patterns in the bilateral lung fields. Pulmonary TB was suspected. Though acid-fast smears for 3 sets of sputum samples in early August 2011 were negative, Mycobacterium tuberculosis was isolated on 20 August 2011, and was susceptible to all first-line anti-TB drugs. Beginning on 23 August 2011, she received standard anti-TB treatment consisting of isoniazid, rifampin, pyrazinamide, plus ethambutol for 2 months, followed by isoniazid plus rifampin for another 4 months. One week after commencing anti-TB treatment, her fever subsided and the sore throat and odynophagia improved; she recovered completely during the next 2 weeks. The follow-up chest radiography 2 months after starting anti-TB treatment showed clear lung fields. Follow-up laryngoscopy in March 2012 revealed complete recovery of the laryngeal le-

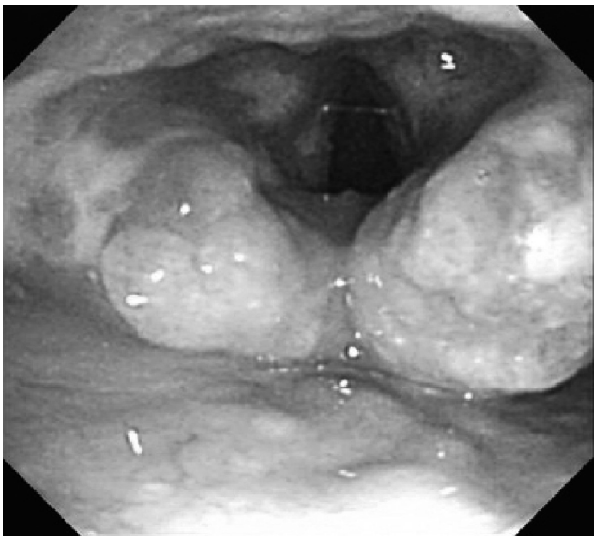

Fig. 1. Laryngoscopy showed granular change with multiple ulcers as the over bilateral aryepiglottic folds, epiglottis and vocal cords.

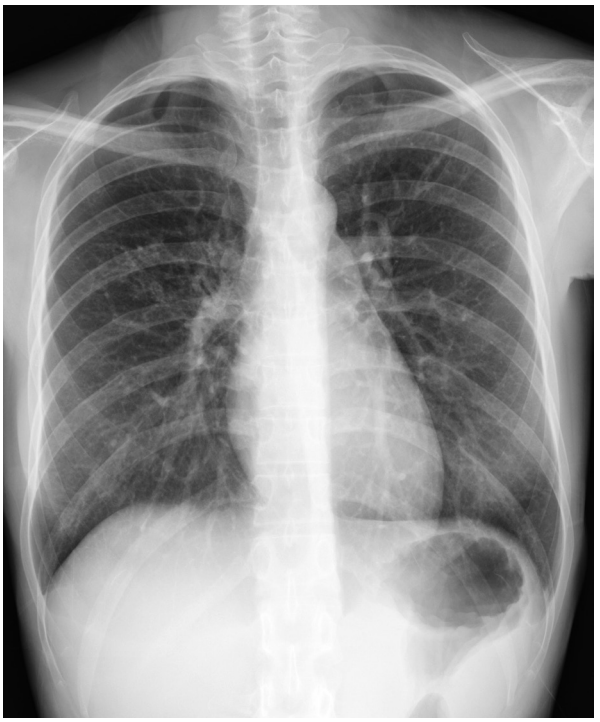

Fig. 2. Chest radiography before anti-TBtreatment showed infiltrations in the right upper lung field.

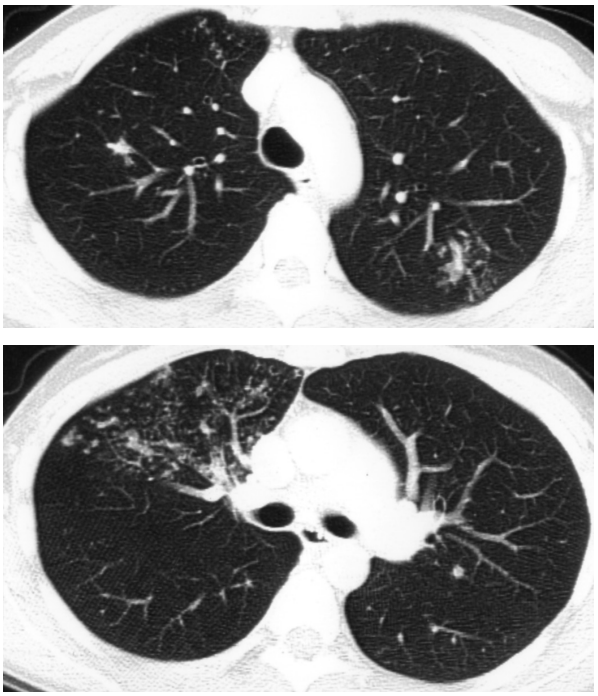

Fig. 3. Chest CT revealed scattered nodular opacities and tree-in-bud patterns in the bilateral lung fields.

sions. During the whole disease course, she had no gastrointestinal symptoms and colofibroscopy located no lesions. Costicosteroids were never prescribed during this period. Laryngeal TB, rather than Crohn's disease with laryngeal involvement, was favored.

Discussion

In the pre-antibiotic era, laryngeal TB occurred in 35-83% of patients with pulmonary TB and was associated with a high mortality rate (45-90%) [8]. Incidence decreased to less than 1% with the introduction of modern anti-TB treatment [6]. Laryngeal TB rarely developed without the accompaniment of active pulmonary TB [9], and could occur as a primary site of infection or as a result of hematogenous spread [10]. Increase in the number of immunocompromised host due to diseases (such as acquired immunodeficiency syndrome) or medications increased the incidence of atypical presentations of TB [8]. Definite diagnosis of laryngeal TB relies on tissue culture, and may require about 2 weeks on average to obtain a positive result [11]. The diagnosis can be made earlier if histological examination of laryngeal biopsy revealed granulomatous inflammation with caseous necrosis and presence of AFB [8].

Crohn's disease is a non-infectious, lifelong disease arising from an interaction between genetic and environmental factors and is more common in developed countries [4]. The diagnosis of Crohn's disease is established by a combination of clinical presentation, endoscopic appearance, radiology, histology, surgical findings and, more recently, serology [4]. Though there is no "gold standard", colofibroscopy with multiple biopsy specimens is recommended as the first-line diagnostic procedure [12]. The typical histopathologic findings are focal chronic inflammation, focal crypt irregularity and granulomas [4]. Presence of non-caseating granulomas, small collections of epithelioid histiocytes and giant cells is not diagnostic for Crohn's disease, because these can also be observed in infectious processes [4]. Extra-intestinal manifestation of Crohn's disease is rare, but it has been reported to involve the nasal cavity, supraglottic structures, glottis, skin, and respiratory tract [13-14], and responds well to corticosteroids [1,3]. When Crohn's disease involves the upper gastrointestinal tract, there is almost always concomitant disease in the small bowel or colon [15]. In addition, biopsies of buccal mucosa from patients with Crohn's disease have been shown to have a correlation with disease activity [15]. Inflammatory bowel disease is now considered to result from an in-

appropriate inflammatory response to intestinal microbes in a genetically susceptible host [16], which implies that disease extension to some degree may be positively correlated with intestinal disease activity.

In clinical practice, the CDAI is used to assess the disease activity of Crohn's disease [4]. The CDAI for our patient in June 2011 was 56 points (stool pattern: 14, fever: 20; weight: 22), which was considered to be a remittent status according to the evidence-based consensus of the European Crohn's and Colitis Organization (ECCO) in 2010 [4].

In our case, TB, rather than Crohn's disease was likely to be responsible for the laryngeal lesions, for the following reasons. First, the Crohn's disease in this patient was in a remittent status, based on the CDAI score. Second, pulmonary TB was culture-confirmed and may reasonably involve the larynx by bronchogenic spread. Third, a therapeutic response was obvious after anti-TB treatment without using corticosteroids for Crohn's disease. This case is a reminder that in TB-endemic areas, TB should still be considered a possibility when there is a histological finding of granuloma without caseous necrosis or AFB, even in patients with Crohn's disease.

References

1. Ephgrave K. Extra-intestinal manifestations of Crohn's disease. Surg Clin North Am 2007; 87: 673-80.
2. Yang J, Maronian N, Reyes V, *et al*. Laryngeal and other otolaryngologic manifestations of Crohn's disease. J Voice 2002; 16: 278-82.
3. Lu DG, Ji XQ, Zhao Q, *et al*. Tracheobronchial nodules and pulmonary infiltrates in a patient with Crohn's disease. World J Gastroenterol 2012; 18: 5653-7.
4. Van Assche G, Dignass A, Panes J, *et al*. The second European evidence-based consensus on the diagnosis and management of Crohn's disease: Definitions and diagnosis. J Crohn's Colitis 2010; 4: 7-27.
5. Siroy A, Wasman J. Metastatic Crohn's disease: a rare cutaneous entity. Arch Pathol Lab Med 2012; 136: 329-32.
6. Shin JE, Nam SY, Yoo SJ, *et al*. Changing trends in clinical manifestations of laryngeal tuberculosis. Laryngoscope 2000; 110: 1950-3.
7. Best WR. Predicting the Crohn's disease activity index from the Harvey-Bradshaw Index. Inflamm Bowel Dis 2006; 12: 304-10.
8. Yencha MW, Linfesty R, Blackmon A. Laryngeal tuberculosis. American Journal of Otolaryngology 2000; 21: 122-6.
9. Kandiloros DC, Nikolopoulos TP, Ferekidis EA, *et al*. Laryngeal tuberculosis at the end of the 20th century. J Laryngol Otol 1997; 111: 619-21.
10. Ramadan HH, Tarazi AE, Baroudy FM. Laryngeal tuberculosis: Presentation of 16 cases and review of the literature. J Otolaryngol 1993; 22: 39-41.
11. Lu D, Heeren B. Comparison of the Automated Mycobacteria Growth Indicator Tube System (BACTEC 960/MGIT) with Löwenstein-Jensen medium for recovery of mycobacteria from clinical specimens. Am J Clin Pathol 2002; 118: 542-5.
12. Coremans G, Rutgeerts P, Geboes K, *et al*. The value of ileoscopy with biopsy in the diagnosis of intestinal Crohn's disease. Gastrointest Endosc 1984; 30: 167-72.
13. Ulnick KM, Perkins J. Extraintestinal Crohn's disease: case report and review of the literature. Ear Nose Throat J 2001; 80: 97-100.
14. Lemann M, Messing B, D'Agay F, *et al*. Crohn's disease with respiratory tract involvement. Gut 1987; 28: 1669-72.
15. Wagtmans MJ, van Hogezand RA, Griffioen G, *et al*. Crohn's disease of the upper gastrointestinal tract. Neth J Med 1997; 50: 2-7.
16. Abraham C, Cho JH. Mechanisms of disease inflammatory bowel disease. N Engl J Med 2009; 361: 2066-78.

克隆氏症病人的喉頭肉芽性炎症：結核病或是克隆氏症之腸外侵犯

鄭少仲　王振源 *

克隆氏症和結核菌感染在病理檢查下同樣為肉芽腫炎症，若無發現乾酪性壞死或耐酸性桿菌，兩者難以區分。我們報告一例 31 歲女性患有病情穩定的克隆氏症，並新診斷肺結核，喉頭病灶切片顯示為肉芽腫性炎症，但是並未發現乾酪性壞死或是耐酸性桿菌，病人接受標準抗結核藥物治療後，喉頭病灶經追蹤也證實消失。*(胸腔醫學 **2014; 29: 189-193)***

關鍵詞：耐酸性桿菌，乾酪性壞死，克隆氏症，肉芽腫性炎症，喉頭結核

行政院衛生署立桃園醫院　內科部，* 台灣大學附設醫院　內科部
索取抽印本請聯絡：王振源醫師，台灣大學附設醫院　內科部　胸腔科，10002 台北市中山南路 7 號

Metastasizing Ameloblastoma (Malignant Ameloblastoma) – An Unusual Cause of Multiple Lung Nodules

Che-Liang Chung, Tzu-Hsiu Tsai, Wei-Yu Liao, Chong-Jen Yu

Ameloblastoma is an uncommon benign, locally aggressive odontogenic neoplasm that accounts for approximately 1% of all tumors and cysts of the jaw. Despite the propensity for local recurrence, ameloblastoma rarely exhibits malignant behavior, but disseminates (malignant ameloblastoma), with the lung as the most common metastatic site. Herein, we report the case of a 43-year-old woman who had desmoplastic ameloblastoma of the mandible and underwent marginal mandibulectomy for removal of the primary tumor. Three years following surgical resection, multiple nodules were found incidentally in the bilateral lungs on computed tomography scan of the chest. The diagnosis of metastasizing ameloblastoma without cellular atypia was confirmed pathologically after wedge resection of 2 of the nodules by video-assisted thoracoscopic surgery. There was no local recurrence at the primary site along with the occurrence of pulmonary metastasis. This patient received follow-up without immediate treatment for the metastasizing ameloblastoma and, in the following 2 years, no radiological progression of the pulmonary metastasis was seen. ***(Thorac Med 2014; 29: 194-199)***

Key words: ameloblastoma, malignant ameloblastoma, multiple lung nodules, odontogenic neoplasm, pulmonary metastasis

Introduction

Ameloblastoma, a rare odontogenic neoplasm arising from the epithelium of the dental lamina, was first reported in the literature in 1885, using the term "adamantinoma" [1]; this slow growing and locally invasive tumor accounts for approximately 1% of all tumors and cysts of the jaw [1-4]. In 1930, the term "ameloblastoma" was suggested to replace adamantinoma [1]. Ameloblastoma of the jaw is the second most common odontogenic tumor, and usually derives from the mandible (80%) and less often from the maxilla [5]. Despite the high propensity for local recurrence if not adequately removed, well-differentiated ameloblastoma rarely exhibits malignant behavior, but develops dissemination (metastasizing ameloblastoma),

Department of Internal Medicine, National Taiwan University Hospital, Taipei, Taiwan
Address reprint requests to: Dr. Tzu-Hsiu Tsai, Department of Internal Medicine, National Taiwan University Hospital, No. 7, Chung-Shan South Road, Taipei 10002, Taiwan

with the lung as the most common metastatic site [5-8]. We report the case of a 43-year-old woman who had ameloblastoma of the mandible and underwent marginal mandibulectomy for removal of the primary lesion, which relapsed with multiple metastatic tumors in the bilateral lungs 3 years after the surgery.

Case Report

In October 2010, a 43-year-old woman presented to our clinic for evaluation of a left lower lung nodule incidentally found on chest radiography. The patient had been healthy until 3 years prior to this visit, when she had a painless gingival swelling in the anterior area of the lower jaw. Diagnosis of desmoplastic ameloblastoma of the mandible was made by incisional biopsy. Histopathology disclosed nests of ameloblastic odontogenic epithelium and dense fibrous connective tissue stroma. The patient then underwent marginal mandibulectomy and iliac bone graft repair in August 2007. All the section margins were clear, except the inferior section line. The patient was then followed up periodically, and during the next 3 years, clinical examinations of the primary surgical site revealed no evidence of local recurrence.

At this presentation, the patient was asymptomatic. No lymphadenopathy of the neck was noted, and other physical examinations were unremarkable. Chest radiograph (Figure 1) showed a sharply marginated nodule without calcification in the left lower lung field. Computed tomography (CT) scan of the chest (Figure 2A, B) disclosed multiple well-defined nodules at the bilateral lung parenchyma, predominantly in the lower lobes. The largest, which was located at the basal left lower lobe, was about 1.4 cm in size. One of the nodules was found to be cavitated.

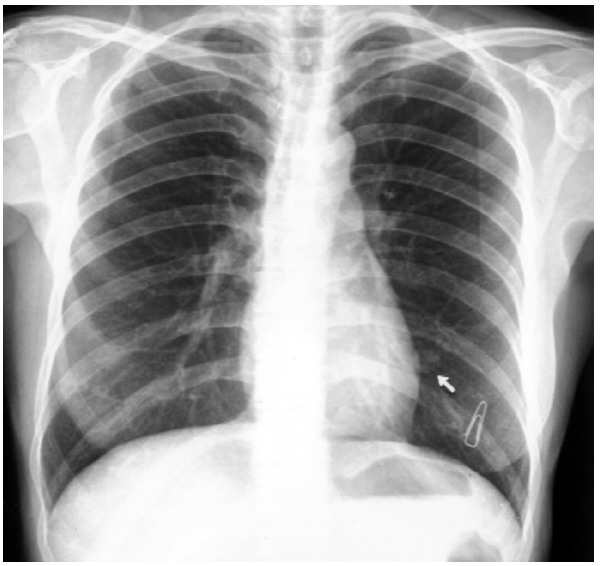

Fig. 1. Chest radiograph 3 years after resection of ameloblastoma in the mandible incidentally showed a nodule (arrow) at the left lower lung field. The clip marks the location of the left nipple.

The diagnosis of metastasizing ameloblastoma was confirmed pathologically (Figure 3) after wedge resection of 2 of the left lung nodules by video-assisted thoracoscopic surgery (VATS). In the histopathology, the tumors were characterized by the presence of epithelial islands outlined by peripheral palisading columnar to cuboidal cells and central spindle to stellate cells. No necrosis, mitosis or cellular atypia was seen. The tumor cells, irrespective of the palisading columnar cells or the stellate spindle cells, were positive for cytokeratin and p63, but negative for S-100 and chromogranin. TTF-1 positive alveolar cells were found lining the outermost surfaces of the tumor nests. These samples had pathological features similar to the tumor in the mandible, confirming the diagnosis of metastatic ameloblastoma. However, there was no local recurrence at the primary site along with the occurrence of pulmonary metas-

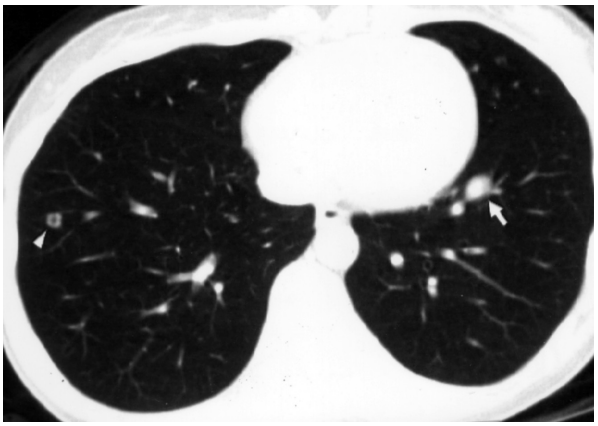

(A)

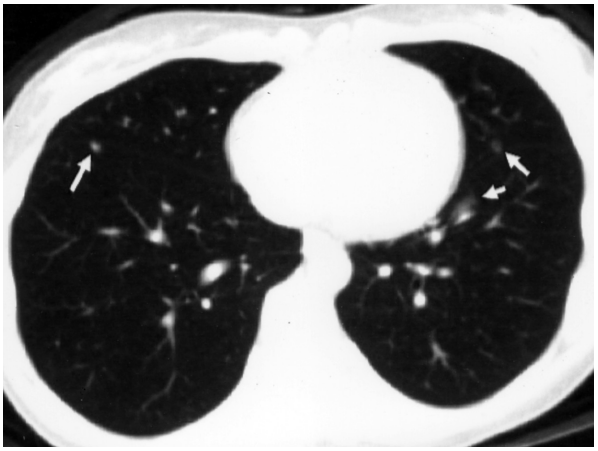

(B)

Fig. 2. (A and B) Computed tomography scan of the chest showed multiple nodules at the bilateral lungs (arrows), with a nodule cavitated (arrowhead) in the right lower lobe of the lung.

tasis.

The patient did not undergo surgical resection for the remaining lung nodules, and neither chemotherapy nor radiation therapy was given. The patient had regular follow-up thereafter. No clinical or radiological evidence of progressive pulmonary disease was documented in the following 2 years. CT scan of the chest performed 10 months after resection of the lung nodules showed that the metastatic nodules remaining in the lungs were relatively stable in number and size.

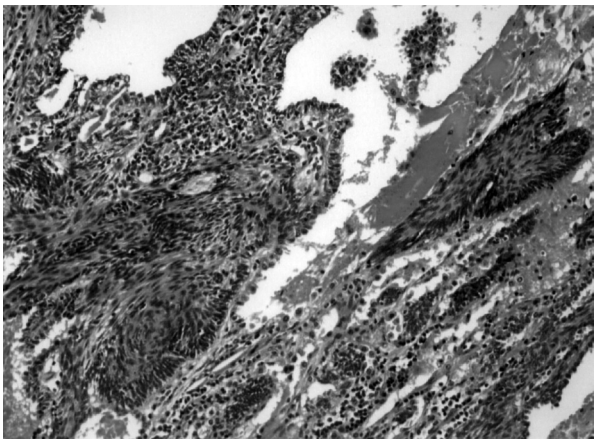

Fig. 3. The tumor was pathologically characterized by the presence of epithelial islands, outlined by peripheral palisaded columnar to cuboidal cells, and central spindle to stellate cells.

Discussion

Ameloblastoma of the jaw is basically benign, but is locally aggressive with a high incidence of local recurrence [1-2]. Malignant variants comprise either ameloblastoma with metastases (malignant ameloblastoma) or an infiltrating lesion with histological features of carcinoma (ameloblastic carcinoma) [9]. In the WHO classification system, malignant ameloblastoma is defined as "an ameloblastoma that metastasizes in spite of a benign histological appearance" (well-differentiated appearance), and ameloblastic carcinomas are tumors characterized by malignant histologic features (poorly differentiated appearance with pleomorphism, hyperchromasia, mitosis, and necrosis), independent of the presence of metastasis [2,9-10].

Metastases occur in roughly 2% of patients with benign ameloblastoma of the jaw [2,5], and 75% to 80% of these involve the lung [5-8]. Other sites of metastases include the cervical

lymph nodes, brain, kidneys, spleen, diaphragm, heart, and soft tissue [6]. It is worth noting that most patients with ameloblastoma do not have a simultaneous diagnosis of metastatic disease at the initial evaluation [6-7,11].

In a recent review of reports of ameloblastoma from 1928, 27 cases with malignant ameloblastoma were found. Of the 27 cases of metastasizing ameloblastoma that were identified based on a convincing pathology, the majority of primary tumors were detected between the third and fifth decades of life (range, 6-74 years of age). There appears to be no gender predilection [7]. About 80% of the primary tumors originated in the mandible and the rest in the maxilla, which is consistent with cases of primary ameloblastoma of the jaw [1-2,6,13].

The duration from operation for the primary tumor to the first metastasis ranged from 2 months to 42 years, with a median of about 14 years [2], which is consistent with another report (average, 18 years; range, 3 to 45 years) [7]. There are reports of patients who presented with pulmonary metastasis but without evidence of local recurrence at the primary site (similar to our case) [7-8,14].

There is considerable evidence from clinical and postmortem studies that ameloblastoma metastasizes from the jaw through hematogeneous or lymphatic spread. Extensive local disease, duration of the presence of the primary tumor, frequent surgical procedures, and multiple local recurrences have been reported to be associated with metastasis of ameloblastoma [2,7]. In some cases, aspiration of tumor cells at the time of oral surgery has been proposed as a possible mechanism of intrapulmonary spread [2,5,7]. Irrespective of the mechanisms involved in the metastasis process, the clinical behavior of metastatic tumors is usually similar to that of the primary tumor, namely, indolent but persistent growth of the lesions at the metastatic sites [7]. Hence, despite multiple pulmonary metastases, patients with metastatic ameloblastoma typically had a reasonable quality of life and survival, although it has been the cause of death in certain reported cases [7]. Nevertheless, if rapid growth and widespread metastasis are observed, ameloblastic carcinoma or primary squamous cell carcinoma of the lungs should be suspected [9].

Survival after diagnosis of metastasis varies in different reports, ranging from 3 years to more than 10 years. The most effective treatment for ameloblastoma may be prompt and thorough resection of the primary tumor to prevent local recurrence and metastasis; adjunctive chemotherapy or radiation therapy has not been shown to provide a benefit for survival or sustained remission [2,7]. Follow-up after operation for the primary tumor should be regular, and additional attention should be paid to the common metastatic sites, such as the lungs and neck, in order to detect metastasis as early as possible. Treatment decision-making for metastatic ameloblastoma, including pulmonary metastasis, is limited by the lack of experience with these rare tumors. Surgical removal of operable lesions is often warranted, particularly when the metastatic tumors are located in the lung periphery where wedge resection is possible [2]. In some case reports, patients had good symptomatic improvement after chemotherapy or radiation therapy, but the overall benefit of this treatment modality is still questionable [7]. In our case, no immediate treatment of the pulmonary metastases was initiated, as the patient's condition was good overall without associated symptoms. Follow-up study demonstrated the indolent nature of the metastatic tumors.

In summary, ameloblastoma of the jaw rarely exhibits malignant behavior, but develops dissemination, with the lung as the most common metastatic site. Metastasizing ameloblastoma (malignant ameloblastoma) should be considered when lung nodules develop in patients with a history of ameloblastoma, irrespective of whether there is local recurrence of the primary tumor.

References

1. Rudagi BM, Halli R, Mahindra U, *et al*. Management of large ameloblastoma- a case report. Pravara Med Rev 2010; 2(1): 22-5.
2. Dissanayake RK, Jayasooriya PR, Siriwardena DJ, *et al*. Review of metastasizing (malignant) ameloblastoma (METAM): pattern of metastasis and treatment. Oral Surg Oral Med Oral Pathol Oral Radiol Endod 2011; 111(6): 734-41.
3. Atkinson CH, Harwood AR, Cummings BJ. Ameloblastoma of the jaw. A reappraisal of the role of megavoltage irradiation. Cancer 1984; 53(4): 869-73.
4. Edward HL. Metastasizing ameloblastoma. Cancer 1989; 64(3): 776-80.
5. Newman L, Howells GL, Coghlan KM, *et al*. Malignant ameloblastoma revisited. Br J Oral Maxillofac Surg 1995; 33(1): 47-50.
6. Berger AJ, Son J, Desai NK. Malignant ameloblastoma: concurrent presentation of primary and distant disease and review of the literature. J Oral Maxillofac Surg 2012; 70(10): 2316-26.
7. Van Dam SD, Unni KK, Keller EE. Metastasizing (malignant) ameloblastoma: review of a unique histopathologic entity and report of Mayo Clinic experience. J Oral Maxillofac Surg 2010; 68(12): 2962-74.
8. Georgakas I, Lazaridou M, Dimitrakopoulos I, *et al*. Pulmonary metastasis in a 65-year-old man with mandibular ameloblastoma: a case report and review of the literature. J Oral Maxillofac Surg 2012; 70(5): 1109-13.
9. Benlyazid A, Lacroix-Triki M, Aziza R, *et al*. Ameloblastic carcinoma of the maxilla: case report and review of the literature. Oral Surg Oral Med Oral Pathol Oral Radiol Endod 2007; 104: e14-27.
10. Sciubba JJ, Eversole LR, Slootweg PJ. Odontogenic/ameloblastic carcinomas. In: L Barnes, JW Everson, P Reichart, editors. World Health Organization classification of tumours, pathology and genetics of head and neck tumours. Lyon, International Agency for Research on Cancer (IARC), 2005: 207-8.
11. Laughlin EH. Metastasizing ameloblastoma. Cancer 1989; 64(3): 776-80.
12. Kunze E, Donath K, Luhr HG, *et al*. Biology of metastasizing ameloblastoma. Pathol Res Pract 1985; 180(5): 526-35.
13. Luo DY, Feng CJ, Guo JB. Pulmonary metastases from an ameloblastoma: case report and review of the literature. J Craniomaxillofac Surg 2012; 40(8): e470-4.
14. Ramadas K, Jose CC, Subhashini J, *et al*. Pulmonary metastases from ameloblastoma of the mandible treated with cisplatin, adriamycin, and cyclophosphamide. Cancer 1990; 66(7): 1475-9.
15. Ii S, Tsuchiya H, Takazawa K, *et al*. Adamantinoma of the proximal femur: a case report. J Orthop Sci 2004; 9(2): 152-6.
16. Papagelopoulos PJ, Mavrogenis AF, Galanis EC, *et al*. Clinicopathological features, diagnosis, and treatment of adamantinoma of the long bones. Orthopedics 2007; 30(3): 211-5; quiz 16-7.
17. Szendroi M, Antal I, Arato G. Adamantinoma of long bones: a long-term follow-up study of 11 cases. Pathol Oncol Res 2009; 15(2): 209-16.

轉移性造釉細胞瘤（Metastasizing Ameloblastoma）－多處肺結節之罕見原因

鐘哲良　蔡子修　廖唯昱　余忠仁

造釉細胞瘤是一種不常見的良性、局部侵襲性的齒源性腫瘤。其約佔所有顎腫瘤及顎囊腫的百分之一。儘管很容易局部復發，造釉細胞瘤甚少遠端轉移。在遠端轉移之少數個案中肺為最常見轉移的位置。我們提出討論的個案為一位下頷患患結締組織增強性造釉細胞瘤（desmoplastic ameloblastoma）並接受邊緣性部分下頷骨切除手術（marginal mandibulectomy）之四十三歲女性。術後三年，胸部電腦斷層顯示產生多處肺結節。我們藉由胸腔內視鏡輔助手術切下其中兩顆肺結節，其病理報告顯示為轉移的造釉細胞瘤，跟原發的位置有一樣的組織學特性，並沒有看到細胞的異生（cellular atypia）。而此病例的原發位置並沒有產生腫瘤復發的跡象。在胸腔內視鏡輔助手術後，此病例並未接受其他針對轉移性造釉細胞瘤之治療，而在接下來兩年的臨床追蹤肺轉移並未進一步進展。*(胸腔醫學* ***2014; 29: 194-199)***

關鍵詞：造釉細胞瘤，惡性造釉細胞瘤，多處肺結節，齒源性腫瘤，肺轉移

臺大醫院　內科部　胸腔內科
索取抽印本請聯絡：蔡子修醫師，國立台灣大學醫學院附設醫院　內科部　胸腔內科，台北市中山南路 7 號